WILSON LOOPS AND RIEMANN THETA FUNCTIONS IN THE GAUGE/GRAVITY DUALITY

A Dissertation

Submitted to the Faculty

of

Purdue University

by

Sannah Phi Ziama

In Partial Fulfillment of the

Requirements for the Degree

of

Doctor of Philosophy

August 2013

Purdue University

West Lafayette, Indiana

ProQuest LLC.
789 East Eisenhower Parkway
P.O. Box 1346
Ann Arbor, MI 48106 - 1346

To my dearest mother Weedor Ziama and my brother Karsor Dennis
with gratitude for their love and indefatigable support.

ACKNOWLEDGMENTS

I am deeply grateful to my supervisor Luis M. Kruczenski for his guidance and numerous encouragements, and for his meticulous teaching that fostered my learning of the many things I have come to learn from him over the past five years. I have also learned a lot of things during discussions with Juan Maldacena, Peter Ouyang, Thomas Clark and Sergei Khlebnikov.

My sincere thanks go to the Simons Center for Geometry and Physics for inviting me to several schools and workshops where I learned a significant number of things.

I would like to particularly thank the NSF for a Graduate Research Fellowship, the AGEP for their strategic support including grant #0450373, and Purdue University for a Doctoral Fellowship. I also thank the friendly administration and staff of the Physics Department of Purdue University for their support during the writing of this thesis.

Finally, I am thankful to my family.

TABLE OF CONTENTS

LIST OF TABLES

LIST OF FIGURES

ABSTRACT

Ziama, Sannah P. Ph.D., Purdue University, August 2013. Wilson loops and Riemann Theta Functions in the Gauge/Gravity Duality. Major Professor: Luis M. Kruczenski.

One important implication of the AdS/CFT conjecture is that the expectation value of a Wilson loop operator in a conformally invariant field theory may be computed in the dual string theory by calculating the regularized area of the minimal area surface that ends on the Wilson loop in the boundary of AdS space. As a consequence, Euclidean Wilson loops correspond to minimal area surfaces in Euclidean AdS space. Many examples of Euclidean Wilson loops have been computed including the parallel lines which give the quark-antiquark energy. We approach the study of Wilson loops from the point of view of finding Riemann theta function solution to the cosh-gordon equation. We compute an infinite set of equivalent classes of simple Wilson loops. Each equivalent class consists of Wilson loops that, though having different shapes and lengths, have the same regularized area of their dual minimal area surfaces. An analytic formula for the area of their dual surfaces is derived. Furthermore new examples of Wilson loops which consist of multiple curves are calculated. For instance we compute cases of concentric Wilson loops which may be viewed as perturbed concentric circular Wilson loops. The trace of their monodromy matrix which gives information about the conserved charges is determined to be a simple function of the spectral parameter.

1. Introduction

In the t'Hooft limit, which is defined as a limit of $N \to \infty$ while keeping $g_{YM}^2 N$ fixed, it has been proposed that strongly coupled planar $\mathcal{N} = 4$ $SU(N)$ super Yang-Mills gauge theory corresponds to weakly coupled type **IIB** string theory on $AdS_5 \times S^5$ space [1, 2]. This is the so called AdS/CFT correspondence or Holography correspondence – a duality between gauge theory on one hand and string theory on the other. One important class of objects that has been studied as an evidence for this duality is the Wilson loop. In particular, it was shown [3] and recently generalized [4] that the energy of a static quark-antiquark pair in $\mathcal{N} = 4$ SYM theory can be determined by computing the expectation value of Wilson loops. On the string theory side the problem reduces to finding the area of minimal area surfaces that end in the boundary of AdS space. The boundary of these surfaces are exactly the Wilson loops on the gauge theory side.

Many examples of Wilson loops have been studied. They may be classified as either open or closed curves. In the case of closed Euclidean Wilson loops (with constant scalar) the most studied one is the circular Wilson loop [5] which is dual to a half-sphere. The only other closed and simple one we are aware of is the two intersecting arcs (lens shaped) [6]. For those Wilson loops which occur as multiple curves, the concentric circles dual to the half-torus were found along with several interesting properties using integrability [7]. For the open curves, the infinite Wilson loops such as the parallel lines [3] and the cusp [8] are known. However, all of these are symmetrically shaped Wilson loops.

In this work a more generalized class of Wilson loops is studied. Their shapes are not symmetric as those of the known examples. In that sense chapter four of this work may be seen as a generalization of the already known examples of Wilson loops. However, the method employed further reveals that many of the previously known

examples of Wilson loops listed above are related to each other. Specifically, it reveals that these Wilson loops may be obtained from each other by a smooth change of a certain parameter. The work focuses on flat Euclidean Wilson loops which are dual to minimal area surfaces in Euclidean AdS_3 space.

This work emphasizes the use of special mathematical functions – *Riemann theta functions* – because they provide a convenient solution to the *cosh-gordon equation* [9, 10] which is a highly nonlinear equation that poses a serious challenge to solving. The cosh-gordon equation is a disguised form of the sigma model in Euclidean AdS space. Traditionally in string theory one finds a solution to the string equations of motion which, by the AdS/CFT correspondence, gives the Wilson loop as the curve describing its intersection with the boundary of AdS space. This is distinct from our approach in the sense that we begin with a certain Riemann surface and determine the Riemann theta functions associated with it. The Wilson loops are then described by those Riemann theta functions which solve the string equation of motion, thus elevating Riemann theta functions (and by extension their underlying Riemann surfaces) to a central role in the study of Wilson loops. Therefore in order to develop a full understanding of how things work it is necessary to study these special functions and the Riemann surfaces with which they are associated. Although in general Riemann theta functions do not need to be associated to Riemann surfaces; those which provide solution to the string equations of motion must.

In chapter 2 we briefly give some background on the conformal (co)invariant nature of AdS_{d+1} and its boundary. We also review the sigma model in Euclidean AdS_3. We show that the string equations of motion reduces to the generalized cosh-gordon equation that is transformed to the standard cosh-gordon equation for which we seek Riemann theta function solutions.

Since the problem of finding *quasi-periodic solutions* to the cosh-gordon equation leads us to Riemann theta functions, in chapter 3 we give a short overview of the theory of Riemann theta functions and of the hyperelliptic Riemann surfaces which they parametrize . This chapter is purposely intended for readers who are not familiar

with the theory of Riemann theta function and wish to pursue the study of Wilson loops based on the proposed method. Many useful references about these functions and their underlying hyperelliptic Riemann surfaces are provided for the more interested reader who wants to pursue more on these functions. Several well-known *lemmas* are given along with their proofs. The proofs are presented as illustration of the main ideas and in a pedagogically friendly way that doesn't obscure the concept in favor of rigor.

Chapters 4 and 5 contain the new examples of Wilson loops computed using the technique presented here.

Chapter 4 focuses on an infinite class of *simple Wilson loops*. A simple Wilson loop is a single smooth curve with a dual minimal area surface. It is shown that unlike the previously known examples of Wilson loops these have general shapes due to their flexibility to be continuously deformed. Also shown is the interesting fact that the deformation is controlled by the spectral parameter that appears in integrability theory, and that the *regularized area* of the dual minimal area surface is invariant under this deformation of the boundary Wilson loop. Perhaps the most important contribution here is that the (regularized) area of the minimal surface is given by an *analytic formula*.

Finally, in chapter 5 more complicated examples of Wilson loops consisting of multiple curves are computed. The area of their dual surfaces are also computed using analytic formulas. The concentric circular Wilson loop is generalized to concentric curves which are not necessarily circular. Furthermore, these concentric Wilson loops can be viewed as perturbations of the concentric circular Wilson loops. This notion of perturbation is shown explicitly by studying the behavior of the Wilson loop under a shrinking of some of the *branch cuts* of a hyperelliptic Riemann surface. Another type of Wilson loop computed is the *cyclical Wilson loop*. These are Wilson loops which are concentric curves that have a *turning number* (the winding number of the unit tangent about the origin) associated with the individual curves. The turning number can be controlled by imposing conditions on the periodicity of the solutions, which

invariably implies controlling the periodicity of ratios of Riemann theta functions. The chapter finishes with new examples of *n-leaf symmetric Wilson loops* which possess a tunable symmetry. They are named that way because of their resemblance to clovers. The number of leafs is determined by the periodicity imposed on the solutions. The ubiquitous role that the periodicity of the solutions plays indicates that many more interesting properties of Wilson loops may be understood by getting a better understanding of the theory of Riemann theta function.

2. Sigma Model in AdS_3 Space

In this chapter we study semiclassical string theory in the AdS_3 space. We begin first by reviewing *holography* of physical theories in AdS_{d+1} and how it relates to Wilson loops.

2.1 Wilson loops in AdS/CFT : A brief overview

We review how the notion of Wilson loop emerges in the AdS/CFT conjecture and the important role it plays.

The AdS/CFT conjecture or Holography conjecture was proposed by Maldacena [1] and further explained by Witten [2]. The main idea of the proposal is that in the limit of large N, where N is the rank of the gauge group of a conformally invariant field theory, this field theory residing on the boundary of $d+1$ dimensional anti-de Sitter space is dual to type **IIB** string theory on AdS_{d+1} times a compact space. The most understood example of this conjecture is the 4 dimensional $\mathcal{N}=4$ $SU(N)$ SYM gauge theory with coupling constant g_{YM}. According to the conjecture, in the t'Hooft limit this theory is equivalent to the tree approximation to supergravity in $AdS_5 \times S^5$. The string coupling constant g_s is proportional to g_{YM}^2 and as $\lambda = g_{YM}^2 N$ gets large but fixed, the superstring theory becomes a weakly coupled theory. This theory is well approximated by the supergravity which is the dual theory to $\mathcal{N}=4$ SYM gauge theory.

Conformal Symmetry and Euclidean AdS Boundary

Recall that the *Poincaré upper half-space model* of hyperbolic space or sometimes referred to as the upper half-space model is described as follows: Take the upper half

space $\mathcal{H}^{d+1}_{\mathcal{R}}$ of $\mathcal{R}^{d+1}$ with coordinates $(x^1, x^2, \cdots, x^d, z)$, with $z > 0$. The quadratic form on this space is

$$ds^2 = \frac{R^2}{z^2}(dx^+ dx^- + (dx^i)^2 + dz^2)\,, \quad i = 3, \cdots, d\,. \tag{1.1}$$

Setting $x^+ = x^2 + i\,x^1$ and $x^- = x^2 - i\,x^1$ leads to the more familiar quadratic form on Euclidean AdS_{d+1}

$$ds^2 = \frac{R^2}{z^2}((dx^i)^2 + dz^2)\,, \quad i = 1, \cdots, d\,. \tag{1.2}$$

The isometry group of this space is $SO(d+1,1)$. This can be readily seen by considering the hyperboloid model of AdS_{d+1}, $\mathbf{H}^{d+1}_{\mathcal{R}}$. Define $\mathcal{R}^{d+1,1}$ by the coordinates $\{x^1, \cdots, x^{d+1}, \tau\}$. Then $\mathbf{H}^{d+1}_{\mathcal{R}}$ is the upper sheet of the hyperboloid defined by $|x|^2 - \tau^2 = -R^2$ in $\mathcal{R}^{d+1,1}$. Here the metric $m_{\mathbf{H}}$ on $\mathbf{H}^{d+1}_{\mathcal{R}}$ is given by

$$m_{\mathbf{H}} = i^* m_{\mathcal{R}}\,, \tag{1.3}$$

where $m_{\mathcal{R}}$ is the metric on $\mathcal{R}^{d+1,1}$ and i is the inclusion map $i : \mathbf{H}^{d+1}_{\mathcal{R}} \hookrightarrow \mathcal{R}^{d+1,1}$. Thus it becomes clear that indeed $SO(d+1,1)$ acting on $\mathbf{H}^{d+1}_{\mathcal{R}}$ leaves the metric invariant.

When $d = 2$ this isometry group becomes the more familiar $SL(2,\mathbb{C})$. This is how $SL(2,\mathbb{C})$ which is isomorphic to the $2d$ conformal symmetry group, $Conf(\mathcal{R}^2)$, may be viewed as the symmetry group of AdS_3 .

The boundary of $\mathcal{H}^{d+1}_{\mathcal{R}}$ is a copy of $\mathcal{R}^d$ located at $z = 0$. The quadratic form (1.1) or (1.2) does not extend over the closure of the Poincaré upper half-space, $\overline{\mathcal{H}}^{d+1}_{\mathcal{R}}$. To get a quadratic form that extends over $\overline{\mathcal{H}}^{d+1}_{\mathcal{R}}$ we multiply ds by a function g which is nonnegative on $\overline{\mathcal{H}}^{d+1}_{\mathcal{R}}$ and that has a first order zero on the boundary ($g = z$ for example) and then the restriction of (1.1) to $\partial\mathcal{H}^{d+1}_{\mathcal{R}}$ the boundary of $\mathcal{H}^{d+1}_{\mathcal{R}}$ becomes

$$d\tilde{s}^2 = g^2\, ds^2 = R^2(dx^+ dx^- + (dx^i)^2)\,, \quad i = 3, \cdots, d\,. \tag{1.4}$$

The function g is not unique and using a different function ge^{ϕ} for a real function ϕ on $\overline{\mathcal{H}}^{d+1}_{\mathcal{R}}$ would lead to a new quadratic form

$$d\tilde{s}^2 \to g^2\, e^{2\phi}\, ds^2 \tag{1.5}$$

on the boundary $\partial\mathcal{H}^{d+1}_{\mathcal{R}}$. So the boundary metric is defined up to a conformal factor and therefore the dual theory has to be conformally invariant. Particularly important are global conformal transformations of the boundary coordinates which in the bulk correspond to the $SO(d+1,1)$ symmetry group of AdS_{d+1} space.

Note that the boundary $\mathcal{R}^d$ is not compact. The conformal group acts on a compact manifold. We can make $\mathcal{R}^d$ compact by "*gluing*"[1] two copies of $\mathcal{R}^d$ into a final compact manifold S^d .

Expectation values of operators in a CFT may be computed in the dual theory in AdS under the provisions of theAdS/CFT conjecture. One operator that fits this description is the Wilson loop operator [3]. One way to see this is that due to the conformal symmetry of both AdS and its boundary, a theory may be viewed separately as a CFT on the boundary of AdS or as a string theory in the bulk of AdS [2]. Therefore under the conditions of AdS/CFT one should in principle be able to compute expectation values of gauge theory operators by computing corresponding quantities in the string theory. So Wilson loops provide an opportunity to test the conjecture or to give supporting evidence for it. This is why computation of Wilson loops plays an important role in the AdS/CFT conjecture.

2.2 Sigma Model in Euclidean AdS_3

A convenient way to imagine Euclidean AdS_3 is to consider it as a subspace of $\mathcal{R}^{3,1}$ defined by the equation

$$-X_0^2 + X_1^2 + X_2^2 + X_3^2 = -1 \ , \tag{2.6}$$

with an obvious $SO(3,1) \cong SL(2,\mathbb{C})$ global invariance. The action of the string in conformal coordinates is given by

$$\begin{aligned} S &= \frac{1}{2}\int \left(\partial X_\mu \bar{\partial} X^\mu - \Lambda(X_\mu X^\mu - 1)\right)\, d\sigma\, d\tau \\ &= \frac{1}{2}\int \frac{1}{Z^2}\left(\partial_a X \partial^a X + \partial_a Y \partial^a Y + \partial_a Z \partial^a Z\right)\, d\sigma\, d\tau, \end{aligned} \tag{2.7}$$

[1] See chapter 4 for a detail explanation of this procedure in the complex setting.

where Λ is a Lagrange multiplier and the μ indices are raised and lowered with the $\mathcal{R}^{3,1}$ metric

$$(v, w) = \sum_{i=1}^{3} v_i w^i - v_0 w^0 \,. \tag{2.8}$$

The complex coordinates z and $\bar{z}$ are related to the world sheet coordinates, $\sigma_a = (\sigma, \tau)$ by $z = \sigma + i\tau$, and $\bar{z} = \sigma - i\tau$. X, Y, Z are called Poincaré coordinates (see (2.26)). The string equations of motion are given by

$$\partial\bar{\partial} X_\mu = \Lambda X_\mu \ , \tag{2.9}$$

where Λ, the Lagrange multiplier is given by

$$\Lambda = \partial X_\mu \bar{\partial} X^\mu = (X_z, X_{\bar{z}}). \tag{2.10}$$

The conformal condition is encoded in the Virasoro constraint

$$(X_z, X_z) = 0 = (X_{\bar{z}}, X_{\bar{z}}). \tag{2.11}$$

The first step to solving the equations of motion is to reduce the problem to an equation with a single unknown scalar field. In AdS_3 space this scalar equation is the cosh-gordon equation

$$\partial\bar{\partial}\alpha = 4\cosh\alpha \,. \tag{2.12}$$

This reduction mechanism referred to as *Pohlmeyer reduction* [12] has been used in the study of many related problems. In the context of Minkowski space-time this procedure was used by Jevicki and Jin [13] and by Kruczenski [14] to find new spiky string solutions, and by Alday and Maldacena [15] to compute certain light-like Wilson loops. In a more geometric guise it was employed [9] to study constant mean curvature surfaces in hyperbolic space. We review the idea and follow closely what was done in [9].

In *Euclidean* AdS_3, form a basis

$$t = (X, X_z, X_{\bar{z}}, N) \tag{2.13}$$

where

$$(X, N) = (X_z, N) = (X_{\bar{z}}, N) = 0, (N, N) = 1 \tag{2.14}$$

Note that (2.6) and (2.11) imply

$$(X, X_z) = (X, X_{\bar{z}}) = 0 \tag{2.15}$$

and

$$(X_z, X_{zz}) = (X_z, X_{z\bar{z}}) = (X_{\bar{z}}, X_{\bar{z}\bar{z}}) = (X_{\bar{z}}, X_{z\bar{z}}) = 0 \tag{2.16}$$

respectively. Define

$$(X_z, X_{\bar{z}}) := 2e^{\alpha}\,, \quad (X_{z\bar{z}}, N) := 2H^h e^{\alpha}\,, \quad (X_{zz}, N) := A^h\,, \tag{2.17}$$

where A^h is the Hopf differential and H^h is the mean curvature of the surface described by the solution to the string equation of motion. Since we are concerned here with a minimal area surface (described by the string equations of motion) we will have a vanishing mean curvature and the second equation in (2.17) is equal to zero. We want to study what happens when the basis undergoes a small motion with the hope that second derivative quantities will tell us something useful about the sigma model. For this we write second derivatives as a linear combination of the basic vectors. Thus we write

$$X_{z\bar{z}} = aX + bX_z + cX_{\bar{z}} + dN\,. \tag{2.18}$$

Then taking inner product with X gives

$$-a = (X, X_{z\bar{z}}) = -(X_z, X_{\bar{z}})$$

which implies $a = 2e^{\alpha}$ due to (2.17). Doing same for the other vectors in the basis gives

$$\begin{aligned} 0 = (X_z, X_{z\bar{z}}) = c(X_z, X_{\bar{z}}) &\implies c = 0 \\ 0 = (X_{\bar{z}}, X_{z\bar{z}}) = b(X_{\bar{z}}, X_z) &\implies b = 0 \\ 0 = (N, X_{z\bar{z}}) = -d & \end{aligned}$$

This shows that

$$X_{z\bar{z}} = 2e^{\alpha}X\,, \tag{2.19}$$

which is exactly the equation of motion (2.9) taking $\Lambda = 2e^{\alpha}$. Note that without the minimal area condition, i.e. $H^h = 0$, equation (2.19) will have an additional term proportional to $H^h N$. Repeating this for the other second derivatives we get

$$X_{zz} = \alpha_z X_z - A^h N$$

and

$$X_{\bar{z}\bar{z}} = \alpha_{\bar{z}} X_{\bar{z}} - \bar{A}^h N \,.$$

Consider motion of the basic vectors given by

$$t_{i,z} = U_{ij} t_j, \qquad\qquad t_{i,\bar{z}} = V_{ij} t_j \,. \tag{2.20}$$

Note that since second derivatives are expressed entirely in terms of first derivatives, quantities such as $t_{i,z}$ and $t_{i,zz}$ are all expressible in terms of first derivatives. Consequently, the matrices U and V contain α and its derivatives, and A^h (and its complex conjugate). Taking second derivatives and imposing the compatibility condition $t_{i,z\bar{z}} = t_{i,\bar{z}z}$ leads to

$$(U_{ij,\bar{z}} - V_{ij,z}) t_j + (U_{ij} V_{jk} - V_{ij} U_{jk}) t_k = 0 \,. \tag{2.21}$$

This equation may be written in matrix form, after dropping the t, as

$$U_{\bar{z}} - V_z + [U, V] = 0 \tag{2.22}$$

with U and V determined from (2.20) as

$$U = \begin{pmatrix} 0 & 1 & 0 & 0 \\ 0 & \alpha_z & 0 & A^h \\ 2e^{\alpha} & 0 & 0 & 0 \\ 0 & 0 & -\frac{1}{2} A^h e^{-\alpha} & 0 \end{pmatrix}, \qquad V = \begin{pmatrix} 0 & 0 & 1 & 0 \\ 2e^{\alpha} & 0 & 0 & 0 \\ 0 & 0 & \alpha_{\bar{z}} & \bar{A}^h \\ 0 & -\frac{1}{2} \bar{A}^h e^{-\alpha} & 0 & 0 \end{pmatrix}.$$

The compatibility equation implies that A^h is a holomorphic function. Furthermore, it leads to a generalized cosh-gordon equation

$$\alpha_{z\bar{z}} - 2e^{\alpha} - \frac{1}{2} A^h \bar{A}^h e^{-\alpha} = 0 \,. \tag{2.23}$$

If in (2.23) we scale the Hopf differential $A^h \to 2A^h$ and similarly for its conjugate, the generalized cosh-gordon equation becomes

$$\alpha_{z\bar{z}} - 2e^{\alpha} - 2A^h \bar{A}^h e^{-\alpha} = 0\,. \tag{2.24}$$

Changing coordinates to $w = \sqrt{A^h}\, z, \bar{w} = \sqrt{\bar{A}^h}\, \bar{z}$ followed by a transformation of the field $\alpha \to \tilde{\alpha} = \alpha - \frac{1}{2}\log A^h \bar{A}^h$, the resulting equation is the standard cosh-gordon equation (2.12). This procedure is equivalent to setting $A^h = 2$ in (2.23).

To connect the scalar field α with the solutions for (2.9) we introduce a hermitian matrix

$$\mathbb{X} = \begin{pmatrix} X_0 + X_3 & X_1 - iX_2 \\ X_1 + iX_2 & X_0 - X_3 \end{pmatrix}. \tag{2.25}$$

Then construct Poincaré coordinates

$$Z = \frac{1}{\mathbb{X}_{22}}, \quad X + iY = \frac{\mathbb{X}_{21}}{\mathbb{X}_{22}}. \tag{2.26}$$

The final connection is to recognize that (2.23) is also the compatibility condition for the system of equations [9]

$$\Phi_z = \tilde{U}\Phi \qquad \Phi_{\bar{z}} = \tilde{V}\Phi \tag{2.27}$$

where $\tilde{U}$ and $\tilde{V}$ are given by

$$\tilde{U} = \frac{1}{2}\begin{pmatrix} 0 & 2\lambda e^{\alpha/2} \\ 2e^{-\alpha/2} & \alpha_z \end{pmatrix} \qquad \tilde{V} = \frac{1}{2}\begin{pmatrix} \alpha_{\bar{z}} & -\bar{A}e^{-\alpha/2} \\ \frac{2}{\lambda}e^{\alpha/2} & 0 \end{pmatrix}. \tag{2.28}$$

The parameter λ is the spectral parameter which emerges in the study of integrable differential equations. Given a solution for the pair of equations (2.27), the Poincaré coordinates are related to (2.27) by

$$X + iY = \frac{a\bar{b} + \bar{d}c}{b\bar{b} + d\bar{d}} \qquad Z = \frac{\sqrt{\det\Phi \det\Phi^{\dagger}}}{b\bar{b} + d\bar{d}} \tag{2.29}$$

where $\Phi = \begin{pmatrix} a & b \\ c & d \end{pmatrix}$. One advantage of Poincaré coordinates is that the boundary of AdS_3 is now a copy of $\mathcal{R}^2$.

The rest of the program is to find a solution for the cosh-gordon equation, then solve the system of equations (2.27) and finally feed the result into (2.29).

3. Hyperelliptic Riemann Surfaces and their Associated Riemann Theta Functions

In seeking quasi-periodic solutions to the cosh-gordon equation, we inherently place a major emphasis on the relevance of Riemann theta functions in this study of Wilson loops. Therefore it is useful to get an understanding of the origin of these functions. As we will see later, when the concept of Riemann theta functions have been developed then the desire solutions in terms of these special functions can be deduced without much attention to the mathematics of these functions or to the Riemann surfaces which give rise to them. For now, as we develop the concept, we study the theory of Riemann theta functions and their connections to Riemann surfaces as much as is needed for our purpose. We need to understand the concept of hyperelliptic Riemann surfaces, which can be attained by gluing together Riemann surfaces. So we begin with a study of this process of "gluing" Riemann surfaces. There is vast mathematics literature on the Algebro-Geometric nature of Riemann theta functions. We review the basics we need here based on [9, 10, 16–20]

3.1 Gluing of Riemann Surfaces

A Riemann surface is a complex manifold of dimension one (in the complex sense). We naturally imagine a Riemann surface as having complex charts and the open subsets on which these charts are defined being themselves Riemann surfaces. One may also look at the situation in the reverse by considering a collection of, a priori, unrelated open sets and patching them together to form a Riemann surface. Indeed, this process of patching together has to be done in a way that allows for the existence of a complex structure on the final Riemann surface. Let us describe this in a rigorous way. First, we need a *gluing datum*.

Definition 1 3.1.1 *A gluing datum consists of the following:*

- *an index set* I
- $\forall\, i \in I$ *a Riemann surface* U_i
- $\forall\, i,\, j \in I$ *open subset* $U_{ij} \subset U_i$ *where* U_{ij} *are considered Riemann surfaces themselves*
- $\forall\, i,\, j \in I$ *an isomorphism* $\phi_{ij} : U_{ji} \to U_{ij}$ *of Riemann surfaces, such that*
  - *a.* $U_{ii} = U_i$, *and*
  - *b.* $\phi_{kj} \circ \phi_{ji} = \phi_{ki}$ *on* $U_{ij} \cap U_{ik}$, $i,\, j,\, k \in I$, *with* $\phi_{ji}(U_{ij} \cap U_{ik}) \subseteq U_{jk}$.

(b) is known as the cocycle condition. In the case $i = j = k$, it implies that $\phi_{ii} = id_{U_i}$ and in the case $i = k$, from $\phi_{ii} = \phi_{ij} \circ \phi_{ji}$, that $\phi_{ji} : U_{ij} \cap U_{ik} \to U_{ji} \cap U_{jk}$ is an *isomorphism*. An isomorphism between Riemann surfaces is a holomorphic bijective map.

We now define a Riemann surface obtained from a gluing datum.

Definition 2 3.1.1 *Suppose* $((U_i)_{i\in I}, (U_{ij})_{i,\,j\in I}, (\phi_{ij})_{i,\,j\in I})$ *is a gluing datum of Riemann surfaces. Then the Riemann surface* X *with injective morphisms* $\psi_i : U_i \to X$ *is said to be the Riemann surface obtain by gluing (with respect to the gluing datum) if the following conditions hold:*

- *1.* $\forall i$ *the map* $\psi_i : U_i \to X$ *gives an isomorphism.*
- *2.* $\psi_j \circ \phi_{ji} = \psi_i$ *on* $U_{ij}, \forall i, j,$
- *3.* $X = \cup_i \psi_i(U_i),$
- *4.* $\psi_i(U_i) \cap \psi_j(U_j) = \psi_i(U_{ij}) = \psi_j(U_{ji}), \forall i, j \in I.$

The Riemann surface constructed this way may or may not be compact; we are interested in those that are compact.

The underlying idea in constructing X goes as follows: begin by taking a disjoint union $\coprod_i U_i$ of the basic Riemann surfaces. Think of $\coprod_i U_i$ as a set consisting of the following subsets:

- singletons, $\{a_i\} \in \{U_i - U_{ij}\}, \forall\, i, j \in I$
- doubletons, $\{x_i, \phi_{ji}(x_i)\}$ where $x_i \in U_i$

Then, let the equivalence relation $\sim$ imply that two points $x_i \in U_i$ and $x_j \in U_j, \forall\, i, j \in I$ are equivalent if and only if $\phi_{ji}(x_i) = x_j$, with $x_j \in U_{ji}$ and $x_i \in U_{ij}$. Clearly there is a surjective morphism $\psi : \coprod_i U_i \to \coprod_i U_i/\sim$ which sends an element in the set $\coprod_i U_i$ to its equivalent class in $\coprod_i U_i/\sim$. Define the desire Riemann surface X as

$$X := \coprod_{i \in I} U_i/\sim \ .$$

We remark that X is endowed with a topology which makes all the injective maps $\psi_i : U_i \to X$ continuous. Furthermore, we have that $\psi_i(U_{i\,j}) = \psi_i(U_i) \cap \psi_j(U_j)$ and $\psi_i(U_i)$ are both open in X.

To reenforce the idea, we give perhaps the simplest example of a Riemann surface constructed this way. Take the index set $I = \{1, 2\}$ which implies we have two sets $U_1 := \mathbb{C}$ and $U_2 := \mathbb{C}$ with open subsets $U_{12} := \mathbb{C}^* = \mathbb{C} \setminus \{0\}$ and $U_{21} := \mathbb{C}^*$, respectively. We have an isomorphism $\phi : \mathbb{C}^* \to \mathbb{C}^*$ which we define as

$$\phi(z) = 1/z\,,$$

which is easy to check defines a gluing datum. The resulting Riemann surface $X := U_1 \coprod U_2/\sim$ is the familiar Riemann sphere $\mathbb{C}_\infty$.

Now that it has been made clear how to construct a Riemann surface from a given gluing datum, it would now be natural to extend this tool to the concept of hyperelliptic Riemann surfaces.

3.2 Hyperelliptic Riemann Surfaces

The hyperelliptic Riemann surfaces will be constructed by gluing two curves, viewed as the zero loci of specified complex polynomials, into a final manifold. Through-

out we will be restricted to the field $\mathbb{C}$. By the set of zero locus of a complex polynomial, $\mathcal{P} \in \mathbb{C}$, we mean

$$V(\mathcal{P}) = \{(\mu, \lambda) \in \mathbb{C}^2 : \mathcal{P}(\mu, \lambda) = 0\} \subseteq \mathbb{C}^2 .$$

So to say a curve X is defined by a polynomial, $\mathcal{P}$, it will mean that X is considered as the set of zeros, $V(\mathcal{P})$, of $\mathcal{P}$.

Take a polynomial in a single variable, $p(\lambda)$, that has degree $2g+1+\delta$, where g is an integer and δ is either 0 or 1 depending on whether g is odd or even respectively.[1] The polynomial is assumed to have distinct roots. Denote by X the smooth curve defined by the equation $\mu^2 = p(\lambda)$ and let $U_1 = \{(\mu, \lambda) \in X \,|\, \lambda \neq 0\} \subset X$, be an open subset of X. Form a second Riemann surface Y, to be glued to X, by the equation $w^2 = q(z) := z^{2g+2}p(1/z)$. The factor z^{2g+2} ensures that $q(z)$ is a polynomial in z and because p has distinct roots so does q. Let $U_2 = \{(z, w) \in Y \,|\, z \neq 0\} \subset Y$ be open. Then there is an isomorphism $\phi : U_1 \to U_2$ given by

$$\phi(\mu, \lambda) = (\mu/\lambda^{g+1}, 1/\lambda) .$$

Define

$$Z := X \coprod Y/\phi,$$

where ϕ denotes the equivalence relation $\sim$ defined via ϕ, to be a Riemann surface of genus g. This Riemann surface admits a degree two covering map to the Riemann sphere by extending λ on X to a holomorphic map $\pi : Z \to \mathbb{C}_\infty$.

Thus, we refer to hyperelliptic Riemann surface *as the surface Z constructed as described above along with a degree two map to the Riemann sphere.*

Indeed, compact hyperelliptic Riemann surfaces can be viewed as the smooth *hyperelliptic curves*

$$\mu^2 = \prod_{i=1}^{N}(\lambda - \lambda_i), \quad N \geq 3, \quad \lambda_i \neq \lambda_j \in \mathbb{C}, \forall\, i, j = 1, ..., N. \tag{2.1}$$

[1] g is the topological genus of the Riemann surface X, i.e. the number of handles of X. It is a deep theorem of Algebraic Geometry that every Riemann surface is an algebraic curve.

For $N = 3, 4$ they are called *elliptic curves*. It is clear that for each value of the independent variable, λ, there are, in general, two distinct values of the dependent variable, μ, and these values are said to lie on the two *sheets* of the Riemann surface. So such a Riemann surface is said to be *two-sheeted* and in general, a Riemann surface given by $\mu^n = \prod_{i=1}^{N}(\lambda - \lambda_i)$ is said to be *n-sheeted*.

There are values of λ, however, for which the two values of μ coincide and it is worth to take note of the behavior of the hyperelliptic Riemann surface at these points. We will adopt the language of Baker [16] in referring to the point on a hyperelliptic Riemann surface corresponding to the value of a pair (μ, λ) as a *place*. The Riemann surface behaves in two possible ways at the point where the values of λ coincide. The first possibility is that the two sheets of the hyperelliptic Riemann surface touch at exactly one point and touch at no where else in the vicinity of the said point. In this case it is possible to draw two small loops around this point with each loop lying entirely in only one of the sheets. When this happens we say the point corresponds to two places of the Riemann surface. The second possibility occurs when the sheets interwind at the point and any small close loop around the point meets both sheets. In this case we say the point equally belongs to the two sheets, and corresponds to one place of the hyperelliptic Riemann surface. Points at which the second scenario occurs are known as *branch points*. A branch point is a point, x on a Riemann surface $\tilde{X}$ such that given a *covering map* (non-constant holomorphic maps between Riemann surfaces), $F : \tilde{X} \to X$ between Riemann surfaces $\tilde{X}$ and X, it is not possible to find a neighborhood $\tilde{U} \ni x$ such that $F|_{\tilde{U}}$ is injective.

From what has been said above, it can be easily deduced that

Lemma 1 3.2.1 *Given a non-constant holomorphic map, $F : \tilde{X} \to X$, between two compact hyperelliptic Riemann surfaces, the set $S_y = F^{-1}(y)$, $\forall\, y \in X$ consists of either one or two places depending on whether the corresponding point is or is not a branch point.*

This implies that S is a discrete set since for any point $x \in \tilde{X}$ it is always possible to find a neighborhood, $\tilde{U} \ni x$ which meets S_y in at most one place $\forall\, y \in X$. Hence

non-constant holomorphic maps between compact hyperelliptic Riemann surfaces are discrete.

It is always possible to find local charts near $x \in \tilde{X}$ and $F(x) \in X$ such that locally F may be represented by a power map

$$z \to z^m, \quad m \in \mathbb{Z}_+ \tag{2.2}$$

and this integer m is independent of the local charts. The number, $m_F(x)$, indicates the number of times F takes the value $F(x)$ and is therefore refer to as the *multiplicity* of the map F at x. In our case for curves described by (2.1), this number is either one or two. Points on a hyperelliptic Riemann surface for which $m_F = 2$ are branch points and the discrete set

$$B = \{x \in \tilde{X} : m_F(x) = 2\} \subset \tilde{X}$$

is finite if $\tilde{X}$ is compact, and the image $F(B) \in X$ is also finite. A covering $F : \tilde{X} \backslash B \to X$ is said to be *unramified*. Topologically, one may describe the number m as follows: It is possible to find neighborhoods, $\tilde{U} \ni x$, $U \ni F(x)$ such that $F^{-1}(y) \cap \tilde{U}$ consists of precisely m points, $\forall\, y \in U \backslash F(x)$. Another significant number is the *branch number* of F at x, $b_F(x) = m_F(x) - 1$. In general $b_F(x) \geq 1$ for branch points and zero for all other points. The *degree of a covering map* $F : \tilde{X} \to X$ is defined as the number

$$d_y(F) = \sum_{x \in F^{-1}(y)} (b_F(x) + 1) \tag{2.3}$$

and this number is independent of the point $y \in X$. From (2.3) it is clear that, as stated in the definition for a hyperelliptic Riemann surface, the independent variable, viewed as a covering map $\lambda : \tilde{X} \to \mathbb{P}^1$ is a degree two map.

Looking back at (2.1) we can readily deduce that the points $(0, \lambda_i)$ are branch points and in general, when $N = 2g + 1$ they consist of the points $(0, \lambda_i), i = 1, ..., N$, and ∞ whereas for $N = 2g + 2$, they are $(0, \lambda_i), i = 1, ..., N$.

There is a prescribed way to give local homeomorphisms near a point on a Riemann surface. Suppose λ has a finite value, say a, then the local coordinate near $\lambda = a$ may be given by

$$(\mu, \lambda) \to (\lambda - a)^{\frac{1}{b_F(\lambda)+1}}, \tag{2.4}$$

and for λ at infinity the homeomorphism is

$$(\mu, \lambda) \to \frac{1}{\lambda^{\frac{1}{b_F(\lambda)+1}}}. \tag{2.5}$$

3.2.1 Basis of Holomorphic One-forms

One distinct feature of hyperelliptic Riemann surfaces is that it is always possible to explicitly write down a basis of the space $H^0(\tilde{X}, \Omega^1)$ of holomorphic one-forms on $\tilde{X}$. We show this but first a few things are in order.

For any hyperelliptic Riemann surface, $\tilde{X}$, given by (2.1), there is an holomorphic automorphism $\sigma : \tilde{X} \to \tilde{X}$ defined by

$$\sigma(\mu, \lambda) = (-\mu, \lambda). \tag{2.6}$$

This automorphism has the property that $\sigma \circ \sigma = id$ so it is called a *hyperelliptic involution*. For the projection map $\pi : \tilde{X} \to \mathbb{P}^1$ we have

$$\pi \circ \sigma = \pi. \tag{2.7}$$

This relation, (2.7), is crucial. It allows us to describe the set, $\mathcal{M}(\tilde{X})$, of all meromorphic functions on $\tilde{X}$ and more relevantly it allows to establish a basis for $H^0(\tilde{X}, \Omega^1)$.

Meromorphic Functions on Hyperelliptic Riemann Surfaces

Suppose $f \in \mathcal{M}(\tilde{X})$, then $\sigma^* f = f \circ \sigma$ also belongs to $\mathcal{M}(\tilde{X})$. Any such f may be written as

$$f = f^+ + f^-, \tag{2.8}$$

a sum of a σ^*-invariant part f^+ and an σ^*-anti-invariant part f^-, with

$$f^+ = 1/2(f + \sigma^* f), \quad f^- = 1/2(f - \sigma^* f). \tag{2.9}$$

Let g be any σ^*-invariant function on a hyperelliptic Riemann surface, $\tilde{X}$, i.e. $\sigma^* g = g$, and let a be a point in $\mathbb{P}^1$ and b in $\tilde{X}$ such that $\pi(b) = a$. Then there is a function, r,on $\mathbb{P}^1$ such that $r(a) = g(b)$. But this implies that $g(b) = r \circ \pi(b) = \pi^* r(b)$. Since g is σ^*-invariant, the function r is well defined and it is unique. So this essentially proves that:

Lemma 2 3.2.1 *Let g be a meromorphic function on a hyperelliptic Riemann surface, $\tilde{X}$, such that $\sigma^* g = g$. Then there is a unique function $r \in \mathcal{M}(\mathbb{P}^1)$ such that $g = \pi^* r = r \circ \pi$.*

The significance of *Lemma 2 (3.2.1)* is that it states that the σ^*-invariant part of all meromorphic functions on a hyperelliptic Riemann surface are pullbacks of meromorphic functions on the Riemann sphere $\mathbb{P}^1$. A natural example of a σ^*-invariant function on a hyperelliptic Riemann surface is the coordinate λ.

To characterize the σ^*-anti-invariant functions on a hyperelliptic Riemann surface, it is natural to look at the coordinate μ, since by the automorphism (2.6) we have $\sigma^* \mu = -\mu$, it is the readily available example. However, due to (2.8) and (2.9), for any meromorphic function f on $\tilde{X}$ the rational function f^-/μ is σ^*-invariant. This implies there exists a unique meromorphic function, R, on $\mathbb{P}^1$ such that $f^- = \mu R$. Thus.

Lemma 3 3.2.1 *If $f \in \mathcal{M}(\tilde{X})$ with $\tilde{X}$ defined by (2.1), then f may be uniquely written as*

$$f = r(z) + \mu R(z)$$

where r and R are meromorphic functions on $\mathbb{P}^1$.

One-forms on Hyperelliptic Riemann Surfaces

We now extend this idea extends to the case of 1-forms which we are more concerned about. 1-forms are constructed from functions so this is why some effort was first devoted to understanding the case of meromorphic functions.

The holomorphic map $\sigma : \tilde{X} \to \tilde{X}$ induces a map

$$\sigma_* : H^0(\tilde{X}, \Omega^1) \to H^0(\tilde{X}, \Omega^1) \tag{2.10}$$

which acts on a holomorphic 1-form, ω in either of two ways: (i). $\omega \to \omega$ or (ii). $\omega \to -\omega$. The first case would inevitably lead to the corresponding situation in *Lemma 2 (3.2.1)*: An ω satisfying $\sigma_*\omega = \omega$ would have to be a pullback of a holomorphic 1-form on $\mathbb{P}^1$. But the space of holomorphic 1-forms on the Riemann sphere is trivial therefore case (i) is not possible, leaving (ii) as the only possibility.

Since λ is σ^*-invariant and μ is σ^*-anti-invariant, as established in the above discussions, the simplest example, in view of what has been said, of a holomorphic 1-form, ω_0 on $\tilde{X}$ should be of the form

$$\omega_0 = \frac{d\lambda}{\mu}$$

so that $\sigma_*(\omega_0) = -\omega_0$ is satisfied. ω_0 is holomorphic because near points $(0, \lambda_i)$ we have local coordinates $\phi = \sqrt{\lambda - \lambda_i}$ according to (2.4), which implies that $\omega_0 = k\, d\phi$ where k is constant. For $\lambda \to \infty$ one has to treat the case when N is odd separately from when N is even. For odd N the local coordinate $\phi = 1/\sqrt{\lambda}$ given by (2.5), leads to $\omega_0 \sim -d\phi$. The same result is found for even N, however with $\phi = 1/\lambda$. Also notice that at points where μ vanishes, $d\lambda$ also vanishes. Therefore ω_0 is indeed holomorphic on $\tilde{X}$.

We can get other holomorphic $1 - forms$ by taking products

$$\omega = f\, \omega_0.$$

But since $\sigma_*(\omega) = -\omega$ must be satisfied, we must have that $\sigma_*(f) = f$, which implies the f is a function of λ only and not of μ. Therefore f is a polynomial in λ. The total degree of ω_0 is $2(g-1)$ for both cases of $N = 2g+1$ and $N = 2g+2$ and we show this explicitly for the odd case.

When $N = 2g + 1$, we see that in the vicinity of infinity we have

$$\omega_0 = \frac{d\lambda}{\mu} \to \frac{d\lambda}{\lambda^{g+1/2}}$$

The local homeomorphism is

$$\phi = \frac{1}{\sqrt{\lambda}}, \quad with \quad d\phi = -\frac{1}{2}\lambda^{-3/2}d\lambda$$

which gives

$$\frac{d\lambda}{\mu} \to -2\phi^{2(g-1)}d\phi. \tag{2.11}$$

This implies that there are $2g-2$ zeros of ω_0 lying above ∞ and so the number of zeros of f cannot exceed this number for $f(\lambda)d\lambda/\mu$ to be holomorphic. So if the degree of f is d, then $2d \leq 2g-2$. Therefore, degree of f cannot exceed $g-1$ and a basis of the space, $H^0(\tilde{X}, \Omega^1)$, of holomorphic $1-forms$ on $\tilde{X}$ is

$$\{\lambda^0\frac{d\lambda}{\mu}, \lambda^1\frac{d\lambda}{\mu}, \cdots, \lambda^{g-1}\frac{d\lambda}{\mu}, \}.$$

The case for even N essentially follows the same line of argument except that the point at infinity is not a branch point and the local homeomorphism is different. This time there are $g-1$ zeros of ω_0 on each sheet of the hyperelliptic Riemann surface and we get a total of $2g-2$ zeros as before. Again we find the same bound on d.

3.2.2 Basis of Cycles on a Hyperelliptic Riemann Surface

Eventually it will be necessary to give a precise description of what it means to integrate a differential form around a loop on a hyperelliptic Riemann surface. So it is important to get a clear understanding of what kind of loops we will integrate along. We begin by looking at (hyperelliptic) Riemann surfaces through a new lens, as a polygon with boundary that gives us a crucial insight into the kinds of loops we will be dealing with.

We take for granted that every compact Riemann surface is homeomorphic to a sphere with handles. The number of handles is indicated by the number $g \in \mathbb{Z}_+$ the *genus* of the Riemann surface. When the Riemann surface is hyperelliptic, then $g = (N-1)/2$ if N is odd, and $g = N/2 - 1$ if N is even.

There is a standard way to represent any sphere with g handles as a $4g$-*gon* in $\mathbb{C}$, such that the interior of the $4g$-*gon* is (simply) connected domain in the $\mathbb{C}$ plane.

Consider a polygon, $\mathcal{P}_{4g}$, with $4g$ sides labeled in counter clockwise direction in the following order

$$a_1, b_1, a_1', b_1', a_2.b_2, a_2', b_2', ..., a_g, b_g, a_g', b_g'$$

Choose orientations of the edges in such a way that the edges a_i' has opposite orientation to a_i and b_i' has opposite orientation to b_i with respect to $\mathcal{P}_{4g}$. The homeomorphism to a sphere with g handles is achieved by identifying the edges a_i with a_i' and b_i with b_i' for $i = 1, ..., g$. On the resulting Riemann surface, the identified edges $a_i \sim a_i'$ and $b_i \sim b_i'$ form closed curves labeled a_i and b_i respectively, for $i = 1, ..., g$.

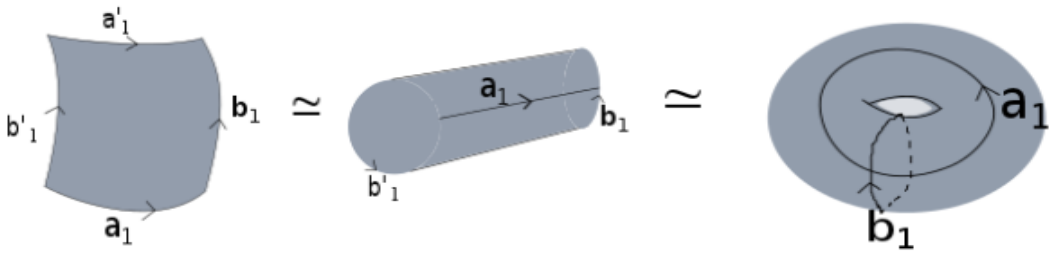

Figure 3.1. *A $g = 1$ Riemann surface obtained from its $\mathcal{P}_4$ representation.*

Any closed curve, γ, on the Riemann surface may be expressed as

$$\gamma = \sum_j (n_j a_j + m_j b_j), \quad n_j, m_j \in \mathbb{Z}\,.$$

These closed curves form the basis of an *abelian group* which we now describe.

A *loop* or closed curve γ on a Riemann surface $\tilde{X}$ is a continuous map $\gamma : [0, 1] \to \tilde{X}$ such that, $\gamma(0) = \gamma(1) = P$, for some $P \in \tilde{X}$. The point P is called the *base*.

Definition 3 3.2.1 *A homotopy of closed curves, γ_0 and γ_1, is a continuos map $\gamma : [0, 1] \times [0, 1] \to \tilde{X}$ such that $\gamma(s, 0) = \gamma_0(s)$, $\gamma(s, 1) = \gamma_1(s)$ and $\gamma(0, t) = \gamma(1, t) = P$. The curves γ_0 and γ_1 are said to be homotopic.*

Two curves can be multiplied if the terminal point of one is the initial point of the other, i.e.

$$\gamma_0 \cdot \gamma_1(t) = \begin{cases} \gamma_0(2t);\ 0 \leq t \leq 1/2 \\ \gamma_1(2t-1);\ 1/2 \leq t \leq 1 \end{cases}$$

if $\gamma_0(1) = \gamma_1(0)$. This concatenation of curves induces a group structure on the homotopy classes of loops based at a point on a Riemann surface. The notions of inverse for curves and identity element are well defined. The inverse of a loop is the curve with opposite orientation; the identity element is the loop which is contractable to a point. The homotopy class of a loop γ is indicated by $\Gamma = [\gamma]$ and the product of two classes is defined as

$$\Gamma_0 \cdot \Gamma_1 = [\gamma_0 \cdot \gamma_1]\,.$$

If P is the terminal and initial point of loops then the homotopy classes of such curves form a group known as the *fundamental group*, $\pi_1(\tilde{X}, P)$. It is easy to show that $\pi_1(\tilde{X}, P)$ is isomorphic to $\pi_1(\tilde{X}, Q)$ for a nearby point Q in $\tilde{X}$. Thus the fundamental group is independent of the base point and may often be denoted by $\pi_1(\tilde{X})$.

The homotopy classes of the curves $a_1, b_1, \cdots, a_g, b_g$ on the Riemann surface labeled $[a_1], [b_1], ..., [a_g], [b_g]$ generate the fundamental group of the Riemann surface. Note that in the $\mathcal{P}_{4g}$ representation of the Riemann surface, it holds that

$$\alpha_1 \cdot b_1 \cdot a_1^{-1} \cdot b_1^{-1} \cdot ... \cdot a_g \cdot b_g \cdot a_g^{-1} \cdot b_g^{-1} = 1. \tag{2.12}$$

We get the *first homology group* by taking the quotient of the fundamental group by the commutative subgroup generated by elements of the form (2.12)

$$H_1(\tilde{X}, \mathbb{Z}) = \frac{\pi_1(\tilde{X}, P)}{[\pi_1(\tilde{X}, \pi_1(\tilde{X})]}. \tag{2.13}$$

This is done to make the fundamental group a commutative group.

Another way to look at the first homology group is to introduce the notions of *chains* and *boundaries*. A chain is a finite formal sum with integer coefficients. On $\tilde{X}$ a *0-chain* is a finite formal sum of points $P = \sum_{P_i \in \tilde{X}} n_i P_i$, and the set of P_i with $n_i \neq 0$ is discrete, and finite since $\tilde{X}$ is compact. Similarly a *1-chain* is a finite formal

sum of curves $\gamma = \sum_i n_i \gamma_i$, and a *2-chain* is of the form $D = \sum_i n_i D_i$ where each D_i is a domain on $\tilde{X}$. The *n-chains* form groups denoted by C_n and a *boundary operator*, ∂_n, is a map that sends a chain from $C_n \to C_{n-1}$. In particular we have that

$$\partial_2 : C_2 \longrightarrow C_1, \qquad \partial_1 : C_1 \longrightarrow C_0$$

and $\partial^2 = 0$. When a closed chain bounds a domain of $\tilde{X}$ it is called a *boundary chain* and they form groups indicated by B_n. In particular, $B_1 \subset C_1$ is the image $\partial_2(C_2(\tilde{X}))$. C_n also contains a subgroup, Z_n, of *∂-closed-n-chains*, i.e.

$$Z_n(\tilde{X}) := \{\gamma \in C_n(\tilde{X}) \ : \partial_n(\gamma) = 0\}.$$

It is clear that $B_n \subset Z_n$ and the group $Z_n(\tilde{X})/B_n(\tilde{X})$ forms the *nth-homology group* $H_n(\tilde{X}, \mathbb{Z})$.

$0 - chains$ have no boundary so $B_0 = \emptyset$. The first homology group is therefore

$$H_1(\tilde{X}, \mathbb{Z}) = \frac{Z_1(\tilde{X})}{B_1(\tilde{X})} = \frac{kernel\, \partial_1 : C_1 \to C_0}{image\, \partial_2(C_2(\tilde{X}))}$$

This view of the first homology group is conceptually easier to understand vis a vis the $\mathcal{P}_4 g$ representation of a hyperelliptic Riemann surface. It is immediately clear that since the cycles $a_1, b_1, ..., a_g, b_g$ do not bound a domain of the hyperelliptic Riemann surface as can be seen in the $\mathcal{P}_4 g$ representation, they are exactly the basis of $H_1(\tilde{X}, \mathbb{Z})$.

The next thing to do naturally is to integrate *n-forms* along n-chains and that is the subject of the next section.

3.2.3 Riemann Period Matrix and Abel-Jacobi Map

We introduce the notion of integration on a hyperelliptic Riemann surface. In particular we are concerned with integrating *Abelian differentials* (*of the first and second kinds*) on chains. This will lead to the definition of the *Abel-Jacobi map* and eventually to the construction of *Riemann period matrix* which is the single most important thing we seek in this chapter.

Functions, Integrals and the Abel-Jacobi Map

The notion of a holomorphic differential is already familiar to us from previous discussions. This notion will now be further extended. An Abelian differential is simply a meromorphic 1-form. There are three kinds of Abelian differentials: An Abelian differential of the first kind is a holomorphic 1- form ω which may be written locally as $f(\lambda)d\lambda$ with $f(\lambda)$ a holomorphic function. An Abelian differential of the second kind is a meromorphic 1-form with its residue vanishing at each of its singular points. An Abelian differential of the third kind is a meromorphic 1-form with general type of singularities; the sum of residues at all its singular points vanishes, however. The notion of multiplicity of an Abelian differential is well defined since it is for a function, f, viewed as a map, F, between a hyperelliptic Riemann surface and the Riemann sphere $\mathbb{P}$. Near, $\lambda \in \tilde{X}$ an Abelian differential ω may be written as

$$\omega(\lambda) = \sum_i c_i(\lambda - \lambda_0)^m d\lambda$$

where m is the multiplicity of ω and its residue is

$$Res_{\lambda_0}(\omega) = c_{-1}.$$

There is a classical theorem due to Riemann on the existence of Abelian differentials for a Riemann surface and it states that the dimension of the space of holomorphic differentials on $\tilde{X}$ is g, the genus of the Riemann surface. We saw in the case of hyperelliptic Riemann surface that the basis of $\Omega^1(\tilde{X})$ is

$$\{...\lambda^{g-j}\frac{d\lambda}{\mu}...\} \qquad j = 1, 2, ..., g.$$

Another important property of Abelian differentials on $\tilde{X}$ is that they are d-closed, i.e. $d\omega = 0$.

This has a significant implication due to the following;

(Poincaré) Lemma 4 3.2.1 *Let ω be a $\mathcal{C}^\infty$ 1-form on a Riemann surface $\tilde{X}$. Suppose that $d\omega = 0$ identically in a neighborhood of a point $x \in \tilde{X}$. Then on some neighborhood U of x there is a $\mathcal{C}^\infty$ function f defined on U with $\omega = df$ on U.*

Thus it is always possible to find a function Ω on $\tilde{X}$ such that

$$\Omega(x) = \int_{x_0}^{x} \omega \tag{2.14}$$

for any point x sufficiently near x_0 on $\tilde{X}$ with $\omega = d\Omega$. The expression (2.14) is known as an *Abelian integral*. The classification scheme for Abelian differentials may also be extended to Abelian integrals: holomorphic $\Omega(x)$ are Abelian integrals of the first kind, meromorphic $\Omega(x)$ are Abelian integrals of the second kind and general $\Omega(x)$ are Abelian integrals of the third kind.

The keen reader may have noticed that the function (2.14) is multivalued due to the dependence of the integral on the path traversed between x_0 and x on an arbitrary Riemann surface $\tilde{X}$. Suppose $\Omega(x)$ represents the integral along the path γ from x_0 to x and $\tilde{\Omega}$ represents the integral along a second path $\tilde{\gamma}$ between x_0 and x. Then the difference between between $\Omega(x)$ and $\tilde{\Omega}(x)$ is the integral along the closed chain $\gamma - \tilde{\gamma}$. This is true for any two paths between any two points on a Riemann surface $\tilde{X}$. The integrals along closed chains solve the multivalueness problem of (2.14).

Consider the space $\Omega^1(\tilde{X})^*$ dual to the space $\Omega^1(\tilde{X})$ which consists of linear functionals $\int_\gamma : \Omega^1(\tilde{X}) \to \mathbb{C}$ where γ is a chain. A linear functional $\int_\gamma$ is said to be a *period* if γ belongs to the first homology group, $H_1(\tilde{X}, \mathbb{Z})$, i.e. γ belongs to a homotopy class, $[\gamma]$ [2]. The set Λ of all periods form a subgroup of $\Omega^1(\tilde{X})^*$ and for any Riemann surface $\tilde{X}$ the *Jacobian of* $\tilde{X}$ is defined as

$$Jac(\tilde{X}) = \frac{\Omega^1(\tilde{X})^*}{\Lambda}.$$

More explicitly, when $\tilde{X}$ is hyperelliptic then the subgroup Λ consists of two types of basis periods, namely the *A-periods* and the *B-periods*

$$A_j = \int_{a_j} d\Omega, \quad B_j = \int_{b_j} d\Omega,\ j = 1, ..., g.$$

And the difference between any two paths between x_0 and x, $\delta\gamma := \gamma - \tilde{\gamma}$, can always be expressed as a chain consisting of *a- and b- cycles*

$$\delta\gamma = \sum_j (m_j a_j + n_j b_j),\ m_j, n_j \in \mathbb{Z},\ j = 1, ..., g.$$

[2]Note that $\int_\gamma = \int_{[\gamma]}$ for any $\gamma \in \tilde{X}$.

This means that any two Abelian integrals with endpoints x_0 and x on $\tilde{X}$ differ by

$$\int_{\delta\gamma} d\Omega = \sum_j (m_j A_j + n_j B_j)\,.$$

So it makes sense to speak of a well defined single valued function Ω on $\tilde{X}$ with the caveat that the value is always modulus periods. For example,

$$\Omega(x_0) = 0 \pmod{\text{period}}.$$

Consider now a map

$$A : \tilde{X} \to Jac(\tilde{X})$$

which maps a 1-form on $\tilde{X}$ to its class in $Jac(\tilde{X})$ and does not depend upon the base point x_0. This map consists of the single valued functions on $\tilde{X}$ and it is known as the *Abel-Jacobi map* of $\tilde{X}$. The functions which will subsequently be dealt with, which will map points from $\tilde{X}$ to $\mathbb{C}$ will be of the Abel-Jacobi type - single valued Abelian integrals.

Riemann Bilinear Relations

In discussing the Abel-Jacobi map, it was necessary to mention the notion of periods. Specifically, the *a-periods* and *b-periods* were shown to form the basis of the space Λ. There exist certain relations among these periods which are important to us. These relations are known as Riemann bilinear relations.

Recall that the function

$$\Omega_\omega(x) = \int_{x_0}^{x} \omega$$

is well defined and single valued on $\tilde{X}$ (mod periods). Given a hyperelliptic Riemann surface $\tilde{X}$, a simply connected *4g-gon* representation denoted here by X_g may be obtained by cutting $\tilde{X}$ along the *a* and *b cycles*. The simply connectedness of X_g implies that $\Omega(x)$ is a single valued function for all paths lying entirely in X_g.

Recall also that the *a-periods* and *b-periods* are given by

$$A_i = \int_{a_i} \omega, \qquad B_i = \int_{b_i} \omega, \qquad i = 1, ..., g\,.$$

Suppose ω and ω' are two $\mathbb{C}^\infty$ 1-forms on $\tilde{X}$, then the first of the Riemann bilinear relations is that

$$\int_{X_g} \omega \wedge \omega' = \sum_{j=1}^{g} (A_j B'_j - A'_j B_j)\,. \tag{2.15}$$

To see this, one needs to use Stoke's theorem as follows:

$$\begin{aligned} \int_{X_g} \omega \wedge \omega' &= \int_{X_g} (d\Omega_\omega \wedge \omega' + \Omega_\omega\, d\omega') \quad \text{since } d\omega' = 0 \\ &= \int_{X_g} d(\Omega_\omega\, \omega') \\ &= \int_{\partial X_g} \Omega_\omega \omega' \quad \text{by Stoke's theorem}\,. \end{aligned} \tag{2.16}$$

Note that, X_g, is a 2-chain with its boundary chain ∂X_g given by

$$\partial X_g = \sum_{j=1}^{g} (a_j + b_j + a_j^{-1} + b_j^{-1})\,.$$

To continue it is important to note further that if a point p_i lies on a_i then there is a corresponding point p'_i on a_i^{-1} which is identified to a_i on $\tilde{X}$. Then

$$\Omega_\omega(p_i) - \Omega_\omega(p'_i) = \int_{x_0}^{p_i} \omega - \int_{x_0}^{p'_i} \omega = \int_{p'_i}^{p_i} \omega = -B_i\,.$$

The last integral is along a path which when viewed on $\tilde{X}$ is homologous, up to opposite orientation, to the basic cycle b_i . Hence the last equality. Similarly, if q_i is a point lying on b_i and its corresponding point q'_i on b_i^{-1}, then

$$\Omega_\omega(q_i) - \Omega_\omega(q'_i) = \int_{x_0}^{q_i} \omega - \int_{x_0}^{q'_i} \omega = \int_{q'_i}^{q_i} \omega = A_i\,.$$

We are now prepare to pick up from (2.16);

$$\begin{aligned} \int_{\partial X_g} \Omega_\omega\, d\omega' &= \sum_{i=1}^{g} \Big(\int_{a_i} + \int_{b_i} - \int_{a_i^{-1}} - \int_{b_i^{-1}} \Big) \Omega_\omega\, d\omega' \\ &= \sum_{i=1}^{g} \int_{p \in a_i} \big(\Omega_\omega(p) - \Omega_\omega(p')\big)\, \omega' \\ &+ \sum_{i=1}^{g} \int_{q \in b_i} \big(\Omega_\omega(q) - \Omega_\omega(q')\big)\, \omega' \\ &= \sum_{i=1}^{g} \big(- B_i\, A'_i + A_i\, B'_i \big)\,. \end{aligned} \tag{2.17}$$

This completes the proof of (2.15).

Also, it can be shown that if ω is a nonzero Abelian differential of the first kind, then

$$Im \sum_{i=1}^{g} A_i(\omega)\, \overline{B_i(\omega)} < 0\,, \tag{2.18}$$

and this is the second of Riemann bilinear relations. The proof of this follows closely that of (2.15). But first it is convenient to write ω in a local coordinate as $\omega = f(z)dz$, and consequently $\overline{\omega} = f(\bar{z})d\bar{z}$. With $z = x + iy$, then $\omega \wedge \omega' = -2i|f|^2 dx \wedge dy$. This implies

$$\begin{aligned} 0 \;&>\; Im \int_{X_g} \omega \wedge \overline{\omega} \\ &=\; Im \sum_{i=1}^{g} \big(A_i(\omega)\, B_i(\overline{\omega}) - A_i(\overline{\omega})\, B_i(\omega) \big) \;\; by \;\; (2.15) \\ &=\; Im \sum_{i=1}^{g} \big(A_i(\omega)\, \overline{B_i(\omega)} - \overline{A_i(\omega)}\, B_i(\omega) \big) \\ &=\; 2\; Im \sum_{i=1}^{g} \big(A_i(\omega)\, \overline{B_i(\omega)} \big)\,, \end{aligned} \tag{2.19}$$

and (2.18) is proved. As a corollary of (2.18), *it holds that there can be no nonzero Abelian differential of the first kind* ω *which has all of its* a-periods *and* b-periods *both entirely real or entirely imaginary, and if for any such* ω *its* $A_i(\omega) = 0$ *(or* $B_i(\omega) = 0$*),* $\forall\, i$*, then it must be that* $\omega = 0$.

Recall that the basis of the space of Abelian differential of the first kind on a hyperelliptic Riemann surface $H^0(\tilde{X},\, \Omega^1(\tilde{X}))$ is written as

$$\{..., \lambda^{g-i} \frac{d\lambda}{\mu}, ...\}\,, \quad i = 1, ..., g\,. \tag{2.20}$$

Recall also that a canonical basis of the first homology group of $\tilde{X}$, $H_1(\tilde{X},\, \mathbb{Z})$, consists of the *a- and b-periods*.

There can be two nonsingular matrices $\mathbf{A}$ and $\mathbf{B}$ defined for Abelian differentials of the first kind ω_i on a hyperelliptic Riemann surface with entries given by

$$A_{i\,j} = \int_{a_j} \omega_i\,, \quad B_{i\,j} = \int_{b_i} \omega_j\,, \quad i, j = 1, ..., g\,, \tag{2.21}$$

and these are known as the period matrices for $\tilde{X}$. The non-singularity is a consequence of the previous argument that if $\forall\, i$, $A_i(\omega) = 0$ or $B_i(\omega) = 0$, then $\omega = 0$.

The first of two important relations satisfied by these matrices is the symmetry relation

$$\mathbf{A^T\,B = B^T\,A}\,. \tag{2.22}$$

This equation follows immediately from the first of Riemann bilinear relations (2.15) as follows; fix two indexes, $i\,, j$, and compute

$$\begin{aligned} 0 &= \int_{X_g} \omega_i \wedge \omega_j\,, \quad \text{both } \omega_i \text{ and } \omega_j \text{ are holomorphic 1-forms} \\ &= \sum_{k=1}^{g} (A_k(\omega_i)B_k(\omega_j) - A_k(\omega_j)B_k(\omega_i))\,, \end{aligned}$$

which means

$$\sum_{k=1}^{g} (A_k(\omega_i)B_k(\omega_j)) = \sum_{k=1}^{g} A_k(\omega_j)B_k(\omega_i))\,. \tag{2.23}$$

Since this is true for all i, j pair, (2.22) is proved. It is therefore no surprise that (2.22) is also known as the first of Riemann bilinear relations in some literature.

It is possible to normalize the basis $\{\omega_i\}$ of $H^0(\tilde{X}, \Omega^1(\tilde{X}))$ to a new basis $\{\tilde{\omega}_i\}$ so that

$$\int_{a_i} \tilde{\omega}_j = \delta_{i\,j}\,, \quad i,j = 1, ..., g\,, \tag{2.24}$$

in which case we have

$$\tilde{\omega}_j = \sum_{k=1}^{g} c_{j\,k}\,\omega_k = \sum_{k=1}^{g} c_{j\,k} \frac{\lambda^{g-k}}{\mu} d\lambda\,, j = 1, .., g\,,$$

and

$$c_{i\,j} = (\mathbf{A}^{-1})_{i\,j}\,,$$

with the $\mathbf{A}$ and $\mathbf{B}$ matrices given by

$$A_{i\,j} = \int_{a_j} \tilde{\omega}_i\,, \quad B_{i\,j} = \int_{b_i} \tilde{\omega}_j\,, \quad i\,, j = 1, ..., g\,. \tag{2.25}$$

In this normalized basis $\{\tilde{\omega}_i\}$ the $\mathbf{B}$ matrix is said to be the normalized period matrix of $\tilde{X}$. Note that in this basis $A = \mathcal{I}$ is the $g \times g$ unit matrix. Using this in (2.22)

reveals that the normalized period matrix $\mathbf{B}$ is symmetric. This brings us to a very important point [17]:

Lemma 5 3.2.1 *With respect to the normalized basis $\{\tilde{\omega}_i\}$, the Riemann period matrix $\mathbf{B}$ is symmetric and the imaginary part is positive definite.*

Proof The symmetry part has been shown above it remains to show the positive definiteness. Write $\omega = \sum_j c_j \tilde{\omega}_j$, $c_j \in \mathbb{R}\,, \forall\, j$. Recall from (2.18) that

$$Im \sum_{i=1}^{g} A_i(\omega)\, \overline{B_i(\omega)} < 0\,,$$

Since by (2.24) we have $A_i(\omega_j) = c_i$, the inequality above becomes

$$Im \sum_{i\,,j}^{g} c_i c_j \overline{B_i(\omega_j)} < 0\,.$$

Considering each c_i as a component of a $g-tuple$ real number, $\mathbf{c}$, the last expression becomes

$$Im(\mathbf{c^T}\, \overline{\mathbf{B}}\, \mathbf{c}) < 0\,.$$

Thus,

$$Im(\mathbf{c^T}\, \mathbf{B}\, \mathbf{c}) > 0\,,$$

which implies that $Im(\mathbf{B}) > 0$. ■

The inequality $Im(\mathbf{B}) > 0$ is known as the second Riemann bilinear relations, and the connection to (2.18) is clear.

3.3 Riemann Theta Functions Associated to a Hyperelliptic Riemann Surface

There is a vast existent literature on Riemann theta functions [9,10,16–19]. In this section we review the minimal knowledge necessary for our purpose. We hope that the ardent reader who may wish to explore more of the subject may find the references we have listed to be useful, perhaps as they were to us. Most of the mathematical

foundation has already been laid in the previous sections of this chapter. Now we introduce the theory of Riemann theta functions and segue in to the previously established concept of a hyperelliptic Riemann surface.

Consider a hyperelliptic Riemann surface , $\tilde{X}$, of topological genus g having fundamental basis cycles $\{a_i, b_i\}, i = 1, \ldots, g$. In general the a_i intersect with the b_i but not with themselves. Whenever an *a-cycle* intersects a *b-cycle* at a point it is always possible to consider the cycles as intersecting at right angles at that point. This is because we are free if necessary to replace a cycle by any member of its homology class that meets the other cycle involved in a right angle at the said point. If a point x_0 is a point of intersection of two cycles, say a_1 and b_2, then the intersection of the cycles is written as $(a_1 \circ b_2)_{x_0}$. There are a possible of two values, ± 1, assigned to an intersection. The value is determined by applying the so called *right-hand-rule* to the tangents to the curves at the point x_0. For instance, if $a_1'(x_0)$ **cross** $b_2'(x_0)$ points out of the page then the value is $+1$ otherwise -1. The value of zero is assigned if the curves do not intersect at the point, for example $(a_i \circ a_j)_{x_0} = 0,\ \forall\, i \neq j, \forall\, x_0 \in \tilde{X}$. This is because the set of intersection points of a_i and a_j, $\forall\, i \neq j$ is empty. The *intersection number* for any two curves a_i, b_j is the integer

$$(a_i \circ b_j) = \sum_{x_0 \in a_i \cap b_j} (a_i \circ b_j)_{x_0}$$

From what has been said the following can be deduced.

Theorem 1 3.3.1 *The intersection number is a skew-symmetric bilinear map*

$$\circ : H_1(\tilde{X}, \mathbb{Z}) \times H_1(\tilde{X}, \mathbb{Z}) \to \mathbb{Z}\,.$$

In the rest of this work we will adopt the basis where

$$(a_i \circ a_j)_x = 0 = (b_i \circ b_j)_x, \quad \forall\, x \in \tilde{X}, \tag{3.26}$$

and

$$(a_i \circ b_j) = \delta_{ij}\,. \tag{3.27}$$

The hyperelliptic Riemann surface is the hyperelliptic curve defined by the function

$$\mu^2(\lambda) = \lambda \prod_{j=1}^{2g} (\lambda - \lambda_j). \tag{3.28}$$

The projection map from $\tilde{X}$ to the Riemann sphere $\mathbb{P}$ has branch points at $0, \infty$, and λ_j.

Consider now $\omega_{i=1\ldots g}$ to be the unique basis of Abelian differentials of the first kind satisfying $\oint_{a_i} \omega_j = \delta_{ij}$, and define the $g \times g$ period matrix as [3]

$$\Omega_{ij} = \oint_{b_i} \omega_j. \tag{3.29}$$

With this choice of basis for the space of holomorphic differentials $\Omega^1(\tilde{X})$ on $\tilde{X}$, it is a fundamental result in the theory of algebraic curves, which we have shown (see *Lemma 5 (3.2.1)*), that the matrix $\mathbf{\Omega}$ is symmetric with positive definite imaginary part. In other words,

$$\mathbf{\Omega} \in \mathcal{H}_g \tag{3.30}$$

where $\mathcal{H}_g$ is the *Siegel upper half space*. The Siegel upper half space is the space of symmetric $g \times g$ matrices with positive definite imaginary part;

$$\mathcal{H}_g = \{\mathbf{\Omega} \in M_{g\times g}(\mathbb{C}) |\, \mathbf{\Omega} = \mathbf{\Omega}^T,\, Im\, \mathbf{\Omega} > 0\}\,. \tag{3.31}$$

Not all matrices belonging to $\mathcal{H}_g$ are those which come from a hyperelliptic Riemann surface. In fact the problem of characterizing all $\mathbf{\Omega} \in \mathcal{H}_g$ which come from a Riemann surface is the exact essence of the Schottky problem. Counting dimensions reveals that the moduli space of hyperelliptic Riemann surfaces has dimension $3g - 3$ for $g > 1$, and that of H_g is $g(g+1)/2$, which indicates a discrepancy when $g \geq 4$.

[3] Sorry for the change of notation from B to Ω. This should not be a source of confusion for the attentive reader.

Definition 4 3.3.1 *Given an* $\mathbf{\Omega}$ *which is the period matrix of a hyperelliptic Riemann surface*$\tilde{X}$*, then the Riemann theta functionassociated to* $\tilde{X}$ *is*

$$\theta(\zeta) := \sum_{n\in\mathbb{Z}^g} e^{\pi i(n\cdot\mathbf{\Omega}\cdot n+2\,n\cdot\zeta)}\,. \tag{3.32}$$

The arguments of the θ *function are* $\zeta = \mathbf{U}z + i\,\bar{z}\mathbf{V}$*, a column vector in* $\mathbb{C}^g$*, and the period matrix* $\mathbf{\Omega}$ *(which we consider fixed and therefore do not explicitly write as an argument). The sum is over all* $n \in \mathbb{Z}^g$*, that is all ordered g-vectors with integer components.*[4]

A brief remark on the quantities $\mathbf{U}$ and $\mathbf{V}$ is in order. Consider the curve $\nu = \sqrt{\lambda}$ which defines a Riemann surface $\widetilde{W}$ realized by gluing two copies of the complex plane with branch cuts $[0,\infty)$. $\widetilde{W}$ is an unramified covering of W defined by

$$W = \{(\nu,\lambda) \in \mathbb{C}^2 \,|\, \nu^2 = \lambda\}\,. \tag{3.33}$$

Then the quantities $\mathbf{U}$ and $\mathbf{V}$ are given by

$$U_k = \oint_{b_k} d\Omega_\infty\,, \quad V_k = \oint_{b_k} d\Omega_0\,, \quad k = 1,\cdots,g\,, \tag{3.34}$$

where

$$\Omega_{\infty,0} = \int_\infty^\lambda d\Omega_{\infty,0}\,, \tag{3.35}$$

are Abelian differentials of the second kind. Furthermore, the asymptotic behavior of these quantities are described by

$$\lambda \to \infty\,, \quad d\Omega_\infty \to d\nu \tag{3.36}$$

and

$$\lambda \to 0\,, \quad d\Omega_0 \to -\frac{d\nu}{\nu^2}\,. \tag{3.37}$$

[4]All vectors *e.g.* n, and ζ are taken to be column vectors (and therefore their transposes n^t, ζ^t are row vectors).

They are also constrained by

$$\oint_{a_j} d\Omega_{\infty,0} = 0\,, \quad j = 1, \cdots, g\,. \tag{3.38}$$

It is common in the literature to find a notation in which $\mathbf{\Omega}$ explicitly appears in the parenthesis as in $\theta(\zeta; \mathbf{\Omega})$; we will not follow such notation here. The only instances when $\mathbf{\Omega}$ is written in the parenthesis is when it is being added to the vector ζ for example as in $\zeta + \mathbf{\Omega} \cdot \alpha$ where α is a column vector. Also we will write $\mathbf{\Omega}_{\alpha',\beta'}$ to denote the quantity $\alpha' + \mathbf{\Omega} \cdot \beta'$ which is a column vector with entries $\alpha'_1 + \mathbf{\Omega}_{i,1}\beta'_1 + \cdots + \alpha'_g + \mathbf{\Omega}_{i,g}\beta'_g\ ,\ i = 1, \cdots, g$.

There is a slightly more general form of Riemann theta function known as Riemann theta function with *characteristic*. The characteristic is written as a column vector of two row g-vectors

$$\begin{bmatrix} \alpha \\ \beta \end{bmatrix} = \begin{bmatrix} (\alpha_1, \cdots, \alpha_g) \\ (\beta_1, \cdots, \beta_g) \end{bmatrix}\,,$$

and the Riemann theta function with characteristic is defined as

$$\theta \begin{bmatrix} \alpha \\ \beta \end{bmatrix} (\zeta) := \theta(\zeta; \beta, \alpha) := \sum_{n \in \mathbb{Z}^g} e^{\pi i[(n+\alpha)\cdot\mathbf{\Omega}\cdot(n+\alpha) + 2\,(\zeta+\beta)\cdot(n+\alpha)]}\,, \tag{3.39}$$

where $\alpha, \beta \in \mathbb{Z}^g$.

Theta functions exhibit quasi-periodicity in the sense that

$$\theta(\zeta + \alpha' + \mathbf{\Omega} \cdot \beta') =: \theta(\zeta + \mathbf{\Omega}_{\alpha',\beta'}) = e^{-i\pi(\beta'\cdot\mathbf{\Omega}\cdot\beta' + 2\,\beta'\cdot\zeta)}\,\theta(\zeta)\,. \tag{3.40}$$

Thus a theta function is not affected by adding the integer vector α' to its argument. (3.40) is derived by a direct computation as follows;

$$\begin{aligned}
\theta(\zeta+\mathbf{\Omega}_{\alpha',\beta'}) &= \sum_{n\in\mathbb{Z}^g} e^{i\pi(n\cdot\mathbf{\Omega}\cdot n+2\,n\cdot(\zeta+\alpha'+\mathbf{\Omega}\cdot\beta'))} \\
&= \sum_{n\in\mathbb{Z}^g} e^{i\pi((n+\beta')\cdot\mathbf{\Omega}\cdot(n+\beta')-2\,n\cdot\mathbf{\Omega}\cdot\beta'-\beta'\cdot\mathbf{\Omega}\cdot\beta'+2\,n\cdot(\zeta+\alpha'+\mathbf{\Omega}\cdot\beta'))} \\
&= \sum_{n\in\mathbb{Z}^g} e^{-i\pi\beta'\cdot\mathbf{\Omega}\cdot\beta'} e^{i\pi((n+\beta')\cdot\mathbf{\Omega}\cdot(n+\beta')+2\,(n+\beta')\cdot(\zeta+\alpha')-2\,\beta'\cdot\zeta-2\,\beta'\cdot\alpha')} \\
&= \sum_{n\in\mathbb{Z}^g} e^{-i\pi(\beta'\cdot\mathbf{\Omega}\cdot\beta'+2\,\beta'\cdot\zeta+2\,\beta'\cdot\alpha')} e^{i\pi((n+\beta')\cdot\mathbf{\Omega}\cdot(n+\beta')+2\,(n+\beta')\cdot(\zeta+\alpha'))} \\
&= e^{-i\pi(\beta'\cdot\mathbf{\Omega}\cdot\beta'+2\,\beta'\cdot\zeta)} \sum_{l\in\mathbb{Z}^g} e^{i\pi(l\cdot\mathbf{\Omega}\cdot l+2\,l\cdot\zeta)}\,.
\end{aligned} \tag{3.41}$$

In the last equality we substituted the sum over n for a sum over $l=n+\beta'$ which is valid since the original sum is infinite over the integer lattice. We also used that $e^{i2\pi m\,n}=1$ for $m\,,n\in\mathbb{Z}^g$.

By similar trick it can be shown that

$$\theta(\zeta+\mathbf{\Omega}_{\alpha',\beta'};\beta,\alpha) =: \theta\begin{bmatrix}\alpha\\ \beta\end{bmatrix}(\zeta+\mathbf{\Omega}_{\alpha',\beta'}) = e^{-i\pi(\beta'\cdot\mathbf{\Omega}\cdot\beta'+2\,\beta'\cdot(\zeta+\beta)}\,\theta\begin{bmatrix}\alpha\\ \beta\end{bmatrix}(\zeta)\,. \tag{3.42}$$

Note that the theta function in (3.32) is just a special form of (3.39) with trivial characteristic, i.e. $\alpha=\beta=0$.

Theta functions that are associated with hyperelliptic Riemann surfaces frequently have one half integer characteristic so it is useful to direct our focus to that case.

Base on what has been said so far we are now in a position to derive few identities which rely entirely upon the definitions given in both (3.32) and (3.39). It is important to know when a Theta function is odd or even and for this we have

$$\theta\big(-\zeta,\frac{1}{2}\beta,\frac{1}{2}\alpha\big) = e^{i\pi\beta\cdot\alpha}\,\theta\big(\zeta,\frac{1}{2}\beta,\frac{1}{2}\alpha\big)\,. \tag{3.43}$$

This implies that the evenness or oddness of a theta function having one half multiples of integer characteristic $\frac{1}{2}\left[\begin{smallmatrix}\alpha\\ \beta\end{smallmatrix}\right]$ depends on whether the quantity $\beta\cdot\alpha$ is even or odd, respectively. A characteristic $\frac{1}{2}\left[\begin{smallmatrix}\alpha\\ \beta\end{smallmatrix}\right]$ is said to be even (odd) if the quantity $\beta\cdot\alpha$ is even (odd). In particular, for $g=3$ the odd characteristic $\frac{1}{2}\left[\begin{smallmatrix}\Delta_1\\ \Delta_2\end{smallmatrix}\right]$ where $\Delta_1=(0,0,1)$ and $\Delta_2=(1,1,1)$ plays a crucial role in this work. And the theta function associated to it will be denoted by $\hat{\theta}(\zeta):=\theta(\zeta;\frac{1}{2}\Delta_2,\frac{1}{2}\Delta_1)$ for the sake of brevity. As a consequence of (3.43) we have

$$\hat{\theta}(-\zeta)=-\hat{\theta}(\zeta)\ , \tag{3.44}$$

and this implies

$$\hat{\theta}(0)=0\,, \tag{3.45}$$

which, as will be shown later, further implies that

$$\theta\Big(\frac{1}{2}\,\mathbf{\Omega_{\Delta_2,\Delta_1}}\Big)=\theta\left(\frac{1}{2}\Delta_2+\frac{1}{2}\,\mathbf{\Omega}\cdot\Delta_1\right)=0\ . \tag{3.46}$$

Quantities such as $\frac{1}{2}\mathbf{\Omega_{\Delta_2,\Delta_1}}$ for which $\theta(\frac{1}{2}\mathbf{\Omega_{\Delta_2,\Delta_1}})=0$ are known as *half periods* of a theta function.

Returning to the identity in (3.43), we can deduce it by a similar trick already used. By replacing ζ by $-\zeta$, and taking care to include the one half in (3.39);

$$\theta(-\zeta;\frac{1}{2}\beta,\frac{1}{2}\alpha) \;=\; \sum_{n\in\mathbb{Z}^g}\exp i\pi\Big[(n+\frac{1}{2}\alpha)^2\mathbf{\Omega}-2\,\zeta(n+\frac{1}{2}\alpha)+\beta(n+\frac{1}{2}\alpha)\Big]\ ,$$

with the understanding that quantities like $n\cdot\mathbf{\Omega}\cdot n=n^2\mathbf{\Omega}$. Then

$$\begin{aligned} rhs &= \sum_{n\in\mathbb{Z}^g}\exp i\pi\Big[(-n-\alpha+\frac{1}{2}\alpha)^2\mathbf{\Omega}+2\,\zeta(-n-\alpha+\frac{1}{2}\alpha)+\beta(-n-\alpha+\frac{1}{2}\alpha)+2\,\beta n+\beta\alpha\Big]\\ &= e^{i\pi\beta\alpha}\sum_{n\in\mathbb{Z}^g}\exp i\pi\Big[(-n-\alpha+\frac{1}{2}\alpha)^2\mathbf{\Omega}+2\,\zeta(-n-\alpha+\frac{1}{2}\alpha)+\beta(-n-\alpha+\frac{1}{2}\alpha)\Big]\ . \end{aligned}$$

Setting $m = -n - \alpha$;

$$\begin{aligned} rhs &= e^{i\pi\beta\alpha} \sum_{m\in\mathbb{Z}^g} \exp i\pi\Big[(m+\frac{1}{2}\alpha)^2\mathbf{\Omega} + 2\,\zeta(m+\frac{1}{2}\alpha) + \beta(m+\frac{1}{2}\alpha)\Big] \\ &= e^{i\pi\beta\alpha}\,\theta(\zeta;\frac{1}{2}\beta,\frac{1}{2}\alpha), \end{aligned}$$

as was to be shown.

The next one is quite general;

$$\begin{aligned} \theta(\zeta+\mathbf{\Omega}_{m,m'};\frac{1}{2}\beta,\frac{1}{2}\alpha) &= \exp i\pi\Big[-2\,m'(\zeta+\frac{1}{2}\mathbf{\Omega}m') + (m\alpha - m'\beta)\Big] \\ &\times\ \theta(\zeta:\frac{1}{2}\beta,\frac{1}{2}\alpha)\,. \end{aligned} \tag{3.47}$$

By definition

$$\begin{aligned} lhs &= \sum_{n\in\mathbb{Z}^g} \exp i\pi\Big[(n+\frac{1}{2}\alpha)^2\mathbf{\Omega} + 2\,(\zeta+m+\mathbf{\Omega}\,m')(n+\frac{1}{2}\alpha) + \beta(n+\frac{1}{2}\alpha)\Big] \\ &= \sum_{n\in\mathbb{Z}^g} \exp i\pi\Big[(n+\frac{1}{2}\alpha)^2\mathbf{\Omega} + 2\,\zeta(n+\frac{1}{2}\alpha) + \beta(n+\frac{1}{2}\alpha)\Big] \\ &\times\ \exp\left[2\,m\,n + m\,\alpha + 2\mathbf{\Omega}\,m'\,n + \mathbf{\Omega}\,m'\,\alpha\right] \\ &= \sum_{n\in\mathbb{Z}^g} \exp i\pi\Big[(n+m'+\frac{1}{2}\alpha)^2\mathbf{\Omega} + 2\,\zeta(n+m'+\frac{1}{2}\alpha) + \beta(n+m'+\frac{1}{2}\alpha)\Big] \\ &\times\ \exp i\pi\big[2\,m\,n + m\,\alpha + 2\mathbf{\Omega}\,m'\,n + \mathbf{\Omega}\,m'\,\alpha - \mathbf{\Omega}(m'^2 + 2\,n\,m' + m'\,\alpha) - 2\zeta\,m' - \beta\,m'\big] \\ &= \exp i\pi\Big[-2\,m'(\zeta+\frac{1}{2}\mathbf{\Omega}\,m') + (m\,\alpha - m'\,\beta)\Big] \\ &\times\ \sum_{n\in\mathbb{Z}^g} \exp i\pi\Big[(n+m'+\frac{1}{2}\alpha)^2\,\mathbf{\Omega} + 2\,\zeta(n+m'+\frac{1}{2}\alpha) + \beta(n+m'+\frac{1}{2}\alpha)\Big]\,. \end{aligned}$$

Setting $l = n + m'$ and summing over l gives (3.47).

The next one which is

$$\begin{aligned} \theta(\zeta+\frac{1}{2}\mathbf{\Omega}_{\beta',\alpha'};\frac{1}{2}\beta,\frac{1}{2}\alpha) &= e^{-i\pi\alpha'(\zeta+\frac{1}{2}\beta+\frac{1}{2}\beta'+\frac{1}{4}\mathbf{\Omega}\,\alpha')} \\ &\times\ \theta(\zeta;\frac{1}{2}\beta+\frac{1}{2}\beta',\frac{1}{2}\alpha+\frac{1}{2}\alpha') \end{aligned} \tag{3.48}$$

looks very similar to (3.47) and one may, by replacing m by $\frac{1}{2}\beta'$ and m' by $\frac{1}{2}\alpha'$ in the latter and keenly following the above proof for (3.47), arrive at (3.48). A much easier alternative way is to do the substitutions in the last line of the above proof for (3.47). One must be careful though, because by naively substituting quantities in (3.47) reveals that only the exponential prefactors will agree on the right hand sides of both identities, the theta functions do not match, however.

A corollary of (3.48) is that

$$\theta(\zeta - \frac{1}{2}\mathbf{\Omega}_{\beta,\alpha}; \frac{1}{2}\beta, \frac{1}{2}\alpha) \;=\; e^{i\pi\alpha(\zeta - \frac{1}{4}\mathbf{\Omega}\,\alpha)}\,\theta(\zeta)\,. \qquad (3.49)$$

This can be seen by substituting $\alpha' = -\alpha$, and $\beta' = -\beta$.

The next identity is of paramount importance;

$$\theta(\zeta; \frac{1}{2}\beta, \frac{1}{2}\alpha) \;=\; e^{i\pi\alpha(\zeta + \frac{1}{2}\beta + \frac{1}{4}\mathbf{\Omega}\,\alpha)}\,\theta(\zeta + \frac{1}{2}\mathbf{\Omega}_{\beta,\alpha})\,, \quad (3.50)$$

in the sense that it gives a relationship between a theta function with one half integer characteristic to theta function with zero characteristic. It is obtained from (3.48) by setting $\alpha = \beta = 0$. It also shows that for $g = 3, \beta = \Delta_2, \text{and}\, \alpha = \Delta_1$, (3.46) holds as was promised.

Finally we have

$$\theta(\zeta; \frac{1}{2}\beta + m, \frac{1}{2}\alpha + m') \;=\; e^{i\pi m\,\alpha}\,\theta(\zeta; \frac{1}{2}\beta, \frac{1}{2}\alpha)\,, \quad (3.51)$$

and its derivation is trivial by now.

3.4 Fay's Trisecant Identity

Perhaps the most important identity among the theta functions and certainly the most important one in this paper is Fay's trisecant identity:

$$\begin{aligned}\theta(\zeta)\,\theta\left(\zeta+\int_{p_2}^{p_1}\omega+\int_{p_3}^{p_4}\omega\right) &= \gamma_{1234}\,\theta\Big(\zeta+\int_{p_2}^{p_1}\omega\Big)\,\theta\Big(\zeta+\int_{p_3}^{p_4}\omega\Big)\\ &+ \gamma_{1324}\,\theta\Big(\zeta+\int_{p_3}^{p_1}\omega\Big)\,\theta\Big(\zeta+\int_{p_2}^{p_4}\omega\Big)\ ,\end{aligned} \tag{4.52}$$

with

$$\gamma_{ijkl}=\frac{\theta(a+\int_{p_k}^{p_i}\omega)\,\theta(a+\int_{p_l}^{p_j}\omega)}{\theta(a+\int_{p_l}^{p_i}\omega)\,\theta(a+\int_{p_k}^{p_j}\omega)}. \tag{4.53}$$

In these formulas p_j are points on the Riemann surface, and a is a non-singular zero of the Riemann theta function, *i.e.* at a the function is zero but not its gradient. In particular cases, for example in genus three $a=\frac{1}{2}\Delta_2+\frac{1}{2}\Omega\Delta_1$ is a zero as noticed from (3.49). Also notice that the contour integral $\int_{p_a}^{p_b}\omega_j$ defines a vector which from now on, following standard convention, will be abbreviated as

$$\int_{p_a}^{p_b}\omega_j\to\int_{p_a}^{p_b}. \tag{4.54}$$

The function γ may be viewed as a generalization of the cross-ratio function on $\mathbb{CP}^1$ to functions on Riemann surfaces. Some immediate properties of this function are:

$$\gamma_{1233}\ =\ \gamma_{1134}\ =\ 1,\quad \gamma_{2134}\ =\ \gamma_{1234}^{-1},\quad \gamma_{1214}=0=\gamma_{1232}. \tag{4.55}$$

There is also another important property of Riemann theta functions which comes handy in many places in the course of our work. We derived this property from the

Fay's trisecant identity. The property is that suppose ζ' is a zero of the Riemann theta function, i.e. $\hat{\theta}(\zeta') = 0$, then

$$\hat{\theta}\left(\zeta' - \int_1^4\right)\,\theta\left(\zeta' + \int_1^4\right) + \hat{\theta}\left(\zeta' + \int_1^4\right)\,\theta\left(\zeta' - \int_1^4\right) = 0\,. \tag{4.56}$$

A notation has been adopted where each point p_i has been set to i and the Abelian differential in the integrals has been dropped for brevity. To show (4.56), we begin by explicitly rewriting the Fay's trisecant identity

$$\begin{aligned}\theta(\zeta)\,\theta\left(\zeta + \int_2^1 + \int_3^4\right) &= \frac{\theta\left(a+\int_3^1\right)\theta\left(a+\int_4^2\right)}{\theta\left(a+\int_4^1\right)\theta\left(a+\int_3^2\right)}\,\theta\left(\zeta+\int_2^1\right)\,\theta\left(\zeta+\int_3^4\right)\\ &+ \frac{\theta\left(a+\int_2^1\right)\theta\left(a+\int_4^3\right)}{\theta\left(a+\int_4^1\right)\theta\left(a+\int_2^3\right)}\,\theta\left(\zeta+\int_3^1\right)\,\theta\left(\zeta+\int_2^4\right)\end{aligned}$$

Since the four points $\{1,2,3,4\}$ are distinct arbitrary points on the Riemann surface we are free to rearrange them as follows; $2 \to 1$, $1 \to 4$, $4 \to \tilde{4}$. The point $\tilde{4}$ lying on the lower sheet of the hyperelliptic Riemann surface is the point corresponding to 4 which lies on the upper sheet.

$$\begin{aligned}\theta(\zeta)\,\theta\left(\zeta + \int_1^4 + \int_3^{\tilde{4}}\right) &= \frac{\theta\left(a+\int_3^4\right)\theta\left(a+\int_{\tilde{4}}^1\right)}{\theta\left(a+\int_{\tilde{4}}^4\right)\theta\left(a+\int_3^1\right)}\,\theta\left(\zeta+\int_1^4\right)\,\theta\left(\zeta+\int_3^{\tilde{4}}\right)\\ &+ \frac{\theta\left(a+\int_1^4\right)\theta\left(a+\int_{\tilde{4}}^3\right)}{\theta\left(a+\int_{\tilde{4}}^4\right)\theta\left(a+\int_1^3\right)}\,\theta\left(\zeta+\int_3^4\right)\,\theta\left(\zeta+\int_1^{\tilde{4}}\right)\end{aligned}$$

Note that the integral $\int_1^{\tilde{4}}$ is equal to $-\int_1^4$ and the point 1 will be chosen as the base point for all integrals, i.e. an integral $\int_i^j, i, j \neq 1$ should be understood as $\int_i^1 + \int_1^j$. This means we can rewrite the above identity as

$$\begin{aligned}\theta(\zeta)\,\theta\left(\zeta + \int_1^4 + \int_1^{\tilde{4}} - \int_1^3\right) &= \frac{\theta\left(a+\int_1^4-\int_1^3\right)\theta\left(a+\int_1^4\right)}{\theta\left(a+2\int_1^4\right)\theta\left(a-\int_1^3\right)}\,\theta\left(\zeta+\int_1^4\right)\,\theta\left(\zeta-\int_1^4-\int_1^3\right)\\ &+ \frac{\theta\left(a+\int_1^4\right)\theta\left(a+\int_1^4+\int_1^3\right)}{\theta\left(a+2\int_1^4\right)\theta\left(a+\int_1^3\right)}\,\theta\left(\zeta+\int_1^4-\int_1^3\right)\,\theta\left(\zeta-\int_1^4\right)\end{aligned}$$

Using the relationships among θ and $\hat{\theta}$ given in (3.49) we have

$$\begin{aligned}\theta(\zeta)\,\hat{\theta}(\zeta)e^{i\pi\Delta_1\cdot(\zeta-\frac{1}{2}\Delta_2-\frac{1}{4}\Omega\cdot\Delta_1)} &= \frac{\theta\Big(a+\int_1^4-\int_1^3\Big)\,\theta\Big(a+\int_1^4\Big)}{\theta\Big(a+2\int_1^4\Big)\,\theta\Big(a-\int_1^3\Big)} \\ &\times\ \theta\left(\zeta+\int_1^4\right)\,\hat{\theta}\left(\zeta-\int_1^4\right)\,e^{i\pi\Delta_1\cdot(\zeta-\int_1^4-\frac{1}{2}\Delta_2-\frac{1}{4}\Omega\cdot\Delta_1)} \\ &+\ \frac{\theta\Big(a+\int_1^4\Big)\,\theta\Big(a+\int_1^4+\int_1^3\Big)}{\theta\Big(a+2\int_1^4\Big)\theta\Big(a+\int_1^3\Big)} \\ &\times\ \hat{\theta}\left(\zeta+\int_1^4\right)\,\theta\left(\zeta-\int_1^4\right)\,e^{i\pi\Delta_1\cdot(\zeta+\int_1^4-\frac{1}{2}\Delta_2-\frac{1}{4}\Omega\cdot\Delta_1)}\end{aligned}$$

After further simplifications of the constant terms and cleaning up, the resulting expression becomes

$$\begin{aligned}\theta(\zeta)\,\hat{\theta}(\zeta) &= e^{-i\pi\Delta_1\cdot\int_1^4}\,\frac{\theta\Big(\int_1^4\Big)\,\theta\Big(a+\int_1^4\Big)}{\theta\Big(a+2\int_1^4\Big)\,\theta(0)}\,\theta\left(\zeta+\int_1^4\right)\,\hat{\theta}\left(\zeta-\int_1^4\right) \\ &+\ e^{i\pi\Delta_1\cdot\int_1^4}\,\frac{\theta\Big(a+\int_1^4\Big)\,\theta\Big(2a+\int_1^4\Big)}{\theta\Big(a+2\int_1^4\Big)\,\theta(2a)}\hat{\theta}\left(\zeta+\int_1^4\right)\,\theta\left(\zeta-\int_1^4\right) \quad (4.57)\end{aligned}$$

The constant terms can still be further simplified again by using the relation (3.49) to arrive at two identities, namely

$$e^{-i\pi\Delta_1\cdot\int_1^4}\,\frac{\theta\left(a+\int_1^4\right)}{\theta\left(a+2\int_1^4\right)}=\frac{\hat{\theta}\left(\int_1^4\right)}{\hat{\theta}\Big(2\int_1^4\Big)} \quad (4.58)$$

and

$$e^{2i\pi\Delta_1\cdot\int_1^4}\,\frac{\theta\left(2a+\int_1^4\right)}{\theta\left(2a\right)}=\frac{\theta\left(\int_1^4\right)}{\theta(0)}\,, \quad (4.59)$$

which when substituted in (4.57) gives

$$\theta(\zeta)\,\hat{\theta}(\zeta) = \frac{\hat{\theta}\Big(\int_1^4\Big)\,\theta\Big(\int_1^4\Big)}{\hat{\theta}\Big(2\int_1^4\Big)\,\theta(0)}\,\left[\theta\left(\zeta+\int_1^4\right)\,\hat{\theta}\left(\zeta-\int_1^4\right)+\hat{\theta}\left(\zeta+\int_1^4\right)\,\theta\left(\zeta-\int_1^4\right)\right]. \quad (4.60)$$

Then (4.56) is proved when ζ is ζ', a zero of $\hat{\theta}$.

Note also that another significance of (4.60) is that it states that the quantity on the left hand side of

$$\frac{\theta\left(\zeta+\int_1^4\right)\,\hat{\theta}\left(\zeta-\int_1^4\right)+\hat{\theta}\left(\zeta+\int_1^4\right)\,\theta\left(\zeta-\int_1^4\right)}{\theta(\zeta)\,\hat{\theta}(\zeta)}=\frac{\hat{\theta}\Big(2\int_1^4\Big)\,\theta(0)}{\hat{\theta}\Big(\int_1^4\Big)\,\theta\Big(\int_1^4\Big)} \tag{4.61}$$

is independent of ζ.

3.5 Quasi-periodic Solution to the Cosh-gordon Equation

One important use of the Fay's Trisecant formula is that it provides a direct way of obtaining directional derivatives of theta functions or of ratios of them. Suppose we take the derivative D_{p_1} of (4.52) and then send $p_2 \to p_1$ we get

$$\begin{aligned} D_{p_1}\ln\left[\frac{\theta(\zeta)}{\theta(\zeta+\int_{p_3}^{p_4})}\right] &= -D_{p_1}\ln\left[\frac{\theta(a+\int_{p_3}^{p_1})}{\theta(a+\int_{p_4}^{p_1})}\right] \\ &\quad -\frac{D_{p_1}\theta(a)\,\theta\left(a+\int_{p_4}^{p_3}\right)}{\theta\Big(a+\int_{p_4}^{p_1}\Big)\,\theta\Big(a+\int_{p_1}^{p_3}\Big)}\frac{\theta\Big(\zeta+\int_{p_3}^{p_1}\Big)\,\theta\Big(\zeta+\int_{p_1}^{p_4}\Big)}{\theta(\zeta)\,\theta\Big(\zeta+\int_{p_3}^{p_4}\Big)}. \end{aligned} \tag{5.62}$$

Here D_{p_1} indicates a directional derivative defined as (summation over j implied):

$$D_{p_1}F(\zeta)=\omega_j(p_1)\frac{\partial F(\zeta)}{\partial\zeta_j}\ , \tag{5.63}$$

and should not be confused with a derivative with respect to p_1 that, if appears, we will denote as ∂_{p_1}. Also, the final expression is simplified using the identities (4.55). We can further take D_{p_3} and then send $p_4 \to p_3$ obtaining:

$$D_{p_3p_1}\ln\theta(\zeta)=D_{p_3p_1}\ln\theta\left(a+\int_{p_3}^{p_1}\right)+\frac{D_{p_1}\theta(a)D_{p_3}\theta\,(a)}{\theta\Big(a+\int_{p_3}^{p_1}\Big)\,\theta\Big(a+\int_{p_1}^{p_3}\Big)}\frac{\theta\Big(\zeta+\int_{p_3}^{p_1}\Big)\,\theta\Big(\zeta+\int_{p_1}^{p_3}\Big)}{\theta^2(\zeta)}. \tag{5.64}$$

(5.64) shows that the second derivative of the logarithm of a theta function contains the theta function. This motivates us to think that solutions of

$$\partial\bar{\partial}\alpha=4\cosh\alpha=2(e^{\alpha}+e^{-\alpha})\ , \tag{5.65}$$

should naturally be sought as logs of theta functions.

We rewrite (5.64) more succinctly,

$$D_{p_3p_1}\ln\frac{\theta(\zeta)}{\theta\left(a+\int_{p_3}^{p_1}\right)}=-\frac{D_{p_1}\theta(a)D_{p_3}\theta\,(a)}{\theta\left(a+\int_{p_3}^{p_1}\right)\theta\left(a+\int_{p_1}^{p_3}\right)}\frac{\theta\left(\zeta+\int_{p_3}^{p_1}\right)\theta\left(\zeta+\int_{p_1}^{p_3}\right)}{\theta^2(\zeta)}. \quad (5.66)$$

This equation is valid for all ζ so we may shift the argument $\zeta\to\zeta+\int_{p_1}^{p_3}$ obtaining another equation which we then subtract from (5.66) leaving us with

$$D_{p_1p_3}\ln\frac{\theta(\zeta)}{\theta(\zeta+\int_{p_1}^{p_3})}= \quad (5.67)$$
$$-\frac{D_{p_1}\theta(a)D_{p_3}\theta(a)}{\theta(a+\int_{p_3}^{p_1})\theta(a+\int_{p_1}^{p_3})}\left\{\frac{\theta(\zeta+\int_{p_1}^{p_3})\theta(\zeta+\int_{p_3}^{p_1})}{\theta^2(\zeta)}-\frac{\theta(\zeta)\theta(\zeta+2\int_{p_1}^{p_3})}{\theta^2(\zeta+\int_{p_1}^{p_3})}\right\}.$$

Define

$$\int_{p_1}^{p_3}\omega:=\frac{1}{2}\Delta_2+\frac{1}{2}\Omega\cdot\Delta_1\ , \quad (5.68)$$

where Δ_2,Δ_1 constitute an integer characteristic and Ω is the period matrix in (3.29). This gives

$$\theta(\zeta+\int_{p_1}^{p_3})=e^{-\pi i\Delta_1\cdot(\zeta+\frac{1}{2}\Delta_2+\frac{1}{4}\Omega\cdot\Delta_1)}\,\theta\begin{bmatrix}\Delta_1/2\\ \Delta_2/2\end{bmatrix}(\zeta). \quad (5.69)$$

This identity will help us further simplify (5.67) but first we make a choice of path from p_1 to p_3 such that $\Delta_1\cdot\Delta_2$ is odd, i.e. $e^{-i\pi\Delta_1\cdot\Delta_2}=-1$. Using these we get a nicer formula

$$D_{p_3p_1}\ln\frac{\theta(\zeta)}{\hat\theta\,(\zeta)}=-\frac{D_{p_1}\theta(a)D_{p_3}\theta\,(a)}{\hat\theta^2(a)}\left[\frac{\hat\theta^2(\zeta)}{\theta^2(\zeta)}+\frac{\theta^2(\zeta)}{\hat\theta^2(\zeta)}\right]. \quad (5.70)$$

It turns out that the coefficient of the quantity in square brackets is unity.

Define

$$\Theta:=\frac{\theta^2(\zeta)}{\hat\theta^2(\zeta)}\,,$$

then (5.70) becomes

$$D_{p_1p_3}\ln\Theta=2\left[\frac{1}{\Theta}+\Theta\right] \quad (5.71)$$

which is a disguised form of the cosh-gordon equation

$$\partial\bar\partial\alpha=4\cosh(\alpha)\,. \quad (5.72)$$

We used that with $\zeta = \mathbf{U}\, z + i\, \mathbf{V} \bar{z}$ then $D_{p_1} = \bar{\partial}, D_{p_3} = \partial$ and more importantly we set,

$$\alpha = 2 \ln \frac{\theta(\zeta)}{\hat{\theta}(\zeta)} \,. \tag{5.73}$$

Therefore, our final expression of the Poincaré coordinates may now be written

$$Z = \left| \frac{\hat{\theta}(2 \int_{p_1}^{p_4})}{\hat{\theta}(\int_{p_1}^{p_4}) \theta(\int_{p_1}^{p_4})} \right| \frac{|\theta(0)\theta(\zeta)\hat{\theta}(\zeta)|\, |e^{\mu z + \nu \bar{z}}|^2}{|\hat{\theta}(\zeta - \int_{p_1}^{p_4})|^2 + |\theta(\zeta - \int_{p_1}^{p_4})|^2} \,, \tag{5.74}$$

$$X + iY = e^{2\bar{\mu}\bar{z} + 2\bar{\nu} z} \, \frac{\theta(\zeta - \int_{p_1}^{p_4}) \overline{\theta(\zeta + \int_{p_1}^{p_4})} - \hat{\theta}(\zeta - \int_{p_1}^{p_4}) \overline{\hat{\theta}(\zeta + \int_{p_1}^{p_4})}}{|\hat{\theta}(\zeta - \int_{p_1}^{p_4})|^2 + |\theta(\zeta - \int_{p_1}^{p_4})|^2} \,, \tag{5.75}$$

with

$$\mu = -D_{p_3} \ln \theta(\int_{p_1}^{p_4}), \qquad \nu = -D_{p_1} \ln \hat{\theta}(\int_{p_1}^{p_4}). \tag{5.76}$$

4. Wilson loops I: Simple curves

The quasi-periodic solutions to the cosh-gordon equation, conveniently expressed in terms of Theta functions, give rise to many different possibilities of Wilson loops; some Wilson loops appear as a single piecewise smooth curve and others appear as multiple piecewise smooth curves. A Wilson loop that belong to the first category is said to be a *simple Wilson loop*, and this chapter is devoted to that case. The next chapter will deal with the latter category.

4.1 Wilson Loops of g=3 Hyperelliptic Riemann Surfaces

The shape of the Wilson loop is determined by the intersection of the minimal area surface with the boundary of AdS_3 . The boundary of AdS_3 , in Poincaré coordinates, is located at $Z = 0$ which, from *Ch3* (5.74) for finite $z, \bar{z}$, implies that either $\theta(\zeta) = 0$ or $\hat{\theta}(\zeta) = 0$. In this work we focus on the second case so we determine the shape of the Wilson loop by

$$\hat{\theta}(\zeta) = 0. \tag{1.1}$$

This equation defines curves in the world-sheet which in turn are mapped to curves in the $Z = 0$ plane of the Poincaré patch using the solution to the equations of motion *Ch3* (5.75).

These solutions do not always lead to a simple Wilson loop. In general the Wilson loops obtained can be very complicated curves; one must select those curves which give rise to simple Wilson loops. Also a Wilson loop could spiral infinitely. There are parameters that can be tuned to prevent some of these pathologies, however. We begin with a study of those Wilson loops that arise from theta functions associated to hyperelliptic Riemann surfaces of genus three.

To be more explicit we will illustrate the main ideas of this section by working with a particular example of a hyperelliptic Riemann surface. First, recall the definition of a hyperelliptic Riemann surface: Let $\tilde{X}$ be a curve defined by

$$\mu^2 = f(\lambda) \tag{1.2}$$

with $f(\lambda)$ a polynomial having distinct roots. Assume that $f(\lambda)$ has degree $2g+1+\delta$ with δ equal to 0 or 1 depending on whether g is odd or even, respectively. Then there is a degree 2 map $\lambda : \tilde{X} \to \mathbb{P}$ and the branch points of λ are exactly the roots of f.

With $g = 3$ let's take our Hyperelliptic curve to be defined by

$$\mu^2 = \lambda(\lambda - a)(\lambda + 1/a)(\lambda - b)(\lambda - \bar{b})(\lambda + c)(\lambda + \bar{c}), \quad a \in \mathbb{R}, b, c \in \mathbb{C} \tag{1.3}$$

The corresponding hyperelliptic Riemann surface with the canonical basis of cycles is displayed in *Figure 4.1*

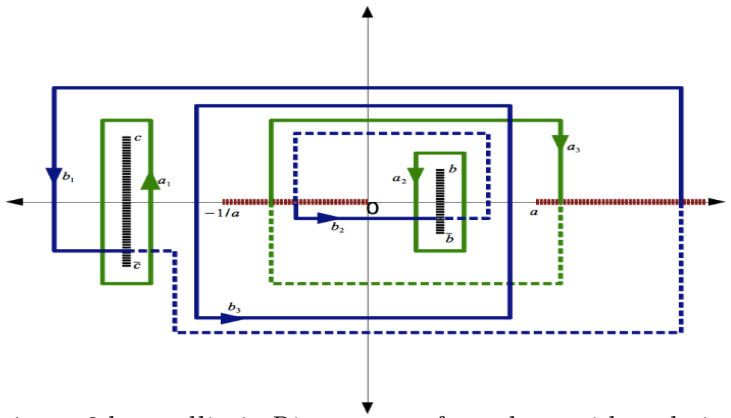

Figure 4.1. *g=3 hyperelliptic Riemann surface along with a choice of basis cycles.*

Take the unique normalized basis of Abelian differentials of the first kind such that $\int_{a_i} \omega_j = \delta_{ij}$. Furthermore consider the Abelian differentials in this basis to be

linear combinations of the previously computed basis of holomorphic differential on a hyperelliptic Riemann surface. That is

$$\omega_j = \sum_{k=1}^{3} c_{j\,k}\tilde{\omega}_k = \sum_{k=1}^{3} c_{j\,k}\frac{\lambda^{3-k}}{\mu}d\lambda\,, j = 1,2,3$$

where

$$c_{j\,k} = (\mathbf{A}^{-1})_{j\,k}\,, \quad A_{j\,k} = \oint_{a_k}\tilde{\omega}_j\,, \quad B_{\mathrm{j}\,k} = \oint_{b_j}\omega_k\,. \tag{1.4}$$

It is clear how to compute the matrices $\mathbf{A}$ and $\mathbf{B}$.

The next set of quantities which are necessary are the vectors found in the expression $\zeta = \mathbf{U}z + i\bar{z}\mathbf{V}$.

Recall that these are given by

$$U_k = \oint_{b_k} d\Omega_\infty\,, \quad V_k = \oint_{b_k} d\Omega_0\,, \quad k = 1,2,3\,, \tag{1.5}$$

where the Abelian differentials of the second kind are given by

$$\Omega_{\infty,\,0} = \int_\infty^\lambda d\Omega_{\infty,\,0}\,. \tag{1.6}$$

From the previous chapter, it was established that the holomorphic one forms on $\tilde{X}$ are of the form $\lambda^j\frac{d\lambda}{\mu}$ where $j \leq g-1$. This means the quantity $d\Omega_\infty$, being meromorphic, goes like

$$d\Omega_\infty \sim \frac{\lambda^j}{\mu}d\lambda \quad \text{with} \quad j \geq 3.$$

Furthermore, from the asymptotic behavior of $d\Omega_\infty$

$$\lambda \to \infty\,, \quad d\Omega_\infty \to d\nu = \frac{1}{2}\frac{d\lambda}{\sqrt{\lambda}}\,,$$

it can be deduced that $j = 3$ and

$$d\Omega_\infty \sim \frac{1}{2}\frac{\lambda^3}{\mu}d\lambda\,,$$

because in the $\lambda \to \infty$ limit, we have $\mu \to \lambda^{7/2}$. In the general case j will be found to be equal to g, the genus of the hyperelliptic Riemann surface.

We are free to add to $d\Omega_\infty$ an holomorphic 1- form without compromising the meromorphicity. So we add a linear combination of holomorphic 1-forms;

$$d\Omega_\infty = \frac{1}{2}\frac{\lambda^3}{\mu}d\lambda + \sum_j \alpha'_j\,\omega_j\,.$$

Using the constraint

$$0 = \oint_{a_k} d\Omega_\infty = \frac{1}{2}\oint_{a_k}\frac{\lambda^3}{\mu}d\lambda + \alpha'_k\,,$$

we determine the constants

$$\alpha'_k = -\frac{1}{2}\oint_{a_k}\frac{\lambda^3}{\mu}d\lambda\,.$$

This allows for the quantity U_k to be given explicitly as

$$U_k = \frac{1}{2}\oint_{b_k}\frac{\lambda^3}{\mu}d\lambda - \frac{1}{2}\sum_j\Big(\oint_{a_j}\frac{\lambda^3}{\mu}d\lambda\Big)\,B_{k\,j}\,. \tag{1.7}$$

By repeating the procedure above for $d\Omega_0$ keeping in mind the asymptotic behavior

$$\lambda \to 0\,,\quad d\Omega_0 \to -\frac{d\nu}{\nu^2}\,,\quad \mu \to i\sqrt{\lambda}\,,$$

it can be determined that

$$V_k = -\frac{i}{2}\oint_{b_k}\frac{\lambda^{-1}}{\mu}d\lambda + \frac{i}{2}\sum_j\Big(\oint_{a_j}\frac{\lambda^{-1}}{\mu}d\lambda\Big)\,B_{k\,j}\,. \tag{1.8}$$

These quantities can now be assembled and substituted into the equations (5.73), (5.74), (5.75) and (5.76) of *Ch3*. (5.74) is particlarly crucial in that the Wilson loops in AdS_3 are defined by the equation

$$Z = 0$$

which can be achieved by setting

$$\hat{\theta}(\zeta) = 0\,.$$

The λ which appears in the Abel map $A_\omega : \tilde{X} \to \mathbb{C}$ that acts on a point in $\tilde{X}$ by

$$x \longmapsto \int_{x_0}^{x}\omega\,,$$

is the so called spectral parameter in the theory of integrability. In this case it provides some sense of symmetry for the Wilson loops. By changing the value of λ while keeping its absolute value at unity, for the reality of the solutions, we can continuously deform a single Wilson loop and get many different shapes. This deformation does not affect the regularized are of the corresponding minimal area surface, however.

In particular, the Wilson loops for two different values of λ and the choice of $a = 2$, $b = 1/2 + i/2$, and $c = 1 + i$ are shown below:

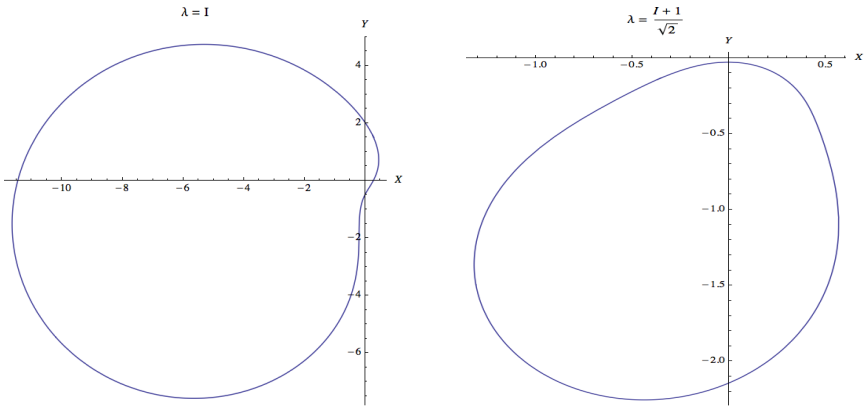

Figure 4.2. *Shapes of a Wilson loop for different values of* λ.

4.2 Analytic Formula for the Area of Minimal Area Surface

Using (1.1) and the accompanying choice of basis cycles on the Riemann surface we found simple Wilson loops in the boundary of AdS_3 like the ones shown in *Figure 4.2*. The shape of these boundary curves depend on the spectral parameter λ but the renormalized area, denoted A_f, does not. So for a given period matrix Ω the solution here is a single parameter family and this parameter leaves the renormalized area invariant. This seems a bit strange at first but perhaps a closer look at the regularization scheme may offer some clarifications.

The vanishing of Z at the boundary of the gravity dual surface makes the total area of these surfaces to blow up. When $\hat{\theta}$ is zero, the field α goes to infinity. So from the formula for the area

$$A = 4 \int e^{\alpha} d\sigma d\tau \,, \tag{2.9}$$

it becomes clear why the area diverges.

Using Fay's trisecant identity, we find an expression for the exponential to be a sum of a finite term and a term that diverges at the boundary where $\hat{\theta} = 0$;

$$\begin{aligned} e^{\alpha} &= D_{p_1 p_3} \ln \theta(0) - D_{p_1 p_3} \ln \hat{\theta}(\zeta) & (2.10) \\ &= D_{p_1 p_3} \ln \theta(0) - \partial\bar{\partial} \ln \hat{\theta}(\zeta). & (2.11) \end{aligned}$$

Integrating the second term at the boundary of the surface obviously leads to divergence so we need to regulate it. In order to do that we observe we may write Z as a product of a non vanishing function and $\hat{\theta}$

$$Z = |\hat{\theta}(\zeta)| h(z, \bar{z}) \,, \tag{2.12}$$

with

$$h(z, \bar{z}) = \left| \frac{\hat{\theta}(2\int_{p_1}^{p_4})}{\hat{\theta}(\int_{p_1}^{p_4})\theta(\int_{p_1}^{p_4})} \right| \frac{|\theta(0)\theta(\zeta)|\, |e^{\mu z + \nu \bar{z}}|^2}{|\hat{\theta}(\zeta - \int_{p_1}^{p_4})|^2 + |\theta(\zeta - \int_{p_1}^{p_4})|^2}. \tag{2.13}$$

Substituting (2.11) into (2.9) and applying Stoke's theorem we get the expression

$$A = 4 D_{p_1 p_3} \ln \theta(0) \int d\sigma d\tau + \oint \hat{n} \cdot \nabla \ln h \; d\ell - \oint \hat{n} \cdot \nabla \ln Z \; d\ell. \tag{2.14}$$

The last integral is divergent and we concentrate now on extracting the leading divergence. The correct AdS/CFT prescription is to cut the surface at $Z = \epsilon$ and write the area as

$$A = \frac{L}{\epsilon} + A_f \,, \tag{2.15}$$

where L should be the length of the Wilson loop and A_f is the finite part which is identified with the expectation value of the Wilson loop through:

$$\langle W \rangle = e^{-\frac{\sqrt{\lambda}}{2\pi} A_f} \,, \tag{2.16}$$

where here λ is the 't Hooft coupling of the gauge theory (not to be confused with the spectral parameter). This prescription is equivalent to subtracting the area $A = \frac{L}{\epsilon}$ of a string ending on the contour of length L and stretching along Z from the boundary to the horizon. To see that the coefficient of the divergence is indeed the length, let us compute

$$A_{\text{div.}} = -\oint_{Z=\epsilon} \frac{1}{Z}\hat{n}\cdot\nabla Z d\ell = \frac{1}{\epsilon}\oint_{Z=\epsilon} |\nabla Z| d\ell \ , \tag{2.17}$$

where we observe that the normal is precisely in the opposite direction of ∇Z because the contour is a curve of constant $Z = \epsilon$ and Z increases toward the inside. On the other hand the length in the boundary is given by

$$L = \oint \sqrt{|\hat{t}.\nabla X|^2 + |\hat{t}.\nabla Y|^2} d\ell \ , \tag{2.18}$$

where $\hat{t}$ is a unit vector tangent to the contour. We can move forward if we write the equation of motion for X as derived form the action *Ch2* (2.7):

$$2\nabla X\cdot\nabla Z = Z\nabla^2 X \ , \tag{2.19}$$

which, when $Z \to 0$, becomes $\nabla X\cdot\nabla Z = 0$ namely ∇X is perpendicular to the normal and therefore parallel to the tangent $\hat{t}$. The same is true for ∇Y so we find

$$L = \oint \sqrt{|\nabla X|^2 + |\nabla Y|^2} d\ell + \mathcal{O}(\epsilon^2). \tag{2.20}$$

Finally the equation of motion for Z is

$$(\nabla Z)^2 - Z\nabla^2 Z = (\nabla X)^2 + (\nabla Y)^2 \ , \tag{2.21}$$

which for $Z \to 0$ implies that $\sqrt{|\nabla X|^2 + |\nabla Y|^2} = |\nabla Z|$. Therefore the length of the Wilson loop is given by

$$L = \oint |\nabla Z| d\ell - \frac{\epsilon}{2}\oint \frac{\nabla^2 Z}{|\nabla Z|}\, d\ell \ , \tag{2.22}$$

and the divergent piece of the area is indeed $A_{\text{div.}} = \frac{L}{\epsilon}$. There is a finite part remaining:

$$\begin{aligned} A &= \frac{L}{\epsilon} + A_{\text{f}} \ , \\ A_{\text{f}} &= 4D_{p_1p_3}\ln\theta(0)\int d\sigma d\tau + \oint \hat{n}\cdot\nabla \ln h \ d\ell + \frac{1}{2}\oint \frac{\nabla^2 Z}{|\nabla Z|}\, d\ell. \end{aligned} \tag{2.23}$$

The integrals are performed on the world-sheet parameterized by σ, τ. The first integral is proportional to the area of the world-sheet. The last two integrals are done over the world-sheet boundary. The final expression can be simplified by rewriting $Z = |\hat{\theta}(\zeta)|h(z,\bar{z})$ and using that $\hat{\theta}(\zeta)$ vanishes on the boundary where the contour integral is performed. It is then easy to check that $h(z,\bar{z})$ term drops out and the final formula for the renormalized area is

$$\begin{aligned} A_{\mathrm{f}} &= 4D_{p_1p_3}\ln\theta(0)\int d\sigma d\tau + \frac{1}{2}\oint \frac{\nabla^2\hat{\theta}(\zeta)}{|\nabla\hat{\theta}(\zeta)|}\, d\ell \\ &= 4D_{p_1p_3}\ln\theta(0)\int d\sigma d\tau + \oint \frac{D_{p_1p_3}\hat{\theta}(\zeta)}{|D_{p_1}\hat{\theta}(\zeta)|}\, d\ell. \end{aligned} \tag{2.24}$$

This gives us an analytical expression for the renormalized area of the minimal surfaces.

In illustrative terms, what this all means is that in order to regularize the integral we cut the surface, as shown in *Figure 4.3*, at a height $\epsilon \to 0$ and then subtract the leading divergent term. The leading term contains information about the length of the Wilson loop.

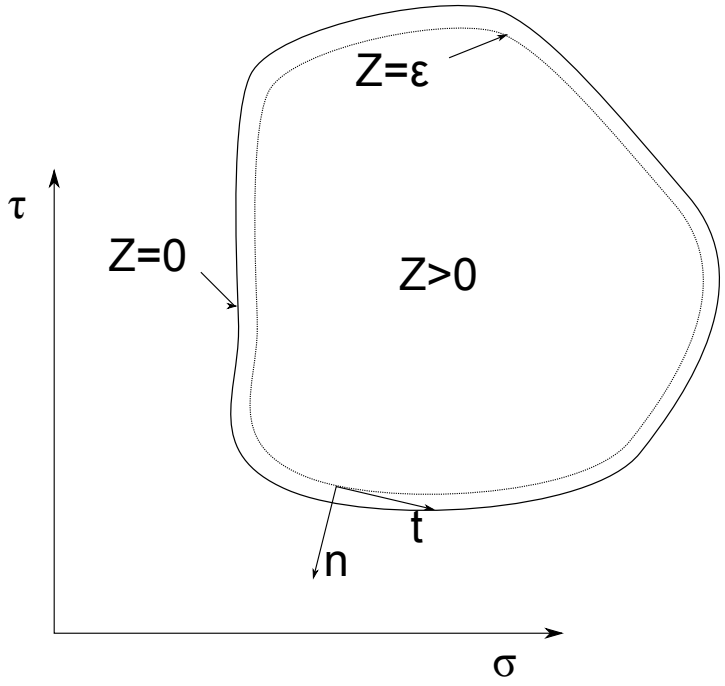

Figure 4.3. *The boundary is determined by the contour $Z = 0$. However the area is computed by integrating up to a contour $Z = \epsilon \to 0$ and then the leading divergence $\frac{L}{\epsilon}$ is subtracted. Here L is the length of the contour in the boundary (not in this (σ,τ) plane).*

We find that the shape of the Wilson loop depends on the spectral parameter λ. For two values

$$\lambda_1 = i, \qquad \lambda_2 = -\frac{1+i}{\sqrt{2}}. \tag{2.25}$$

we obtained

$$L_1 = 13.901, \quad L_2 = 6.449\ , \tag{2.26}$$

$$A_f = -6.598 \quad \text{for both.} \tag{2.27}$$

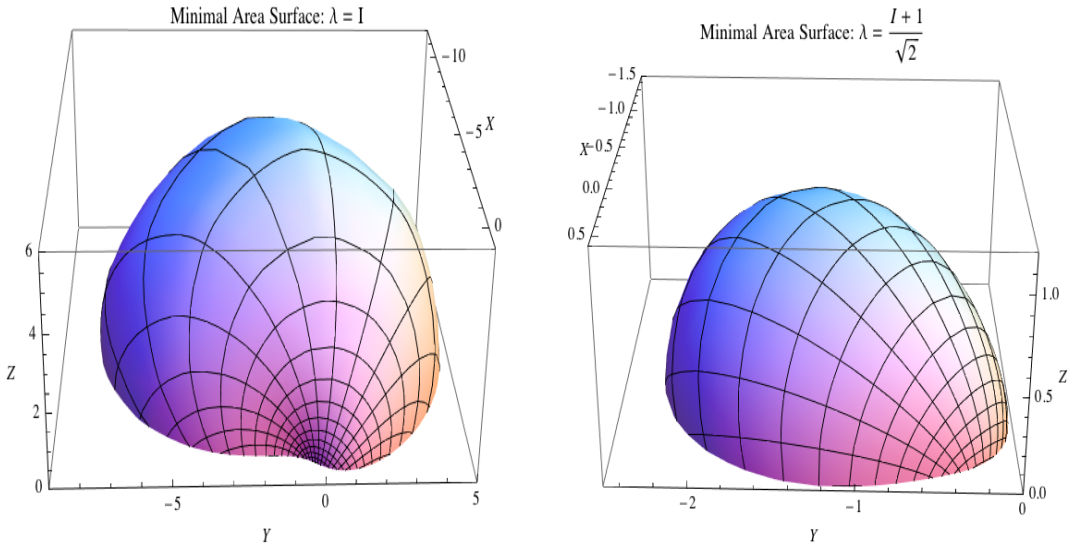

Figure 4.4. *Minimal area surfaces ending on the contours illustrated in Figure 4.2. We emphasize that the surfaces are known analytically and they have the same area.*

5. Wilson loops II: Multiple Curves

We have seen in *Ch4* how simple Wilson loops arise from a $g = 3$ hyperelliptic Riemann surface. This chapter is devoted to the case in which the Wilson loop consists of multiple curves in the boundary of AdS_3 . Some of these Wilson loops are open as in the case of the already known examples of the cusp [8], and the double parallel lines [3]; others are closed as in the cases of the concentric circles [7].

These already known examples can also be attained by applying the proposed technique in the $g = 1$ setting. We will demonstrate this before moving on to the case of $g = 3$ multiple curve Wilson loops. We see that for this higher genus new examples of Wilson loops and their minimal area surfaces may be computed.

5.1 Wilson Loops of g=1 Hyperelliptic Riemann surfaces

The study of $g = 1$ hyperelliptic Riemann surface gives us an opportunity to study some of the previously known examples of Wilson loop from a new perspective. It unveils some structure among these seemingly unrelated Wilson loops. It shows that the story of the cusp Wilson loop segues into that of the concentric circles by adjusting the branch point. In fact it will be shown that the single line, the cusp, the parallel lines, and concentric circles are all related to each other.

As before we begin by describing the elliptic curve;

$$\mu^2 = \lambda(\lambda - a)\big(\lambda + \frac{1}{a}\big)\,, \quad a \in \mathbb{R}\,. \tag{1.1}$$

The corresponding Riemann surface along with the choice of basis cycles is shown in *Figure 5.1.* The Riemann theta functions in the $g = 1$ settings are just the slightly more familiar Jacobi theta functions which can be shown [21] to be related to the Elliptic theta functions; for consistency we continue to use Riemann theta functions with the caveat that the arguments have now become complex scalars.

The $g = 1$ case is further characterized by the fact that we have an explicit relationship between the quantities Ω_∞ and Ω_0;

$$\Omega_+ := \Omega_\infty + i\,\Omega_0 = \frac{\mu}{\lambda}\,, \tag{1.2}$$

and consequently

$$\Omega_- := \Omega_\infty - i\,\Omega_0 = 2\Omega_0 + \frac{\mu}{\lambda}\,. \tag{1.3}$$

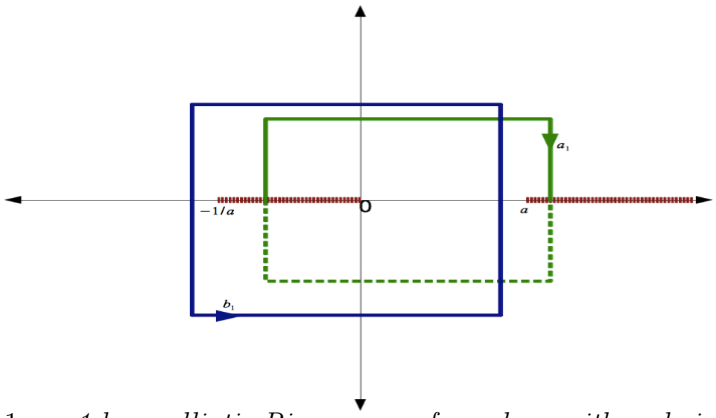

Figure 5.1. *g=1 hyperelliptic Riemann surface along with a choice of basis cycles.*

The two important determinants of the nature of the Wilson loops obtained are the spectral parameter λ and the branch point a. The cases of interest are $\lambda = \pm 1$. For each of these values of λ we have the choice of taking $a > 1$ or $a < 1$. It turns out that for values of a in these intervals the Wilson loops behave the same for both values of λ:

- $\lambda = \pm 1$; $a < 1$: The quantities Ω_+ and Ω_- are both real and the Wilson loop is a cusp. The minimal area surface is a half-cone and the angle of cusp θ is given by

  $$\cos(\theta) = Re\frac{X_2(0)}{X_1(0)}\,, \tag{1.4}$$

  where X_1 and X_2 are the solutions (5.75) along the first and second lines, going counterclockwise from the positive X-axis, that make up the Wilson loop.

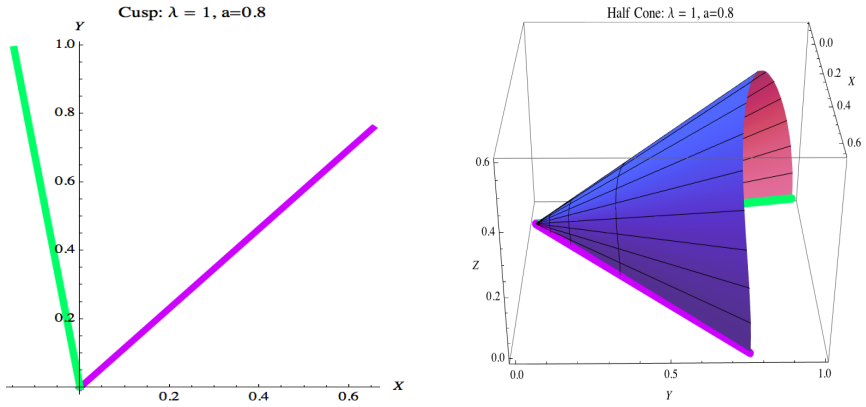

Figure 5.2. *The cusp and its corresponding half-cone.*

- $\lambda = \pm 1$; $a > 1$: The quantities Ω_+ and Ω_- are both imaginary and the Wilson loop is the concentric circles. The minimal area surface is a half-torus.

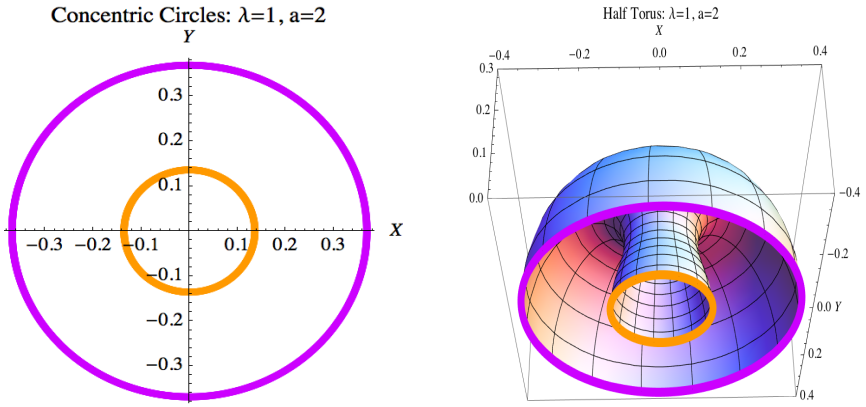

Figure 5.3. *The concentric circles and its corresponding half-torus.*

There are other possibilities and one case of interest is when $\lambda = 1$ and letting a take on values for which the hyperelliptic curve becomes singular. These cases are

- $a \to 0$: The curve is becoming singular and the Wilson loop is a straight line.
- $a \to 1$: The Wilson loop is a pair of parallel lines.
- $a \to \infty$: The curve is becoming singular and the Wilson loop is a circle.

Note that the cases when $a \to 0$ and $a \to \infty$ gave simple Wilson loops which are the subject of the previous chapter. We saw in the previous chapter how the technique generalizes the concept of the circular Wilson loop.

5.2 Closed Wilson Loops for $g = 3$ Hyperelliptic Riemann Surface

We are primarily interested in the genus 3 case and here we have $2g + 1$ finite branch points (and the point at infinity). Also the number of branch cuts being,

$g+1$, will now increase from two to four. Due to the involution $\lambda \to -1/\bar{\lambda}$, the branch point $c = -1/b$. The points $\bar{b}$ and $\bar{c}$ are the complex conjugates of b and c, respectively (See *Figure 4.1*).

In the $g = 1$ case the Wilson loop we get for $\lambda = \pm 1$ automatically is periodic for $a > 1$. In general this is not the case and certainly not for $g = 3$. The image of the curves determined by $\hat{\theta} = 0$ in AdS_3 is typically an infinite spiral. The practical way to get a periodic Wilson loop is to judiciously select the branch points for $|\lambda| = 1$.

Even when the Wilson loop is periodic, it is not guaranteed that it is not a very complex system of curves that intersect with each other or individually self intersect. For example, suppose the world sheet is a horizontal strip bounded by two horizontal curves that map to periodic curves in AdS. In addition, suppose between these horizontal strips there are several closed curves. Then the image of the entire horizontal strip in the boundary of AdS is in general a complicated system of curves. For now, we are interested in studying non intersecting periodic Wilson loops.

Since in $g = 1$ case with $a > 1$ we obtained periodic Wilson loops, we take the $g = 3$ hyperelliptic Riemann surface and make it look as close as possible to the $g = 1$ hyperelliptic Riemann surface. The idea then is that as we shrink the $b\bar{b}$ and $c\bar{c}$ branch cuts we should get results close to the concentric circles. This can be viewed as a perturbation of the concentric circles and this should be manifested in the shapes of the Wilson loops we get. We reemphasize that unlike the $g = 1$ case the solutions are not automatically periodic; we must work tediously to pick a suitable value of $a > 1$ as we move the point b around to get periodic concentric curves.

Along the boundary of the minimal area surfaces the solution may be further simplified using the Fay's trisecant formula. In particular we have that

$$\bar{X} := X - iY = e^{2\bar{\mu}\bar{z}+2\bar{\nu}z}\frac{\hat{\theta}(\zeta + \int_0^\lambda)}{\hat{\theta}(\zeta - \int_0^\lambda)}. \tag{2.5}$$

Since at the boundary we have $Z = 0$ we are concerned with when $\bar{X}$ becomes periodic. Theoretically, we know what conditions need to be satisfied for (2.5) to be periodic and we wish to discuss that in the following section.

5.3 Excursion: Periodicity of a Ratio of Riemann Theta Functions

We first focus on how to get the ratio of theta functions to be periodic. Once this is understood it should be obvious how to achieve periodicity in (2.5).

Consider a g dimensional complex vector space V and a discrete subset $\Lambda \subset V$. Λ is a lattice in V and therefore a subgroup of the additive subgroup of V. The quotient space $X = V/\Lambda$ is a connected compact complex manifold called a complex tori of dimension g. Also the addition in V induces an abelian Lie group structure on X which makes it a complex abelian Lie group. There is a projection map $\pi : V \to X$ such that $\Lambda = ker(\pi)$.

The basic question we want to address here is how to construct meromorphic functions on X. The answer to this question turns out to have an interesting bearing on the problem at hand–the problem of periodicity of the Wilson loops.

To get a meromorphic function f on X one may begin with a meromorphic function h on V such that $h = f \circ \pi$ is the pullback of f. Note that a sensible meromorphic function on X must be Λ-periodic. Thinking of f as a rational function, one would demand that both the denominator and numerator transform in a controllable manner so that the ratio as a whole is Λ-periodic. It is not difficult to prove that such meromorphic function on a complex torus occurs as ratios of translated Riemann theta functions. A translated Riemann theta function is defined as $\theta^{(x)}(\zeta) = \theta(\zeta - \epsilon'/2 - \tau\epsilon/2 - x)$ with simple zeros at $\zeta = x + \Lambda$. The quantities ϵ and ϵ' constitute the usual characteristic of a theta function.

Suppose we have a ratio of product of Theta functions

$$R(\zeta) = \frac{\prod_{i=1}^{m} \theta^{(x_i)}(\zeta)}{\prod_{j=1}^{n} \theta^{(y_j)}(\zeta)} \,. \tag{3.6}$$

It can be shown that for $\Omega \in \Lambda$, $R(z + \Omega) = R(z)$ if and only if the conditions

- $m = n$ and
- $\sum x_i - \sum y_j \in \mathbb{Z}^g$.

are satisfied.

5.4 Back to Periodicity of our Solutions

Since in (2.5) we have $m=n=1$, we only need to find places x_i on the Riemann surface such that the fraction is periodic. This is exactly what amounts to the problem of finding values of a and b so that the ratio of $\hat{\theta}$ is periodic, namely that $\zeta \to \zeta + m$, for $m \in \mathbb{Z}^g$.

For the exponential in (2.5) to be periodic it is clear we need the quantity

$$\omega(z, \bar{z}) = \mu z + \nu \bar{z} = \frac{p}{q}\pi i$$

where $p/q \in \mathbb{Q}$. Since we are studying world sheets bounded by horizontal curves, this means that two points along a boundary curve of the world sheet given in (σ, τ) coordinates that are mapped to the same point in AdS will have the same τ coordinate but different σ. Writing $z = \sigma + i\tau$ and $\bar{z} = \sigma - i\tau$, then $\omega(\sigma+\delta\sigma, \tau) = \omega(\sigma, \tau)+\delta\sigma(\mu+\nu)$ where $\delta\sigma$ is the difference between the sigma coordinates of the two endpoints along a curve bounding the world sheet. So although we said earlier that if we know how to achieve periodicity in the ratio of theta functions then it will be obvious how to get periodic solutions, that statement is true conceptually, but deceiving in practice. This is because it is not that simple to achieve the condition $\delta\sigma(\mu + \nu) = (p/q)\pi\, i$. This condition must be complemented by the one coming from the theta function part of the solution. Also, we want to constrain n periods of the ratio of Riemann theta function into a single period of the exponential so that the concentric curves we find will be distorted from the shape of the concentric circles. The distorted figure will have the same number of sides as n.

We found values for a and b such that we can match several periods of the ratio of the theta functions into a single period of the exponential function. In each case we get concentric Wilson loops which deviate from the concentric circular Wilson loops by deformations that make them appear like they have been pinched in n sides. The values for the branch points are shown in *Table 5.1* and the corresponding Wilson loops and dual minimal area surfaces are shown in *Figures 5.4 and 5.5.*

Table 5.1
Positions of the branch points; n corresponds to the number of periods

n=2	n=3	n=4	n=5
$a = 1.28088$	$a = 1.102149$	$a = 1.035312$	$a = 1.0304752$
$b = 0.5 + 0.01i$	$b = 0.5 + 0.1i$	$b = 0.7 + 0.2i$	$b = 0.7 + 0.3i$

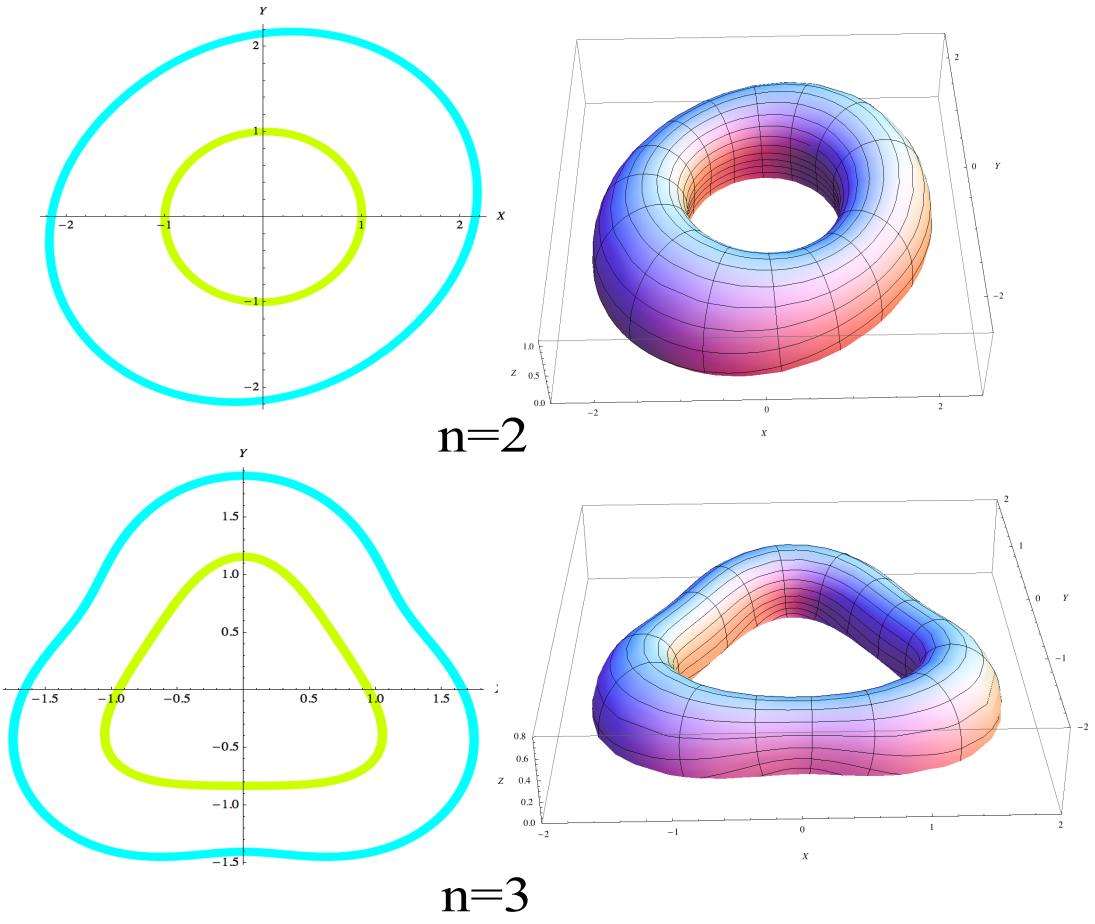

Figure 5.4. *Wilson loops and minimal area surface for n periods*

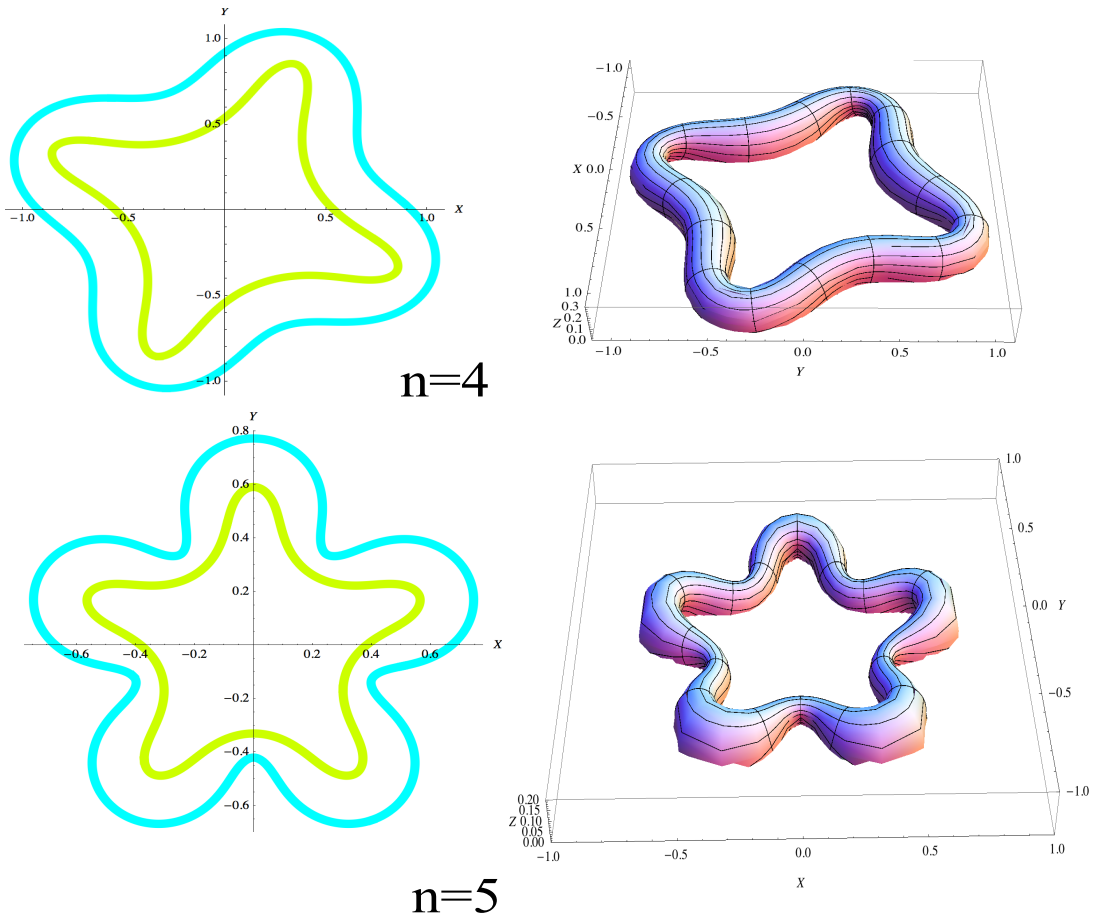

Figure 5.5. *Wilson loops and minimal area surface for n periods*

5.5 Surfaces for Concentric Wilson Loops

To get the surfaces ending on the concentric curves we need the full solutions in Poincaré coordinates. These are given by

$$X + iY = e^{2\bar{\mu}\bar{z}+2\bar{\nu}z}\frac{\theta(\zeta-\int_{p_1}^{p_4})\overline{\theta(\zeta+\int_{p_1}^{p_4})}-\hat{\theta}(\zeta-\int_{p_1}^{p_4})\overline{\hat{\theta}(\zeta+\int_{p_1}^{p_4})}}{|\hat{\theta}(\zeta-\int_{p_1}^{p_4})|^2+|\theta(\zeta-\int_{p_1}^{p_4})|^2}$$

$$Z = \left|\frac{\hat{\theta}(2\int_{p_1}^{p_4})}{\hat{\theta}(\int_{p_1}^{p_4})\theta(\int_{p_1}^{p_4})}\right| \frac{|\theta(0)\theta(\zeta)\hat{\theta}(\zeta)|\,|e^{\mu z+\nu\bar{z}}|^2}{|\hat{\theta}(\zeta-\int_{p_1}^{p_4})|^2+|\theta(\zeta-\int_{p_1}^{p_4})|^2}\,. \tag{5.7}$$

We emphasize that in the boundary where $Z = 0$ the Wilson loop is the image of the set of points where $\hat{\theta}(\zeta)$ vanishes. The solution (5.7) describes the minimal area surface ending on the boundary curves described by $\bar{X}$ in (2.5). These surfaces are essential in the theory because the *regularized area* corresponds to the expectation value of the Wilson loop. So while the the fundamental object in the gauge theory is the Wilson loop, in the gravity dual the corresponding object is the minimal area surface extending into the bulk which connects to the Wilson loop in the boundary of AdS space.

5.6 Stoke's Theorem and the Area of Concentric Wilson Loops

In *Ch4* we showed that the area of the minimal area surfaces may be analytically expressed as [22]

$$A = 4D_{p_1p_3}\ln\theta(0)\int d\sigma d\tau + \int d\sigma d\tau \nabla^2 \ln h - \int d\sigma d\tau \nabla^2 \ln Z\,. \tag{6.8}$$

In the concentric curve case, the preimage of the curves in the boundary of AdS_3 typically looks like a pair of sine-like curves in the world sheet coordinates as shown in *Figure 5.6* below. Stoke's Theorem tells us that to compute the area of a particular surface bounded by concentric Wilson loops, we need to integrate along its

corresponding sine-like curves and along the two vertical boundaries, one at $\sigma = 0$ and the other at $\sigma = \sigma_f$. Here σ_f is the point where the curves end along the σ axis.

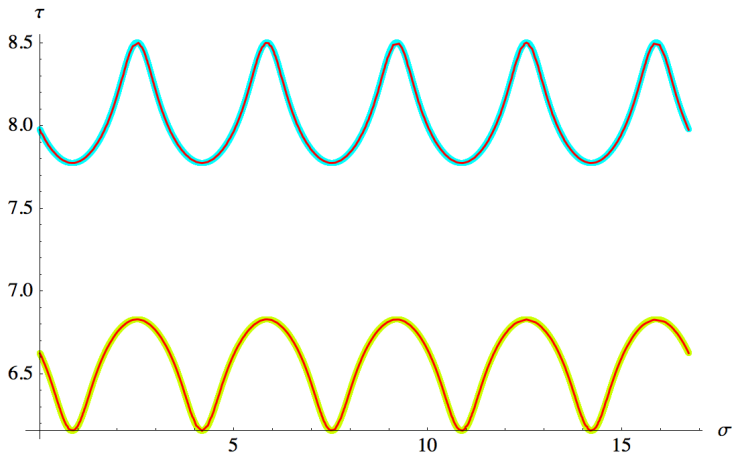

Figure 5.6. *Wilson loops in world sheet coordinates*

We parametrize the sine-like curves by the variable σ, so that the lower curve is now given as $\tau_1(\sigma)$ and the upper one by $\tau_2(\sigma)$. According to Stoke's Theorem, for any smooth real-valued functions Q and P on a regular domain D in $\mathcal{R}^2$, we have that

$$\int_D \Big(\frac{\partial Q}{\partial x} - \frac{\partial P}{\partial y}\Big) dxdy = \int_{\partial D} Pdx + Qdy\,. \tag{6.9}$$

Let us begin with the first term on the right hand side of (6.8) which we denote by A_{const}. When we apply (6.9) by taking $Q = \sigma/2$ and $P = -\tau/2$ we get

$$A_{const} = -2D_{p_1p_3} \ln\theta(0) \Big(\int_2 \sigma\tau_2'(\sigma) - \sigma_f \int_3 d\tau - \int_4 \sigma\tau_1'(\sigma)d\sigma - \int_2 \tau_2(\sigma)d\sigma + \int_4 \tau_1(\sigma)d\sigma \Big) \tag{6.10}$$

where the subscripts 1,2,3,4 on the integrals indicate left, top, right, and bottom boundaries of the domain in the $\sigma - \tau$ plane. Of course the simplest thing to do here is by following elementary calculus and directly write

$$A_{const} = 4D_{p_1p_3} \ln\theta(0) \int (\tau_2(\sigma) - \tau_1(\sigma))d\sigma \tag{6.11}$$

However, we chose to arrive at (6.10) by means of (6.9) because it will turn out that this approach is very useful for the other two more complicated terms in (6.8) where the condition that leads to (6.11) is absent.

For the second term in (6.8), denoted by A_h, we may take $Q = \partial_\sigma \ln h$ and $P = -\partial_\tau \ln h$. We then obtain

$$\begin{aligned} A_h &= -\int_1 d\tau\, \partial_\sigma \ln h|_{\sigma_0} - \int_2 d\sigma\, \partial_\sigma \ln h|_{\tau_2} \tau_2'(\sigma) + \int_3 d\tau\, \partial_\sigma \ln h|_{\sigma_f} \\ &+ \int_4 d\sigma\, \partial_\sigma \ln h|_{\tau_1} \tau_1'(\sigma) + \int_2 d\sigma\, \partial_\tau \ln h|_{\tau_2} - \int_4 d\sigma\, \partial_\tau \ln h|_{\tau_1} \end{aligned} \tag{6.12}$$

Similarly, the last term in (6.8) indicated by A_z becomes,

$$\begin{aligned} A_z &= -\Big(\int_1 d\tau\, \partial_\sigma \ln Z|_{\sigma_0} - \int_3 d\tau\, \partial_\sigma \ln Z|_{\sigma_f} \Big) - \int_2 d\sigma\, \partial_\sigma \ln Z|_{\tau_2} \tau_2'(\sigma) \\ &+ \int_4 d\sigma\, \partial_\sigma \ln Z|_{\tau_1} \tau_1'(\sigma) + \int_2 d\sigma\, \partial_\tau \ln Z|_{\tau_2} - \int_4 d\sigma\, \partial_\tau \ln Z|_{\tau_1} \end{aligned} \tag{6.13}$$

Since Z vanishes along the sine-like curves parametrized as $\tau_1(\sigma)$ and $\tau_2(\sigma)$, we see clearly that only the terms in parenthesis in (6.13) are finite leaving all integrals along sides 2 and 4 which are the two horizontal curves bounding the world sheet to diverge. This is one nice thing about the Stoke's Theorem approach because the divergent part is exposed in very clear manner. To remedy the divergence, we cut the surface at a height ϵ very close to the original boundary, and the integrals are no longer divergent up to the boundary of this cut surface. This is why the string theory is said to have an infrared divergence, but the corresponding gauge theory has an ultraviolet divergence. The preimage of the boundary of the cut surface is then parametrized by two horizontal curves, $t_1(\sigma), t_2(\sigma)$ that lie very close to the original ones and on the inside the world sheet. Once, this is done the formula then becomes

$$\begin{aligned} A_z &= -\Big(\int_{t_1(0)}^{t_2(0)} d\tau\, \partial_\sigma \ln Z|_{\sigma_0} - \int_{t_1(\sigma_f)}^{t_2(\sigma_f)} d\tau\, \partial_\sigma \ln Z|_{\sigma_f} \Big) \\ &- \frac{1}{\epsilon} \Big(\int_2 d\sigma\, \partial_\sigma Z|_{t_2} t_2'(\sigma) - \int_4 d\sigma\, \partial_\sigma Z|_{t_1} t_1'(\sigma) - \int_2 d\sigma\, \partial_\tau Z|_{t_2} + \int_4 d\sigma\, \partial_\tau Z|_{t_1} \Big) \end{aligned} \tag{6.14}$$

It turns out that the first term in parenthesis above vanishes and therefore $A_z = -A_{div}$ where A_{div} is the other grouped item along with its coefficient $1/\epsilon$. Finally, it is clear

that the total area of the minimal area surface can be written as the sum of a term that is finite and a term that diverges as $1/\epsilon$

$$A = A_{conv} + A_{div} \tag{6.15}$$

with

$$A_{conv} = A_{const} + A_h \,, \tag{6.16}$$

and

$$A_{div} = -\frac{1}{\epsilon}\Big(\int_2 d\sigma\, \partial_\sigma Z|_{t_2} t_2'(\sigma) - \int_4 d\sigma\, \partial_\sigma Z|_{t_1} t_1'(\sigma) - \int_2 d\sigma\, \partial_\tau Z|_{t_2} + \int_4 d\sigma\, \partial_\tau Z|_{t_1} \Big) \,. \tag{6.17}$$

5.7 Area Formula and the Length of Boundary Curves

According to the regularization prescription, the divergent part of the total area of the minimal surface should be equal to L/ϵ where L is the length of the Wilson loop. This implies that if (6.17) is correct, it should give us the length of the Wilson loop where in the case of the concentric Wilson loops it is the sum of both the inner and outer curves.

In [22] and *Ch4* of this work we showed that the length of the Wilson loop is

$$L = \int_{2+4} |\nabla Z|\, dl - \frac{\epsilon}{2} \int_{2+4} \frac{\nabla^2 Z}{|\nabla Z|}\, dl \,. \tag{7.18}$$

According to the regularization scheme the regularized area which is the finite part of the total area of the surface ending on the Wilson loop may be obtained by

$$A_{finite} = A - \frac{L}{\epsilon} \,. \tag{7.19}$$

On the other hand we have

$$A_z = \int_D \nabla^2 \log Z d\sigma d\tau = \int_{\partial D} \nabla \log Z \cdot \vec{dl} \tag{7.20}$$

where $\vec{dl} = \hat{n}\, dl$ with $\hat{n}$ the outward normal vector. With the tangent vector to the curve given by $(d\sigma, d\tau)$ we take $\vec{dl} = (d\tau, -d\sigma)$. Going around the loop as before, we obtain

$$A_z = -\Big(\int_1 d\tau \partial_\sigma \log Z|_{\sigma_0} - \int_3 d\tau \partial_\sigma \log Z|_{\sigma_f} \Big) - \Big(\int_2 \frac{\nabla Z}{Z} \cdot \vec{dl} + \int_4 \frac{\nabla Z}{Z} \cdot \vec{dl} \Big) \tag{7.21}$$

We have seen that the first term in parenthesis vanishes when we cut the surface at $Z = \epsilon$, leaving us with the relation

$$-A_z = A_{div} = \frac{1}{\epsilon}\int_{2+4} |\nabla Z|\, dl\,, \qquad at \quad Z = \epsilon$$

Hence the first term in (7.18) is exactly equal to the $\epsilon\, A_{div}$ found in (6.17). So the formula for the regularized area of the surface ending on the Wilson loop becomes

$$A_{finite} = A_{const} + A_h + \frac{1}{2}\int_{2+4} \frac{\nabla^2 Z}{|\nabla Z|}\, dl \tag{7.22}$$

Or more explicitly,

$$A_{finite} = 4D_{p_1p_3}\log\theta(0)\int(\tau_2(\sigma)-\tau_1(\sigma))d\sigma + \int_{\partial D}\nabla\log h\cdot\vec{dl} + \frac{1}{2}\int_{2+4}\frac{\nabla^2 Z}{|\nabla Z|}\, dl \tag{7.23}$$

From $Z = \hat{\theta}\, h$ we can compute that at $Z = 0$ we have $\nabla Z = \nabla\hat{\theta}\, h$ and $\nabla^2 Z = \nabla^2\hat{\theta}\, h + 2\,\nabla\hat{\theta}\cdot\nabla h$. When substituted into (7.23) we get

$$\begin{aligned} A_{finite} = 4D_{p_1p_3}\log\theta(0)\int(\tau_2(\sigma)-\tau_1(\sigma))d\sigma + \int_{\partial D}\frac{\nabla h}{h}\cdot\vec{dl} \\ +\frac{1}{2}\int_{2+4}\frac{\nabla^2\hat{\theta}}{|\nabla\theta|}\, dl + \int_{2+4}\frac{\nabla\hat{\theta}}{|\nabla\hat{\theta}|}\cdot\frac{\nabla h}{h}\, dl \end{aligned} \tag{7.24}$$

Looking at the formula for $\nabla Z = \nabla\hat{\theta}\, h$ it is clear that ∇Z and $\nabla\hat{\theta}$ are in the same direction so that the unit normal may be taken to be $-\nabla\hat{\theta}/|\nabla\hat{\theta}|$. This further simplifies the above equation for A_{finite} giving an expression purely in terms of theta functions and the parametric curves τ_1 and τ_2;

$$A_{finite} = 4D_{p_1p_3}\log\theta(0)\int(\tau_2(\sigma)-\tau_1(\sigma))d\sigma + \frac{1}{2}\int_{2+4}\frac{\nabla^2\hat{\theta}}{|\nabla\theta|}\, dl\,. \tag{7.25}$$

In summary, we have a full analytic program (6.10), (6.12) and (6.17) for computing the regularized area for the minimal area surfaces for the Wilson loops we have found. We applied Stoke's Theorem in separating the finite part of the area from the divergent part and showed that the divergent part is the length of the Wilson loop. In the table below we show numerical results to bolster the theoretical arguments.

We compute the total area numerically at several different values of ϵ using the formula $A = 4\int d\sigma\, d\tau e^{\alpha}$ where $\alpha = 2\log\frac{\theta}{\hat{\theta}}$. We then fit the data to the linear model

$\epsilon\, A = \epsilon\, A_{finite} + L$ and find both the regularized area and the length of the Wilson loops. The results are in *Table 5.2.*

Table 5.2
Area of minimal area surfaces computed by both numerical and analytical methods

Areas	n=2	n=3	n=4	n=5
A by numerical method	$-13.80 + \frac{19.86}{\epsilon}$	$-20.55 + \frac{17.25}{\epsilon}$	$-40.23 + \frac{12.23}{\epsilon}$	$-55.48 + \frac{9.64}{\epsilon}$
A by (6.10),(6.12),(6.17)	$-13.80 + \frac{19.86}{\epsilon}$	$-20.55 + \frac{17.25}{\epsilon}$	$-40.27 + \frac{12.23}{\epsilon}$	$-55.66 + \frac{9.64}{\epsilon}$
A_{finite} by (7.25)	-13.8	-20.55	-40.27	-55.66

5.8 Some Analytic Aspects

Using integrability properties we can make formula (7.25) a bit simpler. First, note that the integral in the first term which is equal to $\int_D d\sigma d\tau$ may be written as

$$\int_D d\sigma d\tau = -\frac{1}{2}\int_{\partial D} \sigma d\tau - \tau d\sigma = -\frac{i}{2}\int_{\partial D} z\, d\bar{z} \tag{8.26}$$

Next, note that

$$\frac{1}{2}\int_{2+4} \frac{\nabla^2 \theta(\hat{\zeta})}{|\nabla \hat{\theta}(\zeta)|}\, dl = \int_{2+4} \frac{D_{13}\hat{\theta}(\zeta)}{|D_1 \hat{\theta}(\zeta)|}\, dl = -2\, i \int_{2-4} D_1 \log\theta(\zeta)\, d\bar{z} \tag{8.27}$$

with the last equality being true only on the boundary where the integral is performed. Putting all this together we obtain a new formula for the area of the surface dual to the Wilson loop as

$$A_{finite} = -2\Im\left\{ D_{13} \log\theta(0) \oint z d\bar{z} + \int_{2-4} D_1 \log\theta(\zeta) d\bar{z} \right\}. \tag{8.28}$$

5.8.1 The Monodromy Matrix

In this section we calculate the trace of the monodromy matrix. The trace of the monodromy matrix gives us the conserved charges in the theory and it should be a function purely of λ.

The monodromy matrix is given by

$$m = \Psi_\sigma \cdot \Psi_\delta^{-1}$$

where σ and δ represent any two points lying between the horizontal curves which map to the Wilson loop in the boundary of AdS. ζ_σ and ζ_δ will be the corresponding vectors at which the theta functions may be evaluated. They are related by $\zeta_\delta = \zeta_\sigma + n(2\pi i)$.

One importance of the monodromy matrix is that its trace measures the deviation of the solution from periodicity. In general it is a function of λ, the spectral parameter. Recall [22] that the matrix ψ is given by

$$\psi = \begin{pmatrix} \psi_1 & \psi_2 \\ \tilde{\psi}_1 & \tilde{\psi}_2 \end{pmatrix},$$

which substituted in the expression for m gives

$$m = \frac{1}{det\,\psi} \begin{pmatrix} \langle\psi_\sigma|\tilde{\psi}_\delta\rangle & -\langle\psi_\sigma|\psi_\delta\rangle \\ \langle\tilde{\psi}_\sigma|\tilde{\psi}_\delta\rangle & -\langle\tilde{\psi}_\sigma|\psi_\delta\rangle \end{pmatrix},$$

where the *bra* and *ket* notation implies

$$\langle\psi_\sigma|\tilde{\psi}_\delta\rangle = \psi_1\,\tilde{\psi}_{2\,\delta} - \psi_{2\,\sigma}\,\tilde{\psi}_{1\,\delta}\,. \tag{8.29}$$

The solutions for ψ was given [22] as

$$\psi_1 = \sqrt{-\lambda}\,\frac{\hat{\theta}(\zeta + \int_0^\lambda)}{\hat{\theta}(\zeta)}\,e^{-\frac{\alpha}{2}}\,e^{\mu z + \nu\bar{z}} \tag{8.30}$$

$$\psi_2 = \frac{\theta(\zeta + \int_0^\lambda)}{\theta(\zeta)}\,e^{\frac{\alpha}{2}}\,e^{\mu z + \nu\bar{z}} \tag{8.31}$$

$$\tilde{\psi}_1 = -\sqrt{-\lambda}\,\frac{\hat{\theta}(\zeta - \int_0^\lambda)}{\hat{\theta}(\zeta)}\, e^{-\frac{-\alpha}{2}}\, e^{-\mu z - \nu \bar{z}} \tag{8.32}$$

$$\tilde{\psi}_2 = \frac{\theta(\zeta - \int_0^\lambda)}{\theta(\zeta)}\, e^{\frac{\alpha}{2}}\, e^{-\mu z - \nu \bar{z}}\,. \tag{8.33}$$

Using *Ch3* (4.61) we compute the determinant of ψ to be

$$det\,\psi = \sqrt{-\lambda}\,\frac{\hat{\theta}(2\int_0^\lambda)\,\theta(0)}{\hat{\theta}(\int_0^\lambda)\,\theta(\int_0^\lambda)}\,. \tag{8.34}$$

We now have the trace formula

$$det\,\psi\, Tr(\psi_\sigma \cdot \psi_\delta^{-1}) = \langle \psi_\sigma | \tilde{\psi}_\delta \rangle - \langle \tilde{\psi}_\sigma | \psi_\delta \rangle\,. \tag{8.35}$$

In expanded form the right hand side becomes

$$\begin{aligned} rhs &= \sqrt{-\lambda}\,\frac{\hat{\theta}(\zeta_\sigma + \int_0^\lambda)\,\theta(\zeta_\delta - \int_0^\lambda)}{\hat{\theta}(\zeta_\sigma)\,\theta(\zeta_\delta)} e^{\frac{1}{2}(-\alpha_\sigma + \alpha_\delta)}\, e^{-\delta\omega} \\ &+ \sqrt{-\lambda}\,\frac{\theta(\zeta_\sigma + \int_0^\lambda)\,\hat{\theta}(\zeta_\delta - \int_0^\lambda)}{\theta(\zeta_\sigma)\,\hat{\theta}(\zeta_\delta)} e^{\frac{1}{2}(\alpha_\sigma - \alpha_\delta)}\, e^{-\delta\omega} \\ &+ \sqrt{-\lambda}\,\frac{\hat{\theta}(\zeta_\sigma - \int_0^\lambda)\,\theta(\zeta_\delta + \int_0^\lambda)}{\hat{\theta}(\zeta_\sigma)\,\theta(\zeta_\delta)} e^{\frac{1}{2}(-\alpha_\sigma + \alpha_\delta)}\, e^{\delta\omega} \\ &+ \sqrt{-\lambda}\,\frac{\theta(\zeta_\sigma - \int_0^\lambda)\,\hat{\theta}(\zeta_\delta + \int_0^\lambda)}{\theta(\zeta_\sigma)\,\hat{\theta}(\zeta_\delta)} e^{\frac{1}{2}(\alpha_\sigma - \alpha_\delta)}\, e^{\delta\omega}\,, \end{aligned}$$

where $\delta\omega = \omega_\delta - \omega_\sigma$. With $\omega = \mu z + \nu \bar{z}$, this means $\delta\omega = \delta\sigma(\mu + \nu)$, where $\delta\sigma$ is the difference between the points δ and σ. Notice also that $\delta\omega$ depends on λ since μ and ν do.

Further simplification of the *rhs* and dividing both sides of (8.35) by (8.34) gives

$$\begin{aligned} Tr(\psi_\sigma \cdot \psi_\delta^{-1}) &= K(\lambda)\, e^{-\delta\omega} \left[\frac{\hat{\theta}(\zeta_\sigma + \int_0^\lambda)\,\theta(\zeta_\delta - \int_0^\lambda) + \theta(\zeta_\sigma + \int_0^\lambda)\hat{\theta}(\zeta_\delta - \int_0^\lambda)}{\sqrt{\hat{\theta}(\zeta_\sigma)\,\theta(\zeta_\sigma)\,\hat{\theta}(\zeta_\delta)\,\theta(\zeta_\delta)}} \right] \\ &+ K(\lambda)\, e^{\delta\omega} \left[\frac{\hat{\theta}(\zeta_\sigma - \int_0^\lambda)\,\theta(\zeta_\delta + \int_0^\lambda) + \theta(\zeta_\sigma - \int_0^\lambda)\hat{\theta}(\zeta_\delta + \int_0^\lambda)}{\sqrt{\hat{\theta}(\zeta_\sigma)\,\theta(\zeta_\sigma)\,\hat{\theta}(\zeta_\delta)\,\theta(\zeta_\delta)}} \right], \end{aligned} \tag{8.36}$$

where the quantity

$$K(\lambda) = \frac{\hat{\theta}(\int_0^\lambda)\,\theta(\int_0^\lambda)}{\hat{\theta}(2\int_0^\lambda)\,\theta(0)}\,.$$

Because the arguments ζ_δ and ζ_σ differ by a period of the theta function, (8.36) can be further simplified to

$$\begin{aligned} Tr(\psi_\sigma \cdot \psi_\delta^{-1}) &= \frac{\left(\hat{\theta}\Big(\zeta_\sigma + \int_0^\lambda\Big)\,\theta\Big(\zeta_\sigma - \int_0^\lambda\Big) + \hat{\theta}\Big(\zeta_\sigma - \int_0^\lambda\Big)\,\theta\Big(\zeta_\sigma + \int_0^\lambda\Big)\right)}{\hat{\theta}(\zeta_\sigma)\,\theta(\zeta_\sigma)} \\ &\times \left(e^{-\delta\omega} + e^{\delta\omega}\right)\, K(\lambda)\,. \end{aligned} \tag{8.37}$$

But the fraction in the equation above is exactly $1/K(\lambda)$ by *Ch3* (4.61) so we have

$$Tr(\psi_\sigma \cdot \psi_\delta^{-1}) = 2\cosh(\delta\omega)\,, \tag{8.38}$$

where $\delta\omega = \delta\sigma(\mu+\nu) = -2\,\delta\sigma\left(D_3 \ln\theta(\int_0^\lambda) + D_1 \ln\theta(\int_0^\lambda)\right)$.

When the trace is evaluated at a value of λ for which the solution $X(s,\lambda)$ is periodic, say a $\lambda = \pm 1$, the quantity $\delta\omega$ being $\delta\sigma(\mu+\nu)$ evaluates to πi because that is exactly the condition imposed on the exponential in $X(s,\lambda)$ necessary for it to be periodic. In that case the trace computes to -2.

5.9 Cyclical Wilson Loops

Recall that in the genus 3 setting the concentric Wilson loops are obtained by matching n number of periods of the ratio of theta function to a single period of the exponential function in (2.5), and by shrinking the $b\bar{b}$ and $c\bar{c}$ branch cuts. So it is natural to ask what happens when, alternatively, n periods of the exponential function is matched with a single period of the ratio of theta functions. It turns out that we get a boundary curve made of self intersecting curves. Each individual curve becomes more like a circle (for some choice of a and b) and the circle goes around n times, hence the name *cyclical Wilson loop*.

We emphasize that these Wilson loops are obtained by making the vertical branch cuts very short and then matching the appropriate periods of the exponential and Theta functions parts of the solutions. We show in *Figure 5.7* an example of a cyclical Wilson loop computed for $n = 2$.

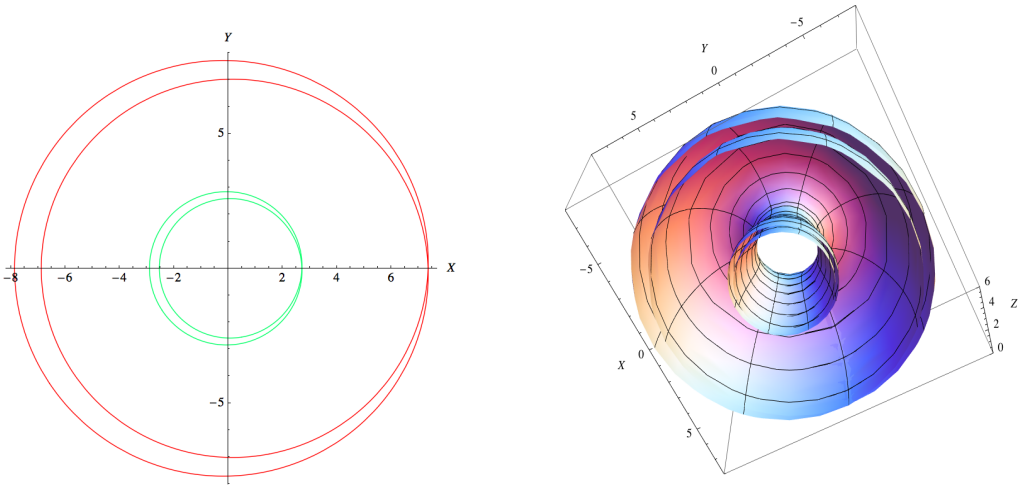

Figure 5.7. *Cyclical Wilson loop and its dual surface:* $n = 2, a = 2.412712, b = 2 + 0.05I$

An interesting thing about the cyclical Wilson loop is that as we shrink the $b\bar{b}$ branch cut even further we approach the concentric circles but the Wilson loops are now becoming n covers of the concentric circles[1]. Below we show two $n = 2$ cyclical Wilson loops that depicts this idea.

[1]Due to the involution $\lambda \to -\frac{1}{\lambda}$ the $c\bar{c}$ branch cut shrinks as we shrink the $b\bar{b}$ branch cut. The branch points a and b determine all the finite branch points.

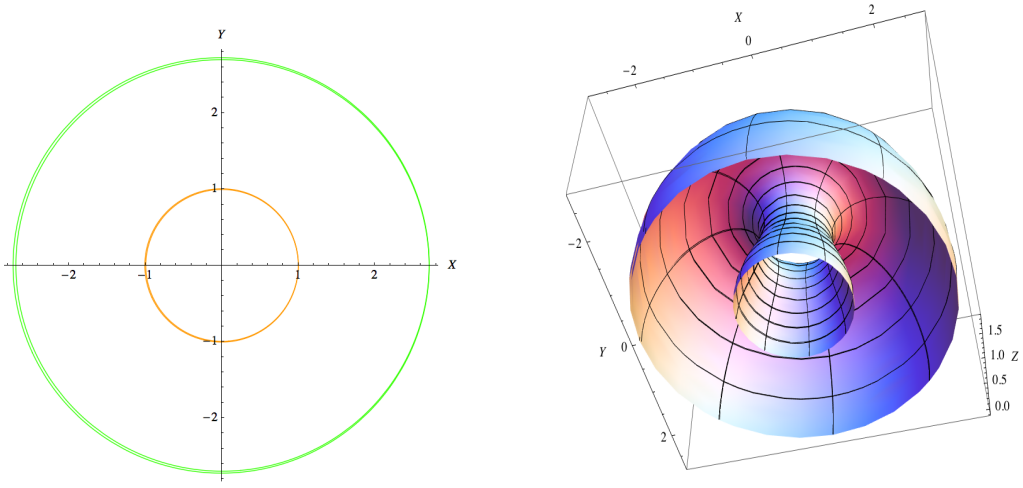

(a). $a = 2.4142,\ b = 2 + 0.005I$

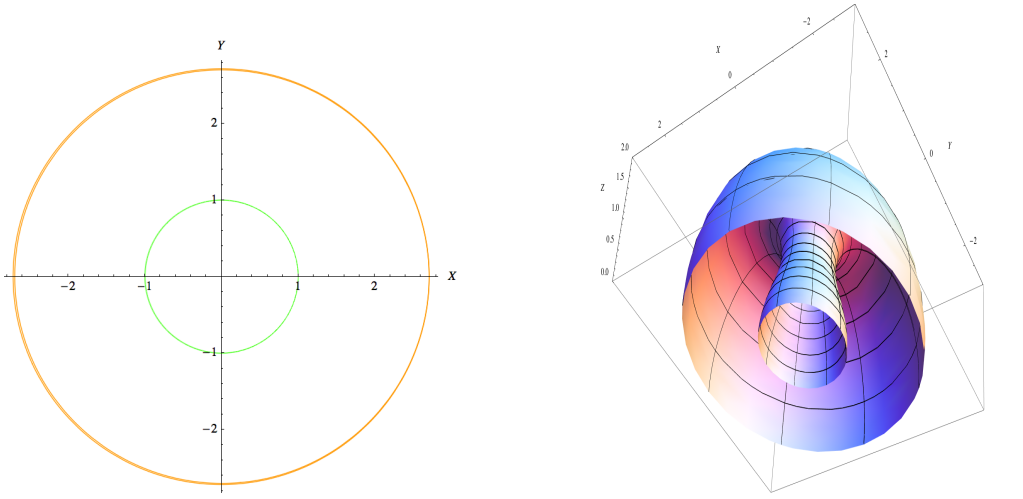

(b). $a = 2.414205, b = 2 + 0.003I$

Figure 5.8. *Cyclical Wilson loops and their corresponding dual surfaces. As we shrink the $b\bar{b}$ branch cut the cycles merge into each other until we get a double cover of the circle.*

It is clear that as we make the imaginary part of b smaller and smaller the the Wilson loops approach the $g = 1$ case with $a > 1$. In general, there are more situations

other than these in which we have more than two boundary curves that behave in more complicated but controllable ways.

5.10 Symmetric n-Leaf Wilson Loops

It is clear by now that so far the Wilson loops that we have discussed which come from hyperelliptic Riemann surfaces of genus three, namely the concentric Wilson loops and the cyclical Wilson loops, were motivated by our previously studied Wilson loops obtained from genus one hyperelliptic Riemann surfaces. In particular, we showed that in the limit that the branch point b approaches the real axis the periodic Wilson loop obtained is a generalization of the concentric circular Wilson loop. Now we are interested in periodic Wilson loops for values of $Im(b) \gg 0$.

For these cases the Wilson loop turns out to be much more complicated. To fully describe these Wilson loops it will be good to begin from their string world sheet description. The Wilson loops are obtained as the image in AdS_3 of the zeros of $\hat{\theta}(\zeta)$ in the string world sheet. So in the world sheet, the curves for this kind of Wilson loop will appear as either closed or open curves. Since periodicity is ensured, images of closed or open curves will always be closed. Sometimes the open curves are horizontal, sometimes they are vertical. Here we focus on cases in which all open curves are horizontal. The minimal area surface in AdS_3 is obtained by mapping the entire bounded region and its two bounding open curves. The bounding curves maps to the boundary of the minimal area surface while the bounded region maps to the surface that extends into the bulk of AdS_3 . Sometimes the region between two open curves in the world sheet contains closed curves. This means the image of entire horizontal strip which now contains closed curves, will consist of a minimal area surface which ends on more than just the images of the open curves.

Also the images of the two open curves and those of the closed curves will in general intersect one another and in some instances self intersect in the boundary of AdS. Although this seemingly gives the impression that the Wilson loop will be

a system of intersecting curves that meander in a chaotic manner, they amazingly display a nice symmetric behavior. More interesting is the fact that the symmetry is governed by the periodicity conditions imposed on the solutions.

Recall that we can match n periods of the exponential function to a period of the theta function part of the solutions or vice versa and obtain different interesting properties. We extend the same idea here and we will particularly focus on the case in which we match n periods of the exponential function to a period of the Theta function part of the solutions. This gives symmetric Wilson loops that look like n-leaf clovers. Such Wilson loops are said to be *n-leaf symmetric Wilson loops*.

We now specifically study the $n = 3$ example of n-leaf symmetric Wilson loops. In *Figure 5.9* we show the zeros of $\hat{\theta}(\zeta)$ over one period of the solutions. The boundary of the minimal area surface will be the images of the closed and open curves.

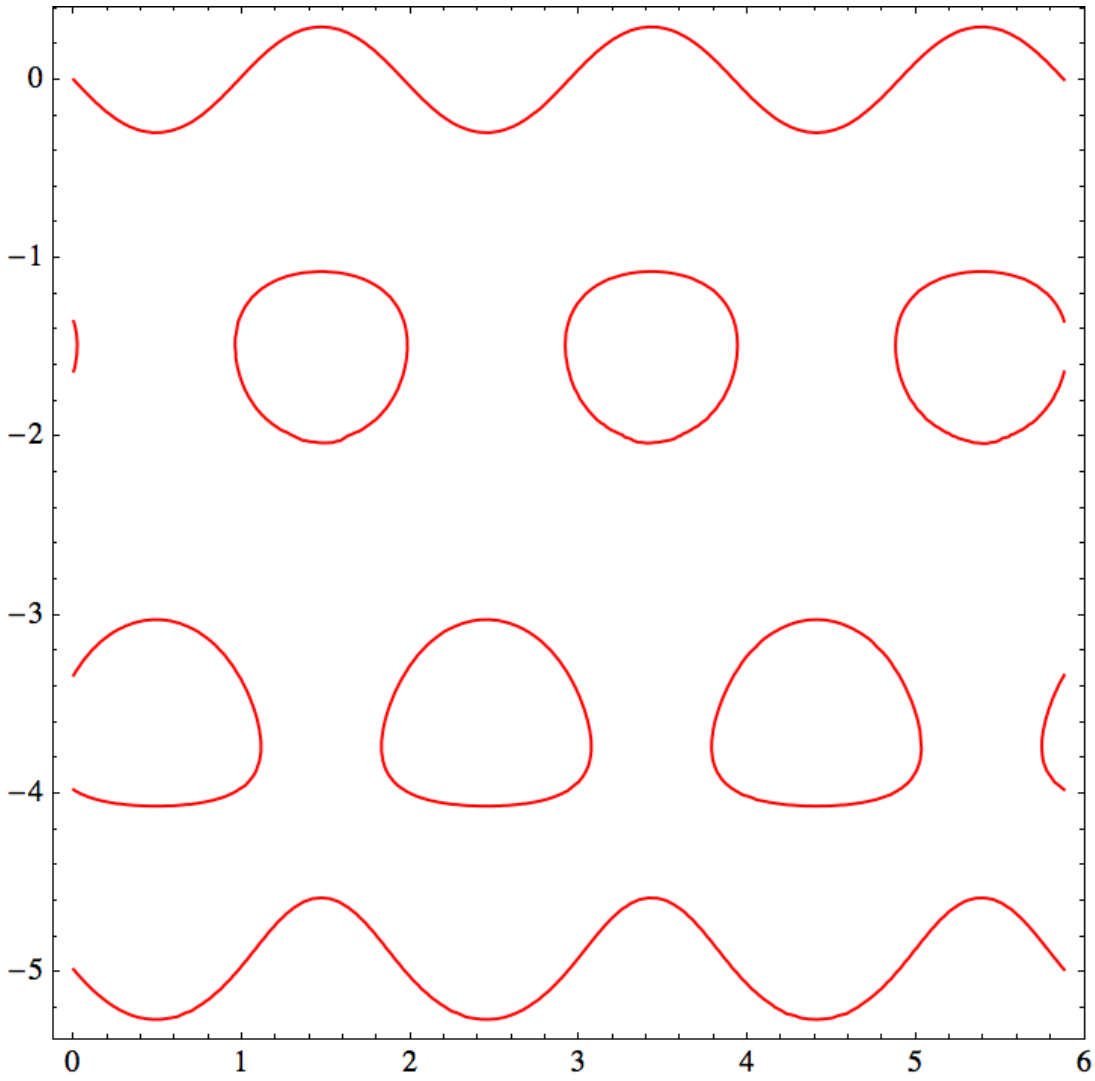

Figure 5.9. *World sheet of* 3*-leaf symmetric Wilson loop.*

We also plot the Z solution over the entire world sheet in order to illustrate that the solutions do end along the zeros of $\hat{\theta}$ and also that the portion of the world sheet between the zeros of $\hat{\theta}$ actually extend into the bulk. This is depicted in *Figure* 5.10.

The figure also shows that since Z achieves a maximum at some point in the world sheet the solution is finite since X and Y are already periodic.

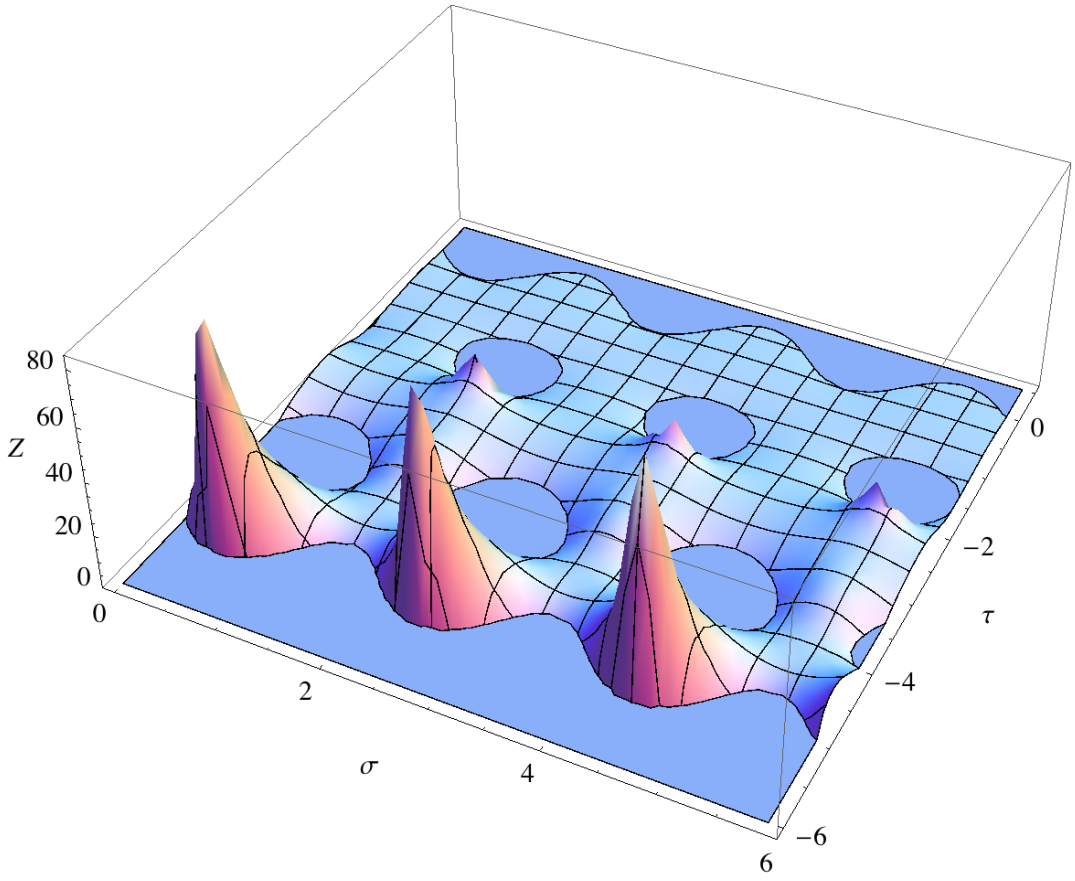

Figure 5.10. *The behavior of the solution Z shows that the surface ends along the zeros of $\hat{\theta}$.*

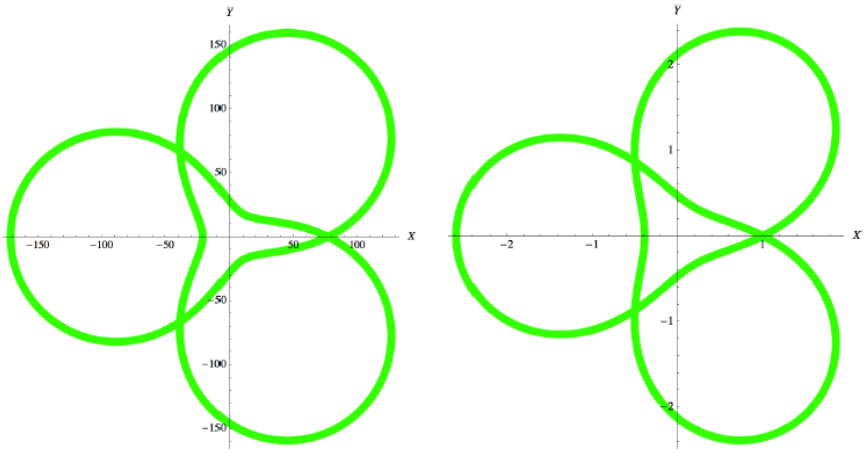

(a). Top sine-like curve. *(b). Bottom sine-like curve*

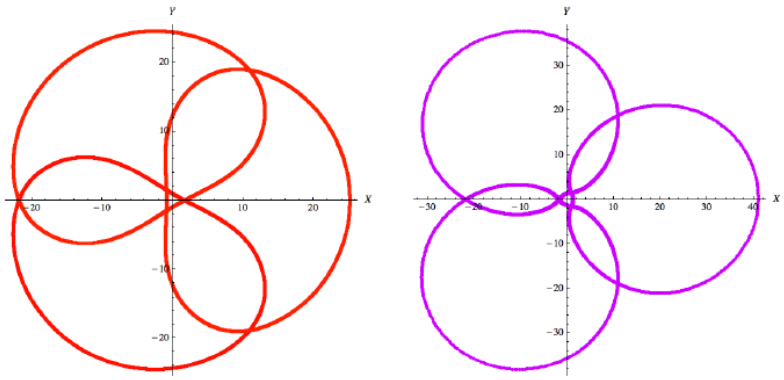

(a). Lowere 3 closed curves. *(b). Upper 3 closed curves*

Figure 5.11. *The boundary curves of the minimal area surface for a* 3*-leaf symmetric Wilson loop. The symmetry is manifest and the images look like three leaf clovers.*

In the boundary of AdS_3 these curves self intersect and form a complex network. This implies a Wilson loop with many self intersections. In the weak 't Hooft coupling limit of a gauge theory, these intersections give rise to logarithmic divergence in the perturbative expansion of the expectation value of the Wilson loop.

To see how the Wilson loop looks like we show a plot of the Wilson loop in the boundary and the gravity dual minimal area surface.

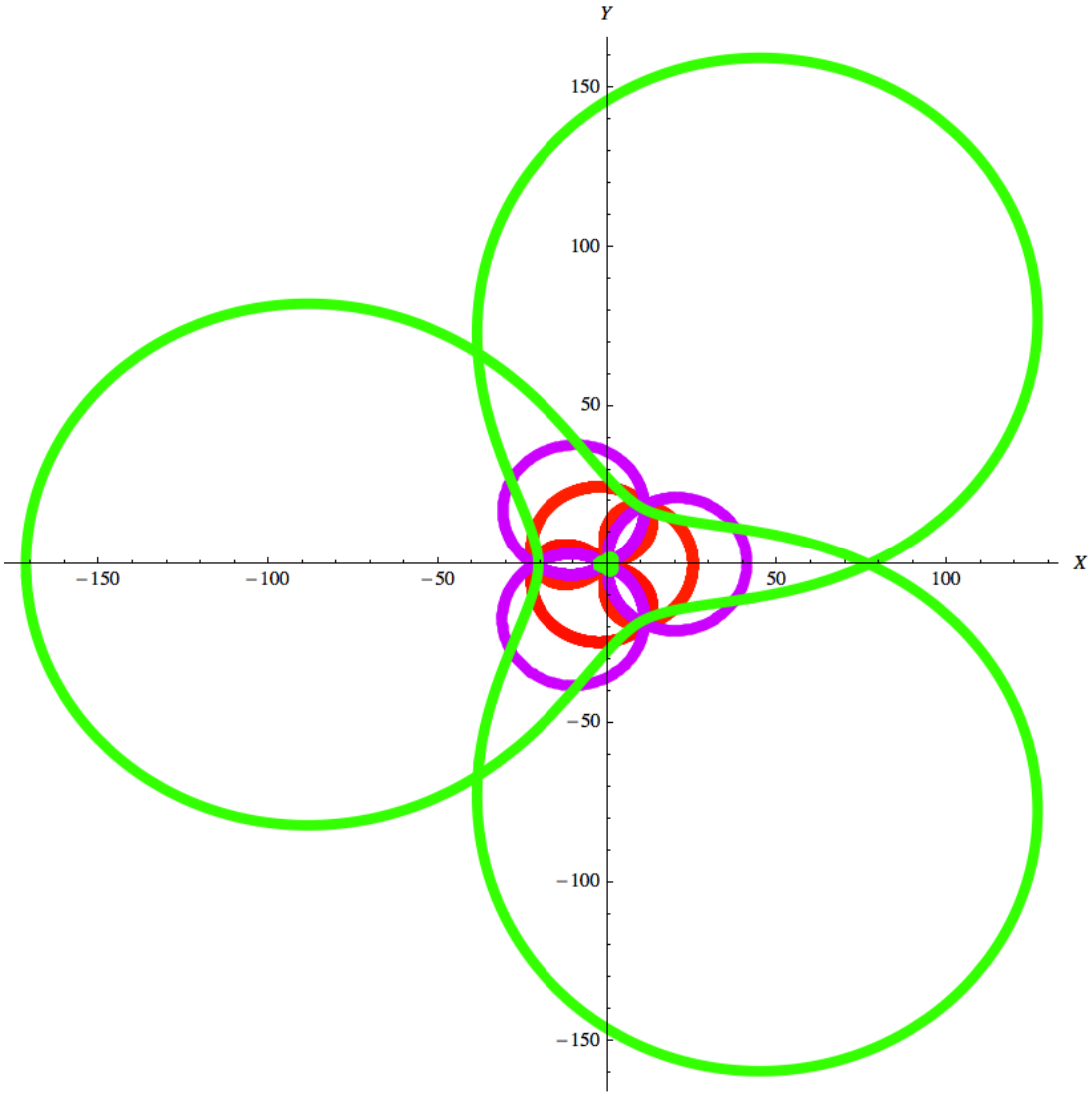

Figure 5.12. 3-*leaf symmetric Wilson loop:* $a = 2.1868, b = 0.5 + 0.5I$

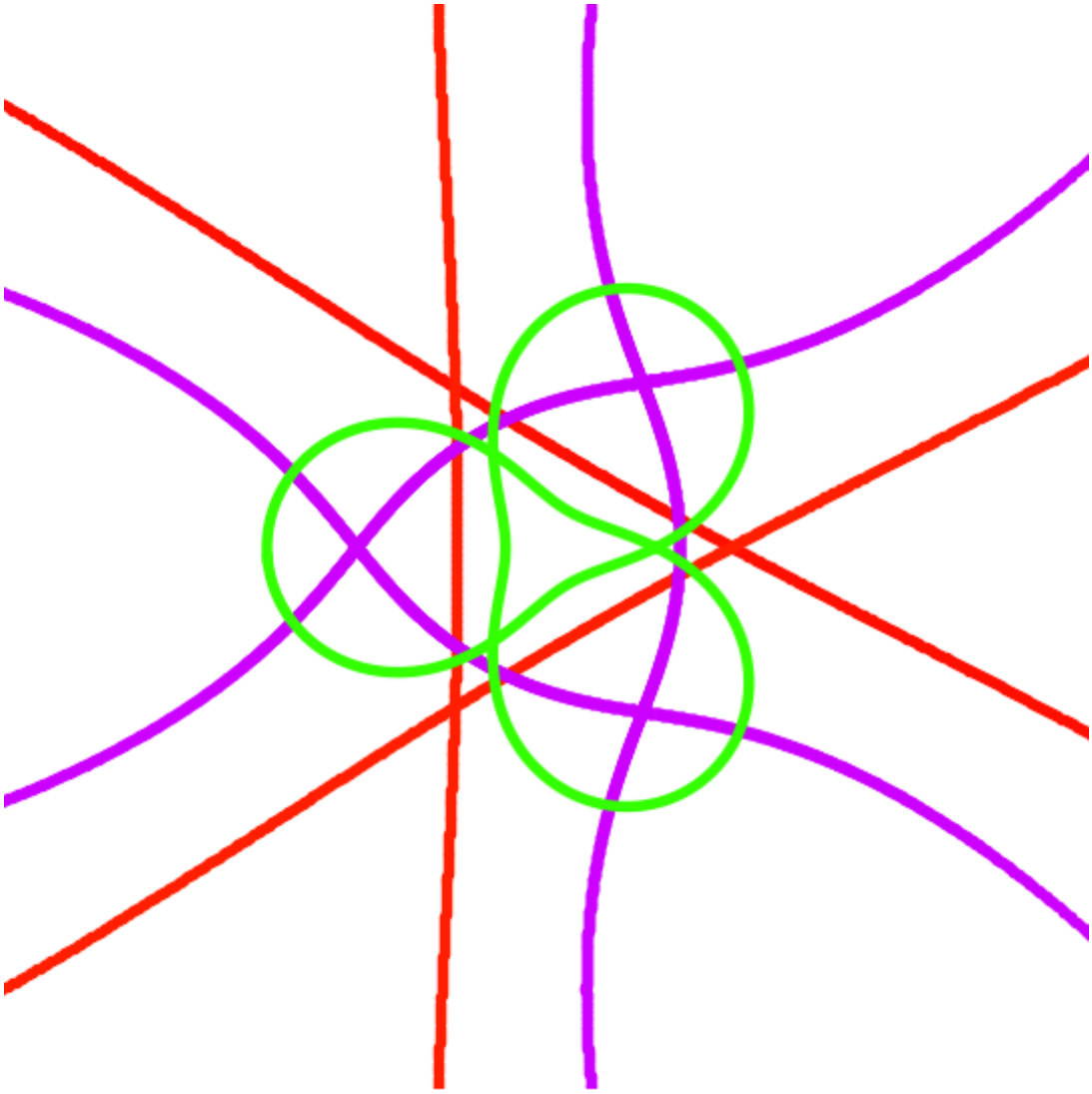

Figure 5.13. *Zoomed in close to the origin of Euclidean* AdS_3

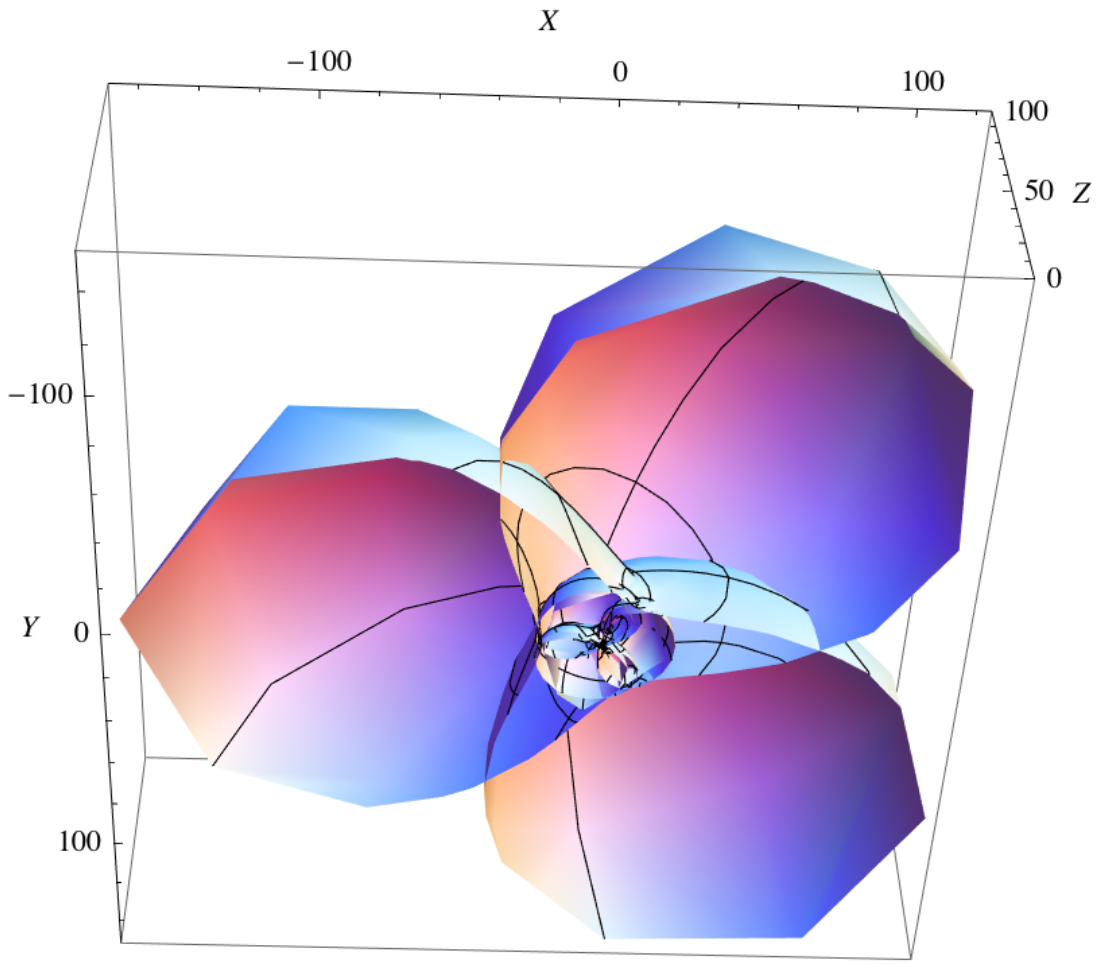

Figure 5.14. *The corresponding minimal area surface is a complex surface in Euclidean AdS_3 space*

6. Conclusion

In this thesis we use existing knowledge of Riemann theta functions to study Euclidean Wilson loops in Euclidean anti de Sitter Space within the context of the Holography conjecture. Using this technique we are able to compute more general examples of Euclidean *simple Wilson loops* whose shapes are not restrictedly symmetric as those of the previously studied examples. We show that these Wilson loops belong to an infinite set of families of Wilson loops, with each family generated by varying the spectral parameter of any single member of that family. Additionally, it is shown that the gravity dual minimal area surfaces of all Wilson loops belonging to the same family have the same *regularized area* regardless of the individual shape and length of the corresponding Wilson loops. The areas of the minimal area surfaces of the Wilson loops we study are computed using derived analytic formulae.

Furthermore, we look at cases when the Wilson loop consists of multiple curves. For example we study noncircular *concentric Wilson loops* and show in a perturbative sense that they are related to the Drukker-Fiol concentric circular Wilson loop. We particularly use the periodicity of the solutions to compute examples where the Wilson loops are controllably deformed. We show also that the trace of their monodromy matrix is a simple function of the spectral parameter which indicates the existence of an infinite number of conserved charges.

Finally, other types of Wilson loops consisting of multiple curves that we consider in this thesis include the *cyclical Wilson loop* and the *n-leaf symmetric Wilson loops*. We emphasize that it is possible to compute these examples because of the quasi periodic nature of Riemann theta functions which we use to express the solutions of the sigma model.

LIST OF REFERENCES

LIST OF REFERENCES

[1] J. Maldacena, "The large N limit of superconformal field theories and supergravity," Adv. Theor. Math. Phys. **2**, 231 (1998) [Int. J. Theor. Phys. **38**, 1113 (1998)], `hep-th/9711200`,
S. S. Gubser, I. R. Klebanov and A. M. Polyakov, "Gauge theory correlators from non-critical string theory," Phys. Lett. B **428**, 105 (1998) [arXiv:hep-th/9802109].

[2] E. Witten, "Anti-de Sitter space and holography," Adv. Theor. Math. Phys. **2**, 253 (1998) [arXiv:hep-th/9802150].

[3] J. M. Maldacena, "Wilson loops in large N field theories," Phys. Rev. Lett. **80**, 4859 (1998) [arXiv:hep-th/9803002],
S. J. Rey and J. T. Yee, "Macroscopic strings as heavy quarks in large N gauge theory and anti-de Sitter supergravity," Eur. Phys. J. C **22**, 379 (2001) [arXiv:hep-th/9803001].

[4] N. Drukker and V. Forini, "Generalized quark-antiquark potential in AdS/CFT," JHEP **1106**,131(2011) [arXiv:1105.5144[hep-th]]

[5] D. E. Berenstein, R. Corrado, W. Fischler and J. M. Maldacena, "The Operator product expansion for Wilson loops and surfaces in the large N limit," Phys. Rev. D **59**, 105023 (1999) [arXiv:hep-th/9809188],
D. J. Gross and H. Ooguri, "Aspects of large N gauge theory dynamics as seen by string theory," Phys. Rev. D **58**, 106002 (1998) [arXiv:hep-th/9805129],
J. K. Erickson, G. W. Semenoff and K. Zarembo, "Wilson loops in N = 4 supersymmetric Yang-Mills theory," Nucl. Phys. B **582**, 155 (2000) [arXiv:hep-th/0003055],
N. Drukker and D. J. Gross, "An exact prediction of N = 4 SUSYM theory for string theory," J. Math. Phys. **42**, 2896 (2001) [arXiv:hep-th/0010274],
V. Pestun, "Localization of gauge theory on a four-sphere and supersymmetric Wilson loops," arXiv:0712.2824 [hep-th].

[6] N. Drukker, S. Giombi, R. Ricci and D. Trancanelli, "Supersymmetric Wilson loops on S**3," JHEP **0805**, 017 (2008) [arXiv:0711.3226 [hep-th]].

[7] N. Drukker and B. Fiol, "On the integrability of Wilson loops in AdS(5) x S**5: Some periodic ansatze," JHEP **0601**, 056 (2006) [arXiv:hep-th/0506058].

[8] M. Kruczenski, "A note on twist two operators in N = 4 SYM and Wilson loops in Minkowski signature," JHEP **0212**, 024 (2002) [arXiv:hep-th/0210115].

[9] M. Babich and A. Bobenko, "Willmore Tori with umbilic lines and minimal surfaces in hyperbolic space", Duke Mathematical Journal **72, No. 1**, 151 (1993).

[10] E. D. Belokolos, A. I. Bobenko,V. Z. Enol'skii, A. R. Its, V. B. Matveev, "Algebro-Geometric Approach to Nonlinear Integrable Equations," Springer-Verlag series in Non-linear Dynamics, Springer-Verlag Berlin Heidelberg NewYork (1994).

[11] D. Brecher, A. Chamblin and H. S. Reall, "AdS / CFT in the infinite momentum frame," Nucl. Phys. B **607**, 155 (2001) [hep-th/0012076].

[12] K. Pohlmeyer, "Integral Hamiltonian systems and interactions through quadratic constraints," Commun. Math. Phys. 46, 207 (1976).

[13] A. Jevicki and K. Jin, "Moduli Dynamics of AdS(3) Strings," JHEP **0906**, 064 (2009) [arXiv:0903.3389 [hep-th]].

[14] M. Kruczenski, "Spiky strings and single trace operators in gauge theories," JHEP **0508**, 014 (2005) [arXiv:hep-th/0410226].

[15] L. F. Alday and J. Maldacena, "Null polygonal Wilson loops and minimal surfaces in Anti-de-Sitter space," JHEP **0911**, 082 (2009) [arXiv:0904.0663 [hep-th]].

[16] D. Mumford, (with the collaboration of C. Musili, M. Nort,E. Previato and M. Stillman), "Tata Lectures in Theta I & II", Modern Birkhäuser Classics, Birkhäuser, Boston (2007),
John D. Fay, "Theta Functions on Riemann Surfaces", Lectures Notes in Mathematics **352**,Springer-Verlag, Berlin Heidelberg, New York (1973),
H. F. Baker, "Abel's Theorem and the Allied Theory, Including the Theory of the Theta Functions", Cambridge University Press (1897).

[17] R. Miranda, "Algebraic Curves and Riemann Surfaces" Graduate Studies in Mathematics, Vol. 5, (1995)

[18] C. Birkenhake and H. Lange, "Complex Abelian Varieties", Grundlehren der mathematischen Wissenschaften **302**, Springer-Verlag Berlin Heidelberg (2004).

[19] H. M. Farkas and I. Kra, "Riemann Surfaces", Graduate Texts in Mathematics, Second Edition, Springer-Verlag, New York, Berlin, Heidelberg (1991).

[20] U. Görtz, T. Wedhorn, "Algebraic Geometry I: Schemes With Examples and Exercises", Vieweg+Teubner Verlag, First Edition, Springer Fachmedien Wiesbaden GmbH (2010).
G. Harder, "Lectures on Algebraic Geometry I: Sheaves, Cohomology of Sheaves, and Applications to Riemann Surfaces", Vieweg+Teubner Verlag, Second Edition, Springer Fachmedien Wiesbaden GmbH (2011).
A. I. Bobenko, C. Klein, "Computational Approach to Riemann Surfaces", Lecture Notes in Mathematics, Springer-Verlag, Berlin, Heidelberg (2011).

[21] M. Kruczenski and S. Ziama, "Wilson loops and Riemann theta functions II", (*publication in progress*).

[22] R. Ishizeki, M. Kruczenski and S. Ziama, "Notes on Euclidean Wilson loops and Riemann Theta functions," Phys. Rev. D **85**, 106004 (2012) [arXiv:1104.3567 [hep-th]].

VITA

VITA

My name is Sannah Phi Ziama and I was born in Liberia. I moved to the USA in 2004 and in that same year I enrolled in a dual degree granting program at IUPUI. I graduated IUPUI in 2008 with a BSc in physics and a MSc in mechanical engineering. In 2008, my curiosity about physics led me to graduate school at Purdue University where I began studying string theory under the supervision of Martin Kruczenski. The subject of my PhD thesis is "Wilson loops and Riemann theta functions in the gauge/gravity duality".

During my undergraduate studies I received several scholarly recognitions and research awards including the LSAMP research award, the Forrest Meiere Prize for Outstanding Undergraduate Physics Major, and the IUPUI UROP research award. I was also awarded the Purdue Doctoral Fellowship, the AGEP Fellowship, and the NSF Graduate Research Fellowship while studying at Purdue University.